Global and Planetary Change 209 (2022) 103736

Contents lists available at ScienceDirect

Global and Planetary Change

journal homepage: www.elsevier.com/locate/gloplacha

Quaternary sediment sources and loess transport pathways in the Black Sea - Caspian Sea region identified by detrital zircon U-Pb geochronology

Chiara Költringer [a,*], Thomas Stevens [a], Martin Lindner [b], Yunus Baykal [a], Amin Ghafarpour [c], Farhad Khormali [c], Natalia Taratunina [d,e], Redzhep Kurbanov [d,f]

[a] Uppsala University, Dept. of Earth Science, 75236 Villavägen 16, Sweden
[b] Department of Chemistry and Physics of Materials, University of Salzburg, Salzburg, Austria
[c] Department of Soil Science, Gorgan University of Agricultural Sciences and Natural Resources, Gorgan, Iran
[d] MSU, Lomonosov Moscow State University, Faculty of Geography, M.V., Leninskie Gori, 1, Moscow 119992, Russia
[e] Department of Stone Age Archeology, Institute of Archeology and Ethnography SB RAS, 17, Ac. Lavrentieva ave., Novosibirsk, 630090, Russia
[f] RAS, Laboratory of Evolutionary Geography, Institute of Geography, Staromonetny, 29, Moscow 119017, Russia

ARTICLE INFO

Editor name: Zhengtang Guo

Keywords:
Detrital zircon U—Pb dating
Loess
Provenance
Sediment routing
East European Plain
Caspian Sea

ABSTRACT

Constraining the controls on the distribution of sediment at a continental scale is a critical step in understanding long-term landscape and climate evolution. In particular, understanding of the role of rivers in wider sediment routing and impacts on aeolian loess formation on a continental scale remains limited. Extensive Quaternary loess deposits are present on the East European Plain and in the Black Sea - Caspian Sea region and are associated with major rivers draining numerous surrounding cratonic and orogenic hinterland areas. Coupled with this, complex changes in local and global sea level have affected the extent and drainage of the Caspian Sea and the Black Sea, and Quaternary glaciations have impinged on the northern margin of the East European Plain. This suggests that sediment routing and loess formation may show complex patterns and controls. Here, we apply U—Pb dating of detrital zircons from fluvial, marine and aeolian (dominantly loess) sedimentary records on the East European Plain and in the Black Sea - Caspian Sea region. This shows a strong control of large rivers on the distribution of sediments at a continental scale in the region, through long-distance transport of several 1000 km, sourced from continental and mountain glacier areas prior to marine or atmospheric reworking and transportation. Strong spatial variability in zircon U—Pb data from loess deposits on the East European Plain reveals multiple diverse sources to the different individual loess sections, whereas no significant temporal variability in loess source is detected during the Late Pleistocene of the Lower Volga loess in South Russia. While the sediment supply from glacial areas via rivers plays an important role for the provenance of East European Plain loess deposits, our data indicate that the stark spatial diversity in loess provenance on the East European Plain is often driven by the input of multiple local sources. Similar to the loess, marine sediments from different basins of the Black Sea and the Caspian Sea also show significant spatial variability. This variability is controlled by the bathymetry of the seas, leading to sedimentary intermixing by sea currents within, but not between different separated sea basins. A direct comparison of marine and aeolian sediments at the same depositional site suggests that although loess and marine sediments are both dominantly sourced from river sediments containing far travelled sedimentary material, local sources play a more important role in many loess deposits.

1. Introduction

One of the most fundamental topics in Earth Sciences is how the material for the formation of sediments is produced, transported and deposited; i.e. the sedimentary cycle. These processes are crucial to constrain in order to understand the long-term development of landscapes, the forcing and effects of climate and environmental change, and a host of other related questions. In particular, knowledge of where and how material is eroded, transported and deposited, and which process agents are active in this (e.g. water, ice, wind, etc.), is essential to link geomorphic work with forcing of other systems, such as climate (e.g. Bridge and Demicco, 2008). Indeed, constraining lags and

* Corresponding author.
E-mail address: chiara.koltringer@outlook.com (C. Költringer).

https://doi.org/10.1016/j.gloplacha.2022.103736
Received 7 May 2021; Received in revised form 2 December 2021; Accepted 7 January 2022
Available online 12 January 2022

pathways in the cycling of sedimentary material is also central to interpretation of rock archives of erosion on land, in terms of climate or landscape processes (e.g. Frostick and Jones, 2002).

Rivers play a major role in this sediment cycling, and climate-landscape interactions can be revealed by analysis of how and where land is denuded via river systems, and how sediment is stored en route to sedimentary basins. Thus, rivers may also play a fundamental role in the distribution of material that later forms aeolian sediments by facilitating the movement of large volumes of sediment to areas where it can easily be deflated and subsequently deposited as loess or aeolian sands (e.g. Smalley et al., 2009; Hällberg et al., 2020). In particular, aeolian dust transport in atmospheric suspension (silt and clay sized particles) is important to understand as a major component of the climate system, both driving and responding to climate change (e.g. Maher et al., 2010; Choobari et al., 2014; Harrison et al., 2001). Examination of the wide scale distribution of dust particles is central to understand how much material has been transported, for how long, and over what pathways. This information is used to better simulate the potential impact of atmospheric dust on the Earth system (Albani et al., 2015). Loess comprises a record of past wind-blown dust, and in particular is dominated by 'coarse dust' (5–20 μm), which itself has specific climate forcing effects and has been significantly underestimated in terms of importance and atmospheric abundance (Adebiyi and Kok, 2020). Constraining prior river transport in dust and loess distribution is a key part in understanding pathways of coarse dust transport, as the extent of this prior fluvial transport has implications for the extent and duration of particle atmospheric transport.

While this importance is well-known, understanding of wide-scale and long-term sediment cycling in loess formation is limited by a lack of knowledge of source and transport of sedimentary material. Loess deposits are extensively preserved over large areas of the mid latitudes, more or less continuously over thousands of km in Eurasia (e.g. Marković et al., 2015; Lehmkuhl et al., 2020). However, the spatial changes in sources for these deposits over a wider, continental scale have seldom been investigated. One of these few studies used bulk geochemistry data and atmospheric modelling to suggest that last glacial dust material in Europe only underwent atmospheric transport of a few hundred km or less (Rousseau et al., 2014). However, the specific role of rivers in wider distribution of material prior to atmospheric transport was not examined, even though several studies propose the importance of river transport in the formation of European loess deposits and river sediment sources are strongly suggested by reconstructed transport directions (e.g. Smalley et al., 2009; Ujvári et al., 2012; Nawrocki et al., 2018; Pańczyk et al., 2020; Baykal et al., 2021).

Despite this uncertainty, the generation of atmospheric dust and ultimately the formation of loess deposits in Europe and western Asia is strongly associated with the overall cool climate during the Quaternary, and its glacial and interglacial cyclicity. Glacial grinding by continental ice sheets and mountain glaciers, as well as cold climate weathering processes in mountains, led to an increased production of fine-grained sedimentary material (Muhs et al., 2003; Smalley and Derbyshire, 1990). Generally, the aeolian deflation of dust is facilitated in cold and poorly vegetated semi-arid and arid areas experiencing strong winds, which are more common in glacial periods (e.g. Pye, 1995). However, transport of material to suitable depocentres where loess can be preserved may require extended fluvial transport prior to aeolian deflation and final deposition. As such, material eventually forming loess can experience several cycles of erosion, accumulation, and transport before its final deposition, and as a result of this can contain sediment from several proto sources, transported via multiple agents and pathways (e.g. Licht et al., 2016).

To test the influence of rivers on sediment supply and subsequent loess formation, to determine the processes and patterns in wide scale sediment cycling, and to facilitate better constraint of the possible effects of dust on climate, environment and landscape, it is important to pinpoint loess provenance in detail using techniques that can reveal multiple proto- and secondary sources, thereby allowing analysis of stepwise dust transport from sources to sink. Furthermore, constraining the provenance of loess distributed over a wide area where sources likely vary geographically, allows analysis of the general role of rivers in wide scale sediment distribution, facilitating insight into recycling and source to sink sediment movement. In addition, the detailed analysis of how loess provenance varies at a continental scale, may yield insight into the controls on wide-scale generation and distribution of aeolian dust during the Quaternary, which is of particular importance in constraining the role of dust in the climate system.

A suitable area to test these factors and their implications is the East European Plain (EEP), including the Black Sea - Caspian Sea region. This area is subject to a complex set of sediment erosion, deposition, reworking and redistribution patterns, controlled by the interaction of fluvial, marine and aeolian systems, which originate from the north (Baltica-Fennoscandia, Urals), south (Caucasus and Iranian mountains), east (central Asian deserts and mountains) and west (Carpathian-Alps and Danube basins) (Fig. 1a). However, the provenance and transport pathways of each of these sedimentary systems remain poorly constrained, as do their relationships and interactions. Targeted provenance studies on loess exist only for Ukrainian deposits in the west of the EEP (Buggle et al., 2008; Nawrocki et al., 2018; Pańczyk et al., 2020) and river provenance data is scarce. Given the complex sedimentary setting in the Black Sea - Caspian Sea region, a provenance tracer is required that can be applied for all these different kinds of sediments and transport pathways to disentangle the origin of the material and transport systems. Detrital zircon U—Pb geochronology represents a powerful single grain analysis technique that has become a widely used method for sedimentary provenance studies and may be a suitable candidate (Fedo et al., 2004 and references therein). Detrital zircons have been successfully used to trace the provenance of various types of siliciclastic sediments and sedimentary rocks (e.g. sandstone, conglomerate), and their metasedimentary equivalents (e.g. Froude et al., 1983; Nutman et al., 1999; Horton et al., 2008; Allen et al., 2006; Vincent et al., 2013; Cawood et al., 2003; Allen et al., 2006; Aleinikoff et al., 2008; Safonova et al., 2010; Stevens et al., 2010; Wang et al., 2011; Garzanti et al., 2013). In loess, single-grain U—Pb dating of detrital zircons can be very source diagnostic in instances where multiple dust sources are expected (Stevens et al., 2010), and overcomes ambiguities in deciphering multiple sources inherent in bulk sample geochemical data. While recycling of zircons through multiple depositional and erosional phases can complicate interpretations, zircons are generally highly suitable for provenance analyses due to their high resistance to mechanical disaggregation and chemical weathering during erosion and transportation (e.g. Moecher and Samson, 2006). This resistance allows examination of crustal proto-sources and constraint of several steps in the generation and transport pathways of loess. Due to the different timing of tectonic events in the study area, diagnostic differences in zircon ages are expected for grains deriving from different orogens bordering the EEP. This makes detrital zircon U—Pb geochronology a potentially powerful tool to understand provenance and sedimentary dispersal systems in the EEP and the Black Sea - Caspian Sea region. Furthermore, the method's suitability for loess provenance studies on the EEP has previously been demonstrated on a smaller scale than considered here (Nawrocki et al., 2018; Pańczyk et al., 2020). As such, here we apply detrital zircon U—Pb analyses to river, aeolian and marine sediments over a wide area of the EEP and south of the Caspian Sea in order to constrain the pathways and mechanisms of sediment routing in the region, and unravel the implications for dust distribution and loess formation.

2. Study area and methodical approach

During Pleistocene cold stages, the northern part of the EEP was covered by the Fennoscandian Ice Sheet (Velichko et al., 2011; Fig. 1a) and the mountain regions of the Urals and Caucasus were glaciated (Astakhov, 2017; Gobejishvili et al., 2011). In addition, periglacial

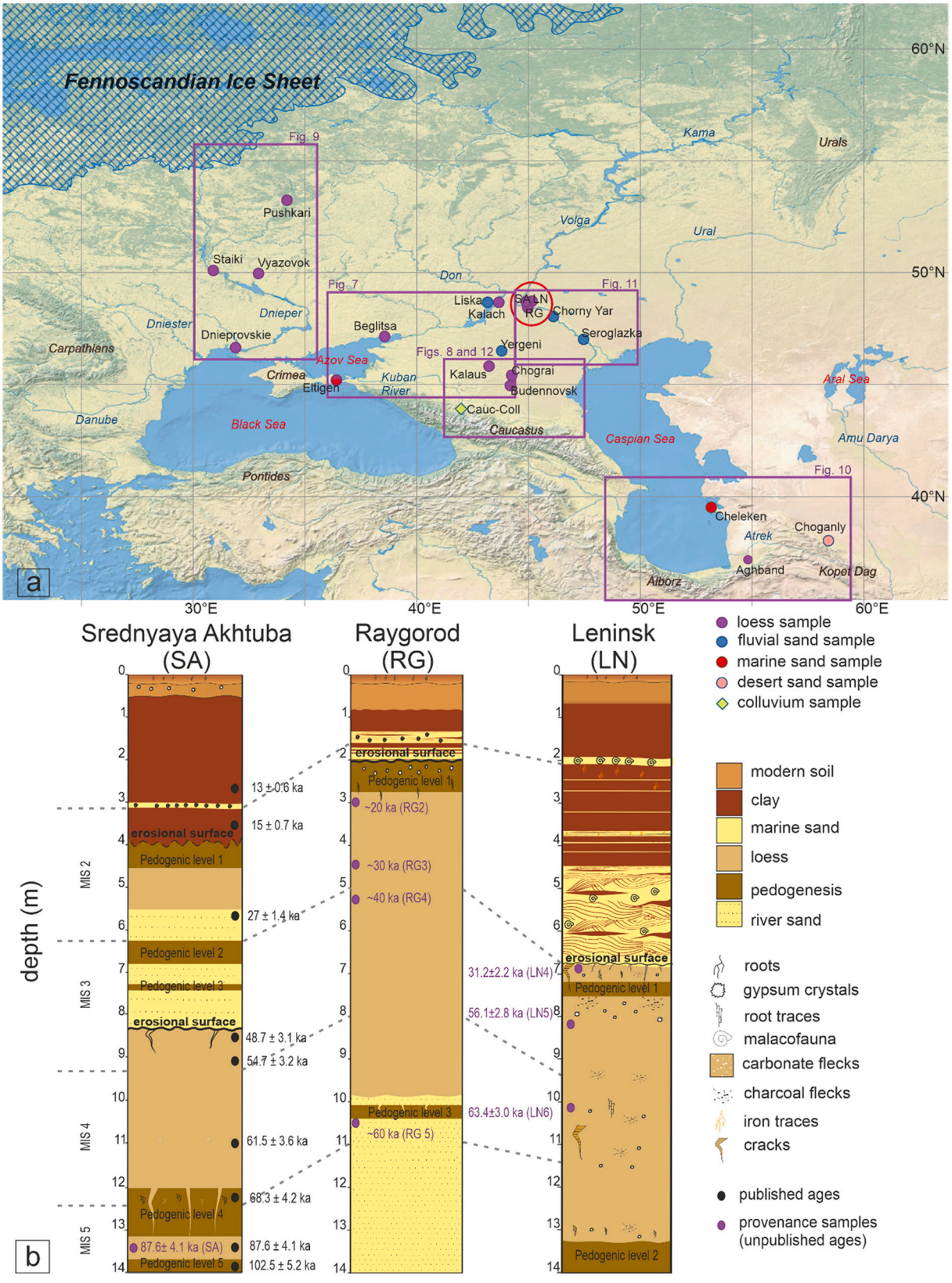

Fig. 1. (a) Map of the study area (EEP and entire Black Sea- Caspian Sea region) with the maximum extent of the Fennoscandian Ice Sheet at 18 ka after Hughes et al. (2016), and showing the sites sampled for this study. The colour coding indicates the sampled material (see legend). The Lower Volga sites shown in Fig. 1b with stratigraphy are marked by the red circle. The purple squares indicate the map details of Figs. 7, 8, 9, 10, 11 and 12. (b) Stratigraphic charts of the three Lower Volga sites, showing the sampling depths and age of the provenance samples (after Költringer et al., 2020). The denoted published ages for SA are optically stimulated luminescence (OSL) ages from Yanina et al. (2017) and Kurbanov et al. (2020), while the ages of the provenance samples are currently unpublished. (For interpretation of the references to colour in this figure legend, the reader is referred to the web version of this article.)

influence reached into the lowlands and far south, almost to the shores of the Black Sea and Caspian Sea (e.g. Goretskiy, 1958; Taratunina et al., 2020; Velichko et al., 2006). The climate in the EEP was overall cold and dry, while precipitation appears to have increased slightly during interstadials (e.g. Dodonov et al., 2006; Liang et al., 2016; Költringer et al., 2020). Generally, precipitation decreased from north to south over the EEP in the Pleistocene (e.g. Buggle et al., 2009), similar to the pattern observed today, with the northern part being dominated by periglacial forest-steppe landscape (Novenko, 2006). At present, the coastal area in the east and north of the Black Sea, around the Azov Sea, as well as the Northern Caspian lowland, is characterized by a dry to temperate continental climate (~300–500 mm a^{-1} mean annual precipitation) and varying types of steppe vegetation (e.g. Sirotenko and Abashina, 1992; Kosarev et al., 2007; Buggle et al., 2009). It is suggested that similar conditions prevailed during the Late Pleistocene in this southern part of the EEP, but were potentially drier, favoring dust entrainment from alluvial, glaciofluvial and coastal sediments by regional and local wind systems and subsequent nearby deposition as loess (Költringer et al., 2020, 2021).

In contrast to the tectonically stable EEP, the South Caspian Basin and its surroundings (Fig. 2) represent a tectonically active region throughout the entire Quaternary, comprising collision and subduction of different tectonic units (e.g. Motavalli-Anbaran et al., 2011). In the southeast of the Caspian Sea in the northeastern foothills of the Alborz mountains and the extensive upland area along the Iranian-Turkmen boarder (Iranian Loess Plateau; Fig. 1.), Pleistocene climate reconstructions suggest a semiarid to subhumid climate, with a strong precipitation gradient from north to south and also from east to west (200–700 mm a^{-1}), and generally poor vegetation cover, similar to today (e.g. Khormali et al., 2020). The Iranian Loess Plateau is located in the semi-arid region of North Iran, where up to >60 m thick loess deposits are preserved. Climatic cyclicity reflecting Pleistocene glacial and interglacial stages in the southern Caspian Sea region seems to broadly overlap with that of the EEP (e.g. Kehl et al., 2021).

Five major river systems drain into the area of the northern Black Sea- Caspian Sea region at present, representing a wide range of possible pathways for sediment to enter the region. From east to west these rivers are: the Volga, the Don, the Dnieper, the Dniester and the Danube; the former four draining generally southwards from the EEP and the latter draining eastwards from the Alps via the Carpathians and Carpathian-Pannonian Basin (Fig. 1a). These and other river sediments likely reflect the geological and environmental situation of their drainage basins and can give information about changes in drainage systems and sediment supply, as well as responses to tectonic or climatic events (e.g. orogeny, glaciation) (Richards, 2002). During the cold Pleistocene phases, all of these river systems were affected by continental or mountain glaciation, with glacial meltwater having an important control on the hydrography and sediment transport of fluvial systems (e.g. Vandenberghe, 1995; Vandenberghe and Woo, 2002). Provenance studies of sediments from rivers from the EEP as well as from the Danube and its tributaries suggest that these sediments generally reflect the exposed geology of the rivers' drainage basins (e.g. Allen et al., 2006; Safonova et al., 2010; Wang et al., 2011; Ujvári et al., 2012; Ducea et al., 2018).

The EEP is geologically comprised of the East European Craton (EEC), which consists of three Late Archean to Early Proterozoic cratonic blocks: Fennoscandia, Sarmatia and Volgo-Uralia (Fig. 2, Bogdanova, 1993). The drainage basins of the Volga (1.4 million km^2), Don (0.42 million km^2) and Dnieper (0.53 million km^2) neighbour each other and cover a large part of the EEP (Safonova et al., 2010). The Volga drains into the North Caspian Sea and its catchment is bordered by the Urals to the east, where its largest tributary, the Kama River, originates (e.g. Golsovo and Belyaev, n.d.). In addition to this Volga input, the Caspian Sea Basin receives significant discharge from the Ural River in the north,

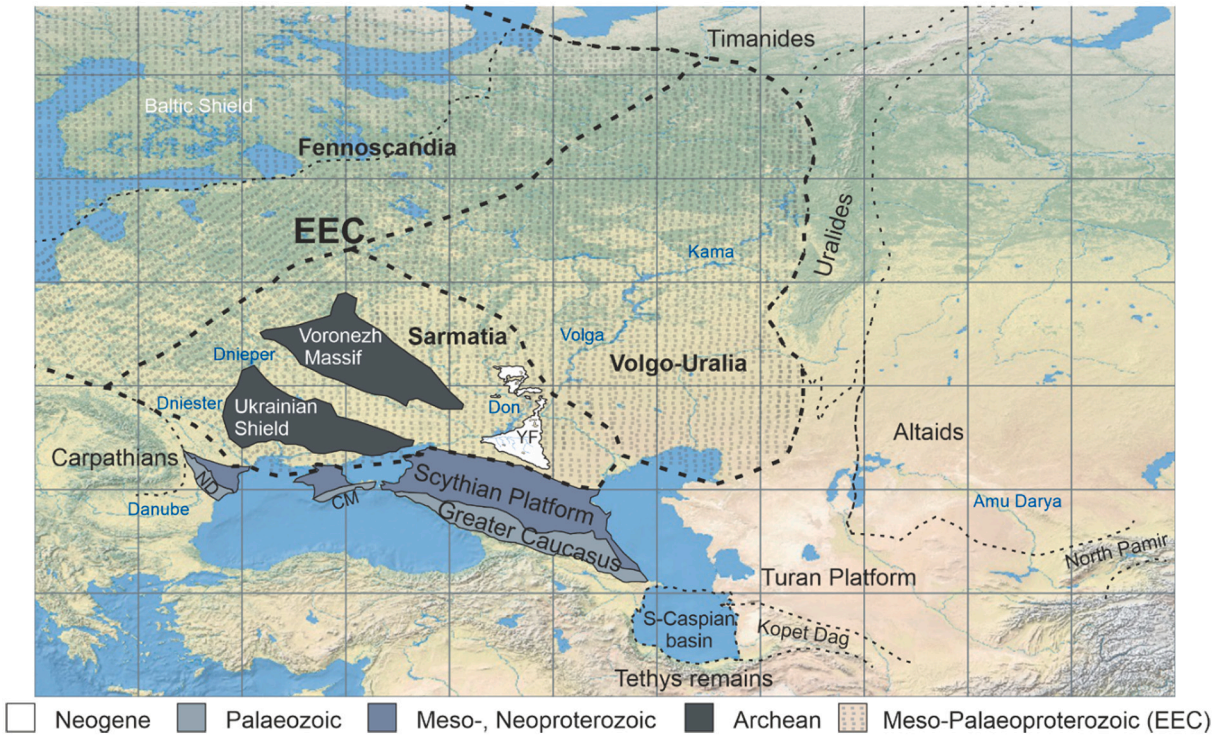

Fig. 2. Selected crustal units and sedimentary formations that are potential primary source regions for sediments in the EEP and the Black Sea- Caspian Sea. For simplicity, the figure only shows units and formations that are most relevant for discussion of EEP sediment sources (for more information see Discussion). The shaded areas denote certain crustal segments or sedimentary formations of the same age. Note that no Archean crust currently crops out in the EEC blocks of Fennoscandia and Volgo-Uralia in the EEP, only in Sarmatia. The Neogene sedimentary Yergeni Formation (analysed in this study) covers the Sarmatian block in the Yergeni uplands and Volga uplands. Also note how the north of the Black Sea is geologically comprised of one Palaeozoic girdle (orogens) and one Meso-, Neoproterozoic girdle (forelands). (ND-North Dobrogea, CM-Crimean Mountains, YF-Yergeni Formation).

the Atrek River in the southeast, and the Samur, Terek and Kura rivers from the Caucasus (Fig. 1). Also, the Palaeo-Amu-Darya River used to drain into the South Caspian over the Uzboy Passage until the Mid Holocene (e.g. Hinds et al., 2004). The Don River flows into the Azov Sea near the city Rostov-on-Don and its catchment area includes the Yergeni uplands as well as part of the Greater Caucasus, which borders its basin in the south. Both the Pleistocene Palaeo-Don as well as the modern Don deeply incise into the Yergeni Formation, named after the Yergeni River, which existed from the Late Miocene to the Early Pliocene and deposited fluvial sediments in the Yergeni uplands (hilly landscape triangularly bordered by Don, Volga and Manych depression) and the Volga uplands north of Volgograd (Karandeeva, 1957, Fig. 2). By contrast, the Dnieper River drains the west of the EEP and parts of the Carpathian foreland (72.1 thousand km^2), and flows into the northwestern corner of the Black Sea, which is comprised of a wide continental shelf with a shallow water depth of ~20 m (e.g. Lericolais et al., 2007). The Danube River also flows into the northwestern corner of the Black Sea, but drains a more extensive area of the Alpine-Carpathian-Dinaric system in central Europe (0.8 million km^2). As such, the rivers draining to the Caspian Sea and Black Sea have a range of source areas from multiple mountain ranges to the west, north and south.

In addition to the fluvial sediments deposited by these rivers, the Black Sea and Caspian Sea area is covered by extensive marine sedimentary deposits associated with past high stands. Marine deposits yield information about the recycling and intermixing of different sediment sources and the influence of sea level oscillation and base level change on sediment supply (e.g. Bridge and Demicco, 2008). Both the Black Sea and the Caspian Sea experienced several phases of transgression and regression, mainly controlled by hydrological changes in their watersheds and global ice volume changes (e.g. Deuser, 1972; Yanko-Hombach and Kislov, 2018). Moreover, the Black Sea sea-level fluctuations are linked to temporary connections during the Quaternary with the Mediterranean Sea through the shallow Bosporus Strait, and with the Caspian Sea through the Manych depression, implying forced water intrusion from the Caspian Sea (e.g. Mangerud et al., 2001; Leonov et al., 2002; Badertscher et al., 2011; Krijgsman et al., 2019; Yanina, 2020; Kurbanov et al., 2018). The Pleistocene glaciations also play a role for these local sea level histories via direct climate forcing or control of river discharges (e.g. Karpychev, 1993; Rychagov, 1997; Badertscher et al., 2011). As a result of these large sea level fluctuations, vast areas of dry continental shelf are today covered by marine terraces, particularly in the flat Northern Caspian lowland (Yanina, 2014).

Aeolian sediments in the form of loess and sands are also extensively represented in the Black Sea - Caspian Sea region (e.g. Panaiotu et al., 2001; Gendler et al., 2006; Buggle et al., 2008; Költringer et al., 2020; Velichko et al., 2009; Zubakov, 1988; Nawrocki et al., 2018; Pańczyk et al., 2020; Khormali and Kehl, 2011a). While deposits in central and eastern Europe are comparably well studied, loess in the southern EEP in southern Russia is less understood and is important in developing a wider understanding of aeolian dust and Eurasian continental atmospheric circulation history. Despite their importance, located towards the middle of the vast Eurasian loess belt, very little is known about the nature, source, transport and accumulation of these Late Pleistocene dust deposits, as well as their importance for understanding Eurasian paleoclimate (Költringer et al., 2020).

The control of the big rivers of the EEP on the Black Sea and Caspian Sea levels has been extensively discussed (e.g. Kvasov, 1979; Grosswald, 1998; Mangerud et al., 2001; Panin et al., 2020). While the focus has mostly been on the influence of rivers on the seas' water budgets, the supply and distribution of sediment in sea basins is also expected to be directly affected by river dynamics and sea level changes (e.g. Tudryn et al., 2016). However, it is not only the marine sediments that are likely to reflect a connection with rivers. As mentioned earlier, loess deposits also often show close linkages to fluvial systems at different scales (Smalley et al., 2009), and such relationships have been demonstrated for loess deposits located in various places, including the Danube Basin, Ukrainian and Polish, and Chinese Loess Plateau loess (e.g. Ujvári et al., 2012; Stevens et al., 2013; Nie et al., 2015; Pańczyk et al., 2020; Baykal et al., 2021). In this river-loess model, loess is transported only a short distance by wind from relatively close by (10s to 100s of kms) deflation zones and the importance of rivers lies in the wider distribution of the material prior to aeolian transport, potentially over thousands of kms from source regions.

The potential role of the large EEP rivers in carrying large amounts of silt particles from glacial outwash of the Fennoscandian Ice Sheet to the southern EEP has been discussed previously (Jefferson et al., 2003; Buggle et al., 2008; Smalley et al., 2009) and Pańczyk et al. (2020) reinforced this connection in their detrital zircon provenance study. Comparable to North American loess, east Ukrainian loess represents a classical 'glacial loess system', in which the material produced by northern continental glaciation is transported to the south via big rivers. Similar is expected for south Russian loess. Indeed, glaciofluvial sediments may have been more or less continuously deposited in the southern EEP since the Early Pleistocene (Gozhik, 1995) and recent scanning electron microscope analyses suggest glacial grinding and river transport for Lower Volga loess (Költringer et al., 2021). Further west, in southern Poland, Baykal et al. (2021) showed a complex history of sediment reworking from both ice sheet and mountain sources before loess deposition. Although untested, this scenario possibly explains also the western and southern Russian loess deposits. Loess in the Danube and Carpathian basins, in contrast, shows a provenance connection to rivers from mountain regions only (Ujvári et al., 2012; Pańczyk et al., 2020).

Considering this, the actual picture of loess formation in the EEP might be complex. Not all SW-Russian loess deposits are necessarily sourced from the large EEP rivers, and instead the Caucasus Mountains might also function as a source area (Sergeev et al., 1986), especially if Caucasus detritus forms a significant component of Don sediments entering the Black Sea. The proximity of abundant marine sediment deposits from Caspian Sea and Black Sea shelfs, dry during parts of the last glaciation, further complicates the situation. These deposits of complex sediment source could represent potential loess sources too. In addition, loose sediment products of non-glacial erosion in the active tectonic region around the South Caspian Basin as well as the deserts to the east of the Caspian Sea cannot be ruled out as source areas for loess deposits around the Caspian Sea, via direct aeolian transport. This diversity in topography and depositional environments implies the possibility of the three major possible modes of loess genesis operating in the region: the continental glacier provenance-river transport mode, the mountain provenance-river transport mode, and the mountain provenance-river transport-desert transition mode (Li et al., 2020). In tectonically active regions, non-glacial erosion and material formation might play a role in these mountain provenance modes. Thus, the EEP - Black Sea - Caspian Sea area represents an ideal place to examine wider scale controls on dust generation, transport and deposition of loess, and to constrain continental scale spatial changes in dust pathways and sources.

3. Sampling and analytical methods

The aim of sample collection was to obtain a wide range of Quaternary sediments of diverse origin, which reflect the past climate and landscape evolution of the EEP and southern Caspian-Black Sea region. We also sample to specifically examine in more detail the temporal and spatial variability of Lower Volga loess (LVL; Fig. 1). Two loess sites along the lower branch of the Volga River in the Northern Caspian lowland in Southern Russia, Leninsk (LN) and Raygorod (RG) (Table 1), were sampled at different stratigraphic depths for temporal provenance variability analysis. Bulk samples of 1–2 kg were taken from optically stimulated luminescence (OSL) dated loess layers: RG2 (~20 ka), RG3 (~30 ka), RG4 (~40 ka); LN4 (31.2 ± 2.2 ka), LN5 (56.1 ± 2.8 ka), LN6 (63.4 ± 3.0 ka) (unpublished ages; Kurbanov et al., 2020, contains

Table 1
Detrital zircon samples and data considered in this study, their sampling location, lithology and age.

Area	Section/ formation	Location		Material	Age	Analysed zircons (n)	Reference
		N	E				
Lower Volga	Leninsk (LN)	48.7221	45.1595	Loess	65–30 ka	865	This study
Lower Volga	Raygorod (RG)	48.4313	44.9665	Loess	~40–20 ka	865	This study
Lower Volga	Srednyaya Akhtuba (SA)	48.7004	44.8937	Loess	87.6 ± 4.1 ka	299	This study
Don	Kalach	48.6648	43.6725	Loess	Unknown Quaternary	291	This study
NE-Azov Sea	Beglitsa	47.1391	38.5611	Loess	30–25 ka	142	This study
E-Crimea	Eltigen	45.1854	36.4049	Loess	60–50 ka	222	This study
SW-EEP	Pushkari	53.2351	34.1927	Loess	MIS 3	78	This study
Manych depression	Kalaus	45.8099	43.2314	Loess	MIS 3–2	287	This study
Manych depression	Chograi	45.4054	44.2456	Loess	MIS 4–3	62	This study
N-Caucasus foothill	Budennovsk	44.9458	44.1828	Loess	MIS 3–2	279	This study
Iranian Loess Plateau	Aghband	37.3701	55.0903	Loess	58–68 ka	257	This study
Lower Volga	Raygorod	48.4313	44.9665	Volga sand	~60 ka	298	This study
Lower Volga	Chorny Yar	48.0320	46.1119	Volga sand	~150–130 ka	300	This study
Lower Volga	Seroglazka	47.0135	47.4599	Volga sand	100–85 ka	304	This study
Don	Liska	48.6701	43.1693	Don alluvium	MIS 4–3	300	This study
Yergeni uplands	no described section	46.4962	43.79947	Yergeni sand	Pliocene	295	This study
East Crimea	Eltigen	45.1854	36.4049	Black Sea sand	~110 ka	244	This study
Turkmen Coast	Cheleken	39.5274	53.1735	Caspian sand	~10 ka	275	This study
Karakum desert	Choganly	38.0337	58.41192	Desert dune sand	Holocene	195	This study
Caucasus	no described section	44.11211	41.8136	Mountain colluvium	Modern	293	This study
SW-EEP	Staiki	50.0937	30.8983	Loess	MIS 2	156	Pańczyk et al., 2020
SW-EEP	Vyazovok	49.9611	32.9215	Loess	MIS 12–2	212	Pańczyk et al., 2020
SW-EEP	Dnieprovskie	46.6435	31.8938	Loess	MIS 6	51	Pańczyk et al., 2020
Black Sea	Dnieper mouth	–		Fluvial sand	Modern	129	Wang et al., 2011
Azov Sea	Don mouth	–		Fluvial sand	Modern	149	Wang et al., 2011
Lower Volga	Volga Volgograd	–		Fluvial sand	Modern	100	Wang et al., 2011
Lower Volga	Chorny Yar	48.03201	46.1119	Fluvial sand	Modern	53	Allen et al., 2006
W-Black Sea	Siret mouth	45.2306	28.00419	Fluvial sand	Modern	110	Ducea et al., 2018
W-Black Sea	N-Dobrogea cumulative	–		Diverse	Neoproterozoic-Palaeozoic	1056	Balintoni and Balica (2016)
Alborz Mountains	cumulative	35.9658	52.5425	Sandstone	Neoproterozoic-Cenozoic	442	Horton et al., 2008
Aspheron Peninsula	Casp. Prod. series	40.4406	50.0715	Sandstone	Late Miocene	219	Allen et al., 2006
Greater Caucasus	Bajocian	41.0321	48.3481	Sandstone	Middle Jurassic	60	Allen et al., 2006
N-Caucasus foreland	Indolo-Kuban	45.4	40.5	Sandstone	Pliocene-Quaternary	65	Vincent et al., 2013
E-Black Sea	Taman	45.1847	36.5999	Sandstone	Pliocene-Quaternary	66	Vincent et al., 2013

limited published ages for these sections). In addition, Lower Volga loess was sampled from one OSL dated layer at Srednyaya Akhtuba (SA, 87.6 ± 4.1 ka) (Fig. 1; Yanina et al., 2017). A stratigraphic description of the three LVL sites can be found in Költringer et al. (2020), Lebedeva et al. (2018), Makeev et al. (2021) and Taratunina et al. (2020). Samples from six other Quaternary loess deposits located in the Northern Black/Azov Sea - Caspian Sea region were taken from deposits of known age wherever available for comparison and to understand wider-scale spatial variability of aeolian dust sources in the region (Table 1, Fig. 1). One loess site located in the western EEP (Pushkari) and one on the northern Iranian Loess Plateau (Aghband) were also sampled (Fig. 1, Table 1). The strategy for secondary (sedimentary) source material sampling considers the availability of material, its exposure to deflation, the geographic distance to the sink, and topographic obstacles on the way. Accordingly, we have sampled fluvial sediments from the Palaeo-Volga and Palaeo-Don rivers, marine sands from the Black Sea and Caspian Sea, as well as mountain colluvium from the northern Greater Caucasus, and desert sands from the Karakum Desert. 1–2 kg bulk samples were taken from sites at each of these locations (Table 1). Additionally, we compare our data to published U—Pb detrital zircon data from further loess sites and potential secondary and primary source areas in the region (Table 1).

Detrital zircon grains were separated from bulk material through sieving (425 μm), Wilfley table washing, Frantz magnetic separation and heavy liquid separation at Uppsala University, Sveriges Geologiska Undersökning (SGU) and the Arizona LaserChron center. To minimize the loss of very fine-grained zircons in loess due to clay coatings and their effects on hydraulic sorting, ultrasonic bathing of the samples was applied following the separation technique of Hoke et al. (2014) to disaggregate the fractions. Zircon separates were mounted on 1″ epoxy mounts and polished to 1 μm finish. High resolution backscattered electron imaging of each mounted sample was performed with a Hitachi 3400 N scanning electron microscope and further used to locate the spots for laser ablation on the zircon grains. Dependent on the zircon yield, a high analysis number (n), with ideally >300 randomly selected zircon grains of all size fractions, was pursued for each sample. This relatively new approach of high n detrital zircon analyses overcomes some limitations inherent in lower n analyses of <100–150 grains per sample. Detrital zircon provenance interpretations are often substantially based on the comparison of relative heights of age peaks in probability plots and this requires large n for statistical robustness (Pullen et al., 2014). Low n analyses (< 115 grains) also harbour the risk of missing significant age peaks entirely (Vermeesch, 2004).

U—Pb dating was carried out at the Arizona LaserChron center. Isotope ratios were measured using a Thermo Element2 high-resolution (HR) multicollector–inductively coupled plasma–mass spectrometer (MC-ICP-MS). Laser ablation was attained for 10 s at ~7 J/cm^2 (constant energy density) with a repetition rate of 7 Hz, using a 9 μm laser beam diameter for analyses (Gehrels et al., 2008; Gehrels and Pecha, 2014; Pullen et al., 2018). The minimum size for analysed zircon grains in this study is 12 μm, in contrast to >25 μm that is commonly used for other loess provenance studies, due to laser size and count number limitations.

This allows consideration of a larger range of zircon grain sizes and makes it less likely that finer zircon fractions will be missed, which might be relevant for interpretation of silt-dominated loess deposits. The following zircon standards were used as reference material for isotope fractionation correction: FC-1 (Paces and Miller, 1993), R33 (Black et al., 2003), and SL (Gehrels et al., 2008). The Nu Instrument's Nu-TRA software and an Arizona in-house Excel spreadsheet (E2agecalc) were used for data normalization and reduction, uncertainty propagation and age calculation. The ^{204}Pb measurement was used for the correction of initial Pb, assuming its composition following Stacey and Kramers (1975). To correct for ^{206}Pb/^{238}U, ^{206}Pb/^{207}Pb, and ^{208}Pb/^{232}Th fractionation and to account for instrumental drift, a sliding-window average of eight reference material analyses was applied. Measurement uncertainties for ^{206}Pb/^{238}U and ^{208}Pb/^{232}Th were attained via regression line analyses, while uncertainties for ^{206}Pb/^{207}Pb and ^{206}Pb/^{204}Pb were defined by standard deviation. Internal (measurement) uncertainties are reported at 1σ, while external (systematic) uncertainties are reported at 2σ level. Reference material FC-1 serves to estimate U and Th concentrations, which are accurate to ~20%. The age cut-off was set at 900 Ma. ^{206}Pb/^{238}U ages were used for ages <900 Ma, while for ages >900 Ma ^{206}Pb/^{207}Pb ages were used for plotting. ^{206}Pb/^{238}U age analyses with uncertainty >10% (1σ) are disregarded and for ^{206}Pb/^{207}Pb age analyses uncertainties >10% (1σ) were included only if the ^{206}Pb/^{238}U age was <400 Ma. Concordance was defined as $\frac{\left(\frac{^{206}Pb}{^{238}U}\right)}{\left(\frac{^{206}Pb}{^{207}Pb}\right)}$, and not reported for ^{206}Pb/^{238}U ages <400 Ma

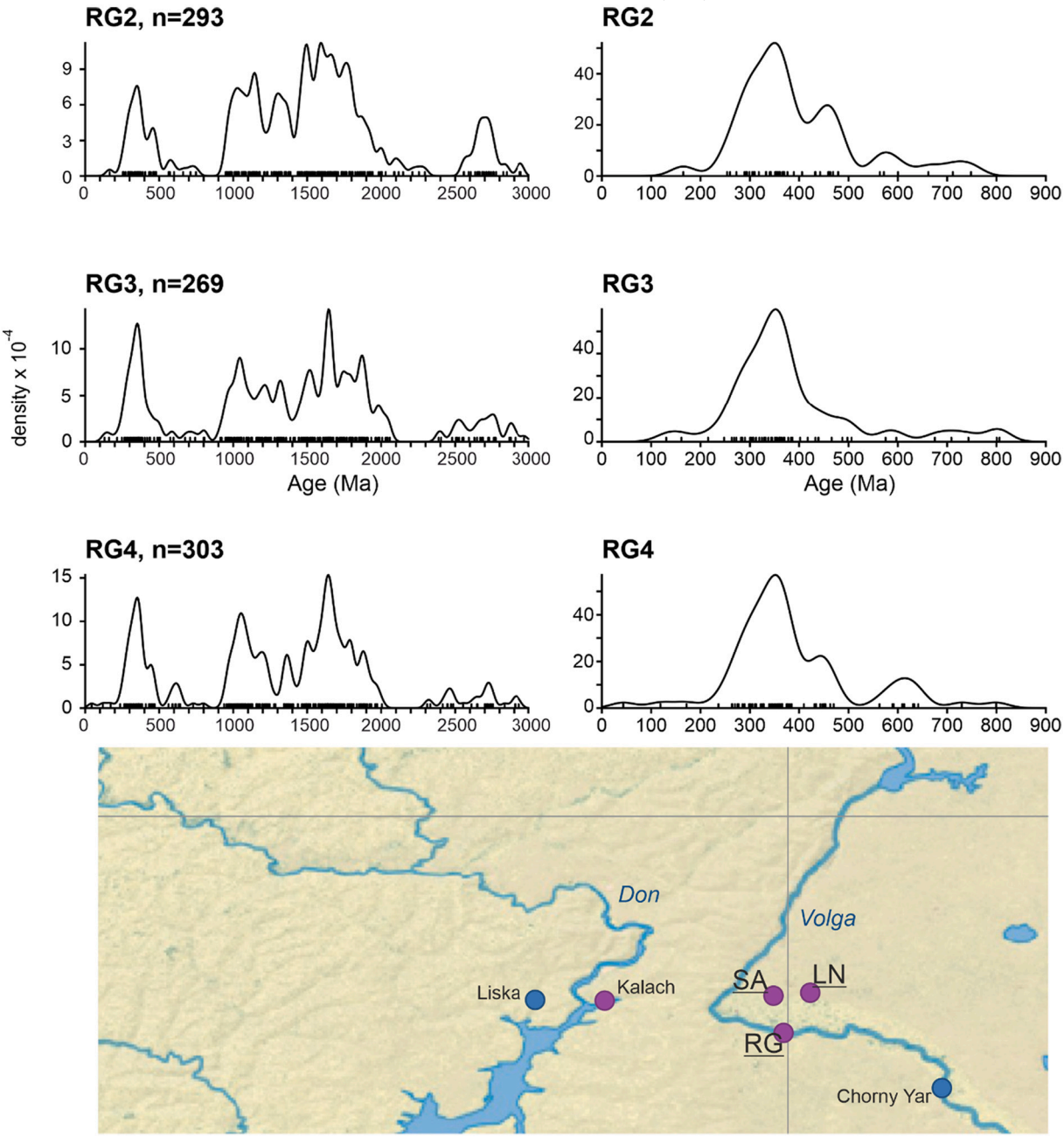

Fig. 3. KDE plots of the three Raygorod samples with RG2 being the youngest and RG4 the oldest (for age and sampling position see Fig. 1b). In the left column all zircons from age 0–3000 Ma are plotted, the right column shows zircons from age 0–900 Ma. Every dash on the x-axis represents one zircon (this way of presentation applies also for following KDE plots of samples in the "Results" section). The map detail shows the position of the three sites (underlined names) in respect to each other as well as other close-by sampling sites. See Fig. 1a for the location of the LVL sites in the EEP and for the legend.

because of the large uncertainty in $^{206}Pb/^{207}Pb$ age. Results showing >20% discordance or > 5% reverse discordance were excluded from further analyses.

All literature published U—Pb detrital zircon data, which is plotted in this study, was reprocessed according to the same criteria as far as the available data and their collection and processing routine allowed (please check the respective publications for methodological details; Table 1). The results of Kernel Density Estimation (KDE) with a fixed bandwidth of 25 Ma are plotted to display the detrital zircon age distribution for each sample (Vermeesch, 2012).

4. Results

4.1. Lower Volga loess

The three samples from Raygorod taken at different stratigraphic depths (RG2 ~ 20 ka, RG3 ~ 30 ka, RG4 ~ 40 ka, Fig. 1b) show slight differences, both in the presence of age fractions, as well as in their abundance. Mesozoic ages are very rare in all three samples ($n = 2$–4; < 2%). All samples have a distinct peak at 360 Ma. In total, the age fraction between 280 and 380 Ma makes up 12% of all measured zircons in RG4 and RG3, and 7% in RG2. Ages from 900 Ma to 2000 Ma are present in all RG samples and account for ~70–76% of measured ages each, however their distribution differs and RG2 shows less sharp individual age peaks than RG3 and RG4. RG4 contains no zircons of age 2000–2300 Ma, and in RG3 zircons of age 2050–2500 are almost absent ($n = 3$), while RG2 shows a very spread age distribution between 2000 and 2300 Ma ($n = 10$). Archean ages in RG3 and RG2 comprise ~10% of the total, while only 5% of analysed zircons in RG4 are older than 2500 Ma. In RG2 these ages are most concentrated at around 2700 Ma (Fig. 3).

The abundance of certain age fractions across the range of zircon ages differs to some extent in the three samples. However, direct comparison is complicated due to the different number of analysed zircons and it is unclear if this variation is simply a function of sampling uncertainty (Pullen et al., 2014) or rather reflects real differences in the population of grains at different sample depths. To test this, random subsamples of 300 grains each were generated from all data combined from the Raygorod site. The resulting KDEs show little variability, which appears mostly in relative peak abundance rather than in the presence or absence of relevant age fractions (Fig. 4).

The KDEs of the three loess samples of different depositional age from Leninsk (LN4 ~ 31 ka, LN5 ~ 56 ka, LN6 ~ 63 ka, Fig. 1b) all show an abundant age fraction at 360 Ma and a similar age peak distribution between 900 Ma and 2100 Ma (Fig. 5). Mesozoic ages are also rare in all the samples, although LN6 contains a higher number of Late Mesozoic ages than LN4 and LN5. The younger samples LN4 and LN5 contain Palaeoproterozoic ages of 2400–2500 Ma years but no Archean ages between 2500 and 2600 Ma, as seen in LN6. Random subsamples of 300 grains were also generated from the combined set of all analysed Leninsk ages. These Leninsk subsamples are also overall similar, showing the same general age peaks but with some differences in age peak heights (Fig. 4). The outcome of this test is discussed further below.

The single analysed Srednyaya Akhtuba sample (SA ~88 ka, Fig. 1b) contains a large age fraction at 360 Ma. No Mesozoic ages younger than Middle Triassic were measured. No ages of around 700 Ma are present, however, this fraction is also very small in the LN and RG samples (1%). The age distribution between 1000 and 2000 Ma is similar to the other Volga loess samples. Only one grain older than 2800 Ma was measured for SA (Fig. 5).

4.2. Loess from the East European Plain and the Caspian Sea region

Loess from the Kalach section on the Don River bank is of unknown Quaternary age and shows the most prominent peak in the sample at 180 Ma. Abundant peaks of similar amplitude occur also at 100 Ma and 360 Ma. Ages between 900 and 2100 Ma, as well as Archean ages, are present and similarly distributed to the ages in the Lower Volga loess (Fig. 6).

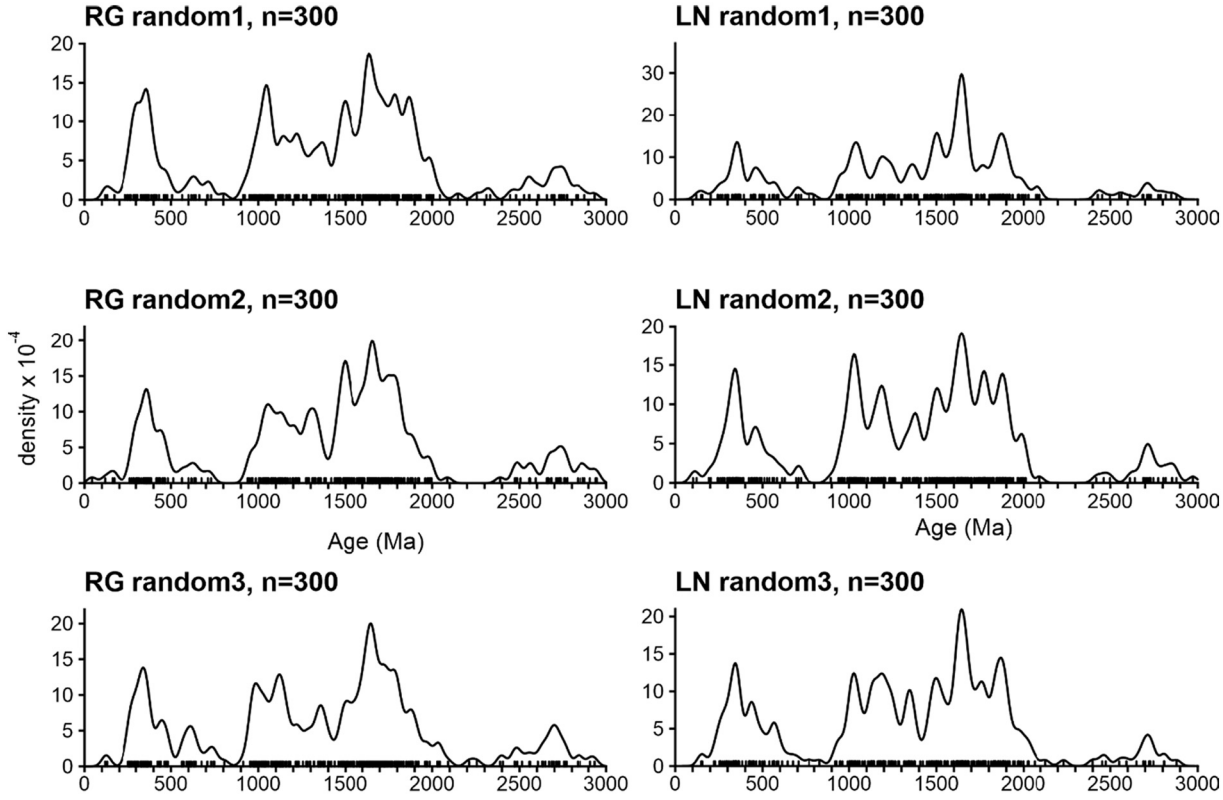

Fig. 4. KDE plots of the random $n = 300$ subsamples from the grouped Raygorod and Leninsk data.

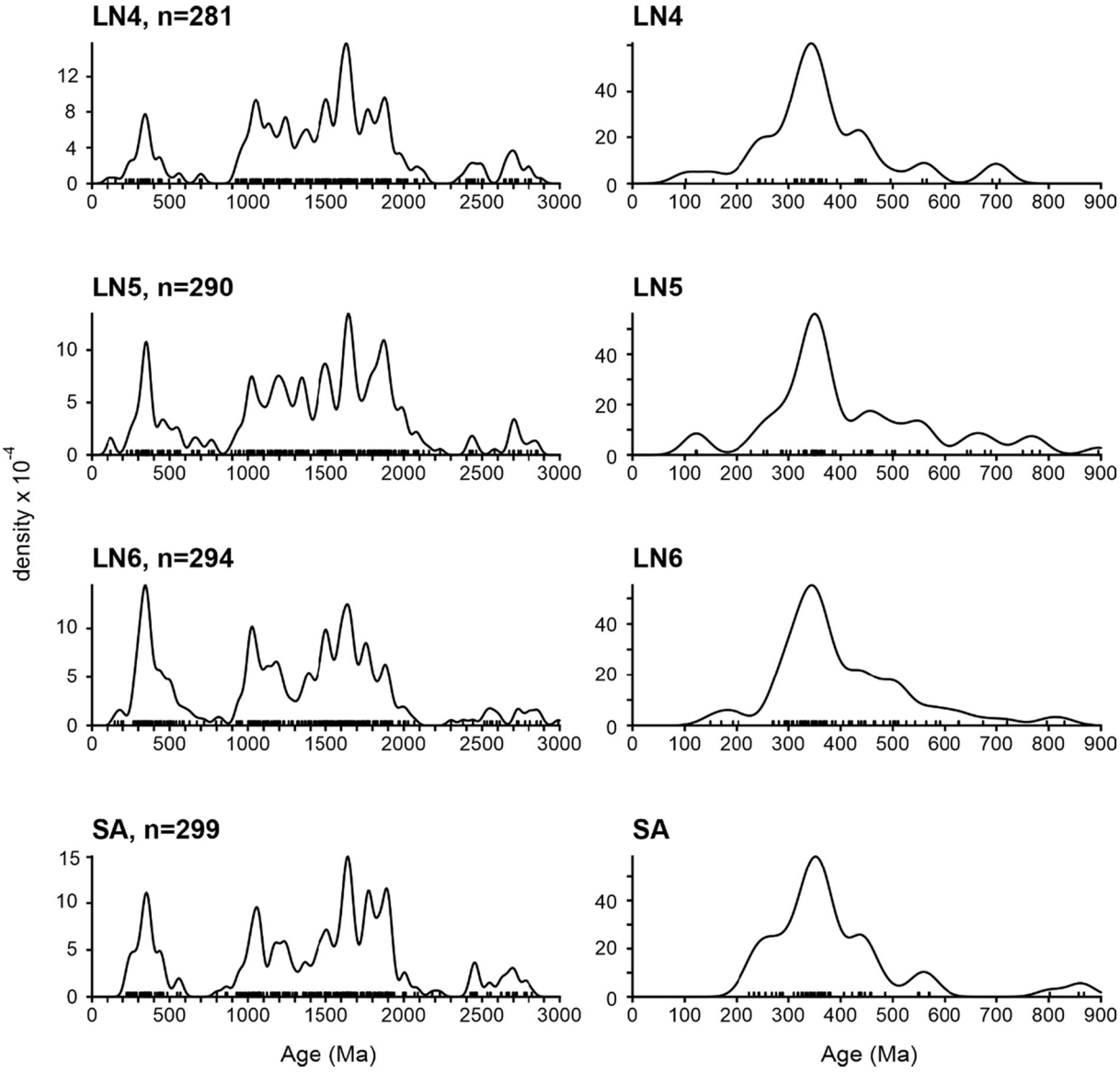

Fig. 5. KDE plots of the three Leninsk samples with LN4 being the youngest and LN6 the oldest, with the oldest LVL sample here from Srednyaya Akhtuba (SA) (see Figs. 1 and 2 for details).

Loess from the Beglitsa section at the Azov Sea (~30–25 ka; Chen et al., 2018) shows a plateau shaped zircon distribution of relatively low abundance between 250 and 450 Ma. A fraction around 300 Ma is defined by a few grains and does not stand out from the other Palaeozoic age populations, which are all defined by only a few grains each and in sum make up 8% of all analysed grains. Proterozoic ages between 1000 and 2100 Ma are present in high abundance (78%) and Early Palaeoproterozoic and Archean ages (11%) show some ages of around 2450 Ma and a broader fraction at 2700–2800 Ma of similar height to the Palaeozoic plateau of ages (Fig. 6). The loess from the Eltigen section on the Crimean Peninsula is 60–50 ka old (Kurbanov et al., 2019) and contains abundant Palaeozoic ages (17%) with a sharp peak at 315 Ma. The abundant age fractions at 450 and 530 Ma define a double peak, while several Neoproterozoic ages date to c. 600 Ma. Meso- and Palaeoproterozoic ages between 1000 and 2000 Ma show similar abundances as the Palaeozoic fractions for three peaks at 1030 Ma, 1630 Ma and 1890 Ma (Fig. 6). Few zircons are older than 2800 Ma ($n = 6$).

Loess from the Manych depression, one site located at the River Kalaus (MIS 3–2), the other section at the River Chograi (MIS 4–3), show very similar zircon age spectra. Both show a major Palaeozoic age peak at 300 Ma, younger than the Palaeozoic peak of 360 Ma that is abundant in many of the previously described samples. Another Palaeozoic peak is seen at 440 Ma. Neoproterozoic ages peak at 620 Ma. Mesoproterozoic ages form a broad peak between 950 and 1150 Ma, while older Meso- and Palaeoproterozoic ages are present in great abundance, peaking at 1480 Ma, 1640 Ma and 1775 Ma. This pattern is clearly defined by the higher-n loess sample from the Kalaus section. Archean ages show a broad double-peak at 2700 and 2800 Ma (Fig. 7). Few zircons are older than 2800 Ma. The Budennovsk section (MIS 3–2) is located proximal to the Manych sites, but in contrast to these sites, which crop out along rivers flowing through the Manych depression, the more southern Budennovsk section is located higher up on the northern foothills of the Greater Caucasus (Fig. 7). The Budennovsk loess sample also contains an abundant age fraction at 300 Ma. An age peak at 450 Ma is well defined and abundant too, while a less pronounced age fraction appears around 600 Ma. The Proterozoic and Archean ages are less frequent compared to the Palaeozoic age fractions (51% and 32%), in contrast to the Kalaus and Chograi samples (Fig. 7).

To the north of the study area, the loess sample from the Pushkari section in the west EEP (MIS 3) does not show any Palaeozoic ages

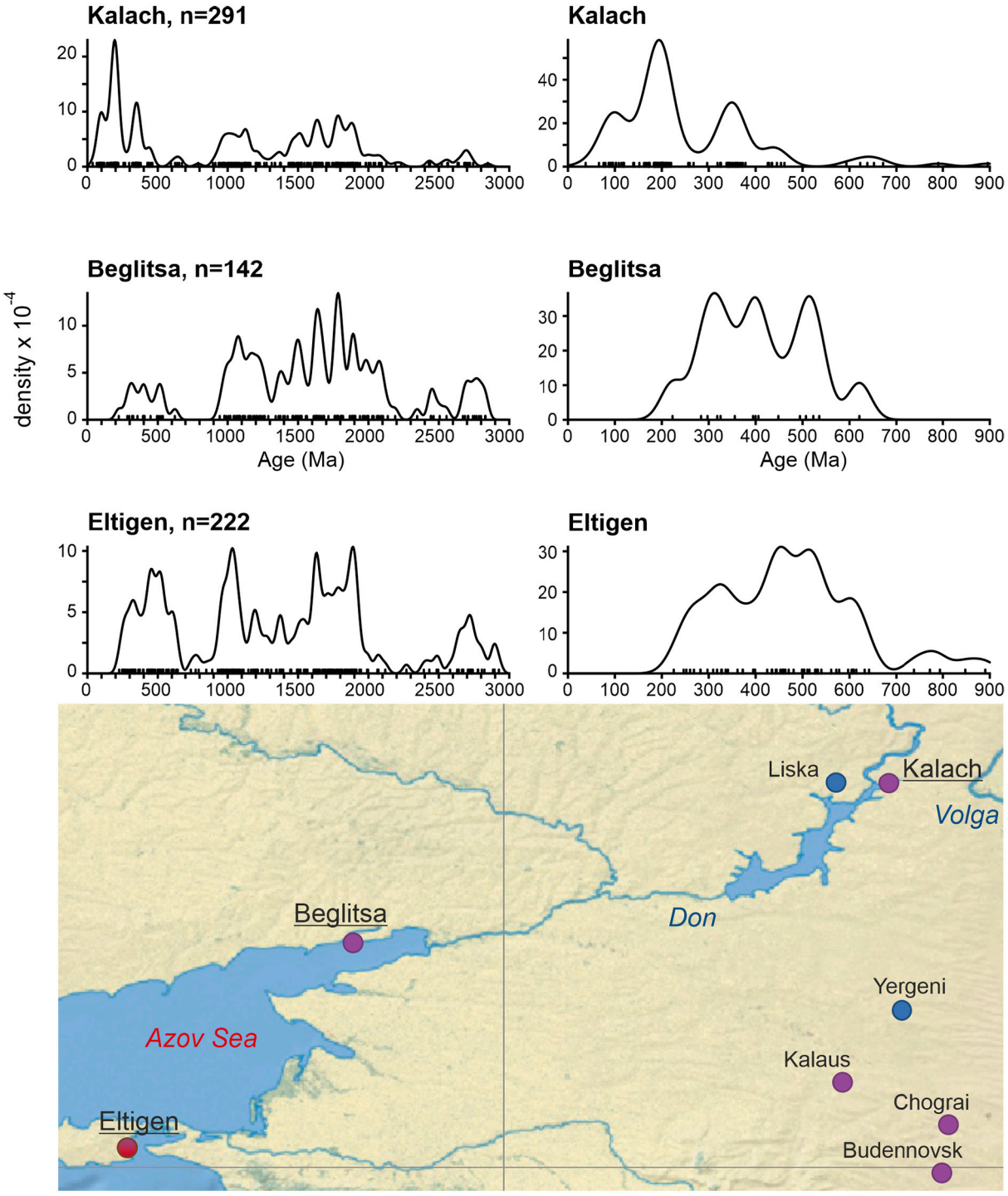

Fig. 6. KDE plots of loess from the Kalach site at the Don River, the Beglitsa site at the Azov Sea, and the Eltigen site on the Crimean Peninsula.

younger than 420 Ma. Only one grain of Neoproterozoic age is present. Meso- and Palaeoproterozoic ages are abundant, particularly between 1000 and 1300 Ma, and 1600 and 1800 Ma, defining four sharp peaks. Only four scattered Archean zircons are present (Fig. 8). By contrast, loess from two Ukrainian sections to the southwest of Pushkari (Staiki and Vyazovok) published in Pańczyk et al. (2020), show late Palaeozoic age populations at around 300 Ma and 420–440 Ma. Few early Cambrian and Neoproterozoic ages are present and scattered between 520 and 620 Ma, and Meso- and Palaeoproterozoic ages are abundant until 2000 Ma. Several Archean ages can be observed (Fig. 8). The data from another Ukrainian loess site analysed by Pańczyk et al. (2020), Dnieprovskie at the Dnieper's mouth into the Black Sea, contains abundant and comparable high peaks for the Early Palaeozoic and Late Neoproterozoic as well as for the Meso- and Palaeoproterozoic (Fig. 8).

U—Pb ages younger than 700 Ma from the Iranian loess site Aghband located on the Iranian Loess Plateau (58–68 ka, Lauer et al., 2017) are extremely abundant (49%), with major peaks at 100 Ma, 250 Ma and 300 Ma. Less abundant age fractions are present at 450 Ma and 620 Ma. Meso- and Palaeoproterozoic ages between 1100 and 1800 Ma, as well as Archean ages, are essentially absent and other Proterozoic ages are low in abundance (Fig. 9). In total 28% of all measured zircons are older than 900 Ma.

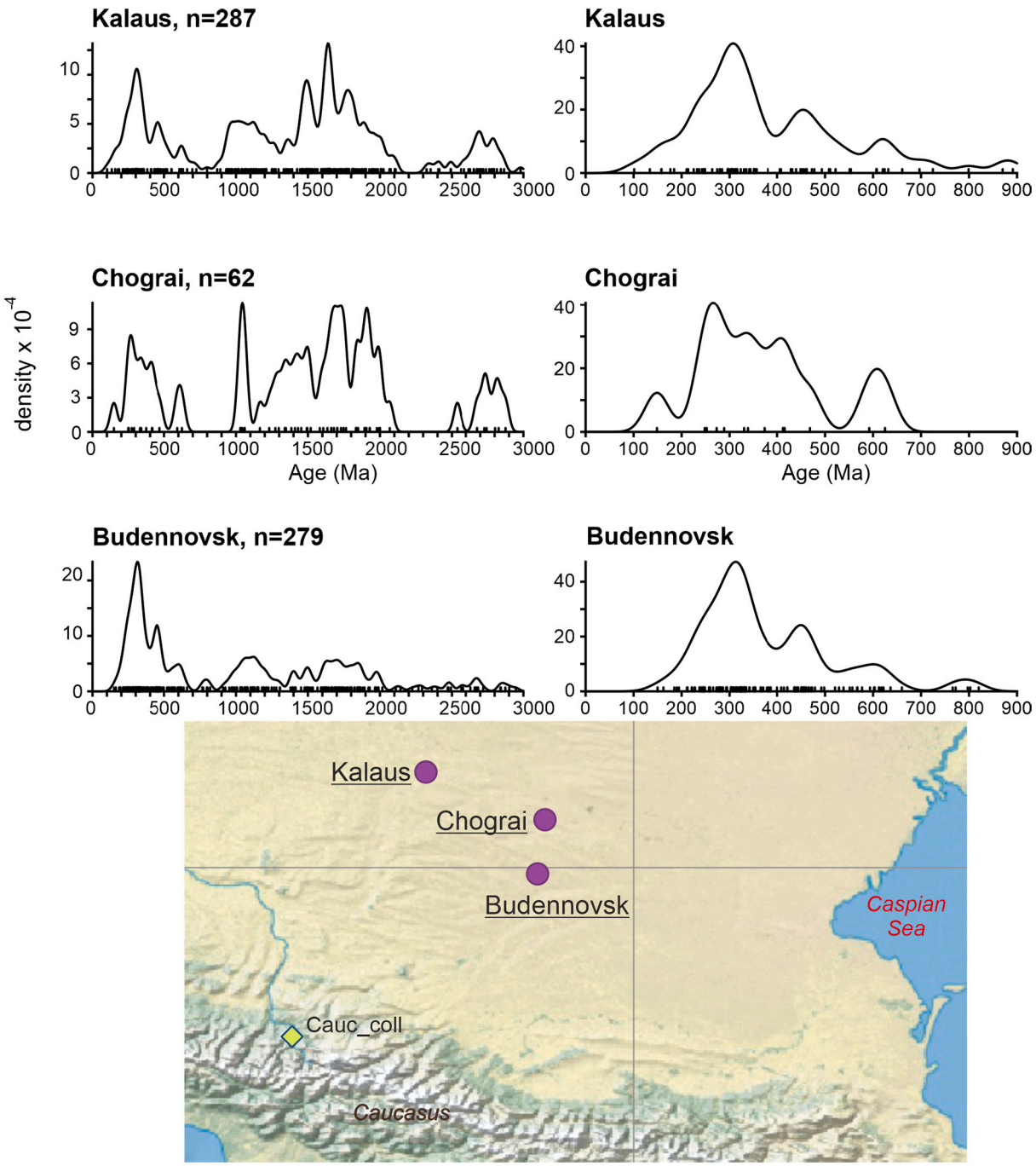

Fig. 7. KDE plots of loess from the Kalaus and Chograi sites in the Manych depression, and the Budennovsk site at the northern Caucasus foothills.

4.3. Other sedimentary material

The Pleistocene Volga River sand sample from Chorny Yar (~150–130 ka; Butuzova et al., 2019) displays a major well-defined peak at 360 Ma and less abundant age fractions of 250 Ma and 580 Ma. Mesoproterozoic ages form a broad plateau between 950 and 1200 Ma and show a peak of broadly the same height at 1480 Ma. Two isolated and well-defined Palaeoproterozoic age fractions define clear peaks at 1600 and 1780 Ma. Archean ages peak at 2700 Ma (Fig. 10). Further downstream, at the section Seroglazka (~85–100 ka; Butuzova et al., 2019; Shkatova, 2010), Volga fluvial sand shows a prominent peak at 360 Ma in its Palaeozoic age distribution. The age fractions around 250 Ma and 450 Ma are represented by fewer grains. Meso- and Palaeoproterozoic ages are generally abundant in the sample with several prominent, narrow peaks, except between 1300 and 1400 Ma, and Archean ages are distributed between 2550 and 2750 Ma (Fig. 10). Similarly, the Volga fluvial sand from Raygorod, age ~ 60 ka (RG5; Fig. 1b, Table 1), contains an abundant 360 Ma age population with a subpopulation at around 300 Ma. Only five spread out zircon ages are younger than this major Palaeozoic population, while Early Palaeozoic ages define a more abundant fraction between 400 and 500 Ma. The few Neoproterozoic ages in the sample occur between 530 and 760 Ma. Meso- and Palaeproterozoic ages, by contrast, are abundant, although again with fewer ages between 1300 and 1400 Ma. In the Archean, a clear age peak occurs at 2700 Ma (Fig. 10).

The KDE for Pleistocene age Don River sand from the Liska section shows a low abundance of ages between 200 and 900 Ma (4%). Meso- and Palaeoproterozoic ages, in contrast, are abundant with several well-

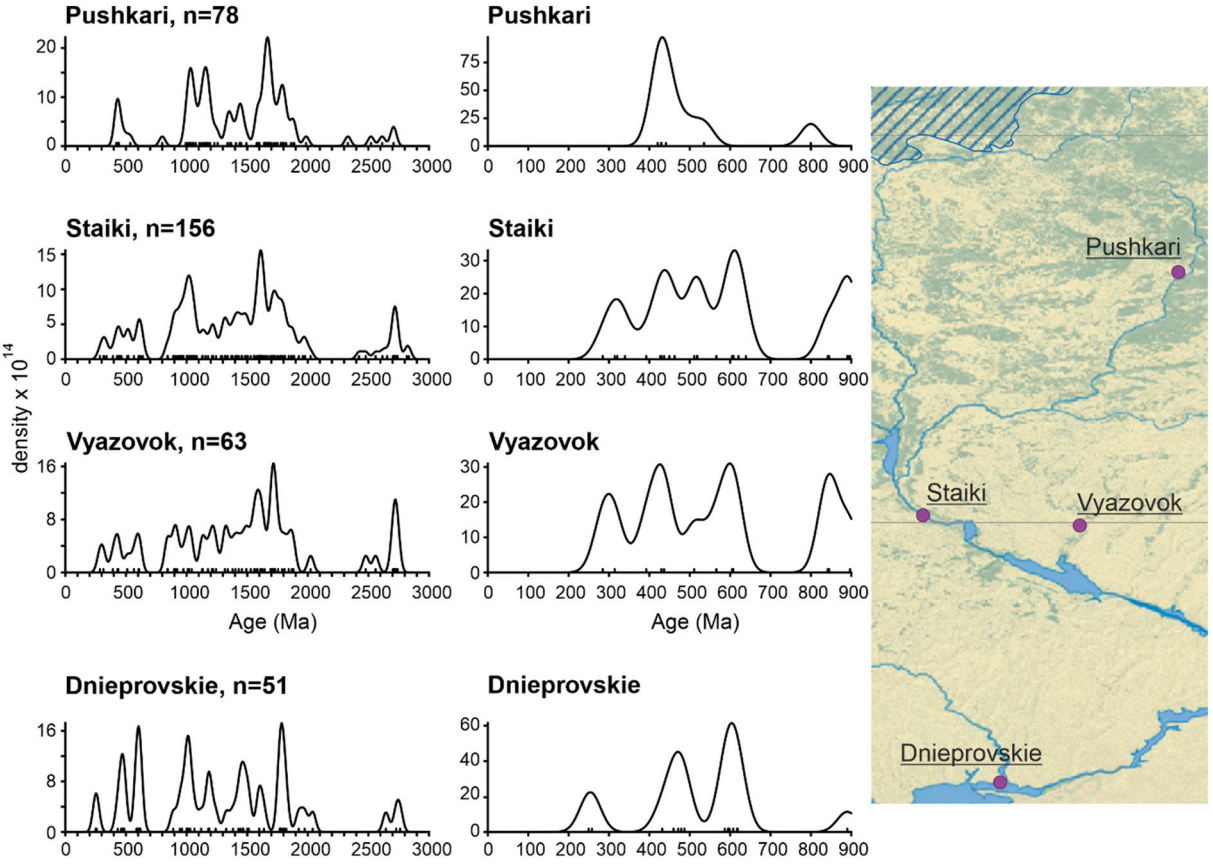

Fig. 8. KDE plots of loess from the Pushkari site on the west Russian EEP (this study), and the Staiki, Vyazovok and Dnieprovskie sites from the Ukrainian EEP (data from Pańczyk et al., 2020).

defined single peaks (87%). Archean ages form a broad peak between 2650 and 2850 Ma (Fig. 11). By contrast, the Yergeni sand sample from the Pliocene age Yergeni formation in the Yergeni uplands shows more Palaeozoic ages (8%): a clearly defined but low peak at 360 Ma, and a subpeak at 440 Ma. Neoproterozoic ages are concentrated in the Late Neoproterozoic with no zircons dating to 700–900 Ma. Mesoproterozoic ages are abundant, especially between 1000 and 1150 Ma, defining one major peak and an older subpeak. Palaeoproterozoic ages form two broader age fractions with double-peaks each, at 1500–1700 Ma and 1800–1900 Ma. While Archean ages are well presented (7%), only four zircons are older than 2800 Ma (Fig. 11). Black Sea sand from the Crimean Eltigen section (~110 ka; Kurbanov et al., 2019) is directly overlain by a sequence of loess, from which the Eltigen loess sample for this study derives. The Black Sea sand sample contains only few, greatly spread out Palaeozoic ages (<5%) in contrast to the overlying loess (Fig. 6). Meso- and Palaeoproterozoic ages are very abundant by contrast (75%), with a broader trough between 1200 and 1400 Ma and an almost total absence of Palaeoproterozoic grains older than 2080 Ma. Archean ages are divided into two fractions: one between 2500 and 2700 Ma and another with ages of around 2800 Ma and older (Fig. 11). Local colluvium from the northern Greater Caucasus of modern depositional age shows quite different peaks, including a very abundant age peak at 280 Ma. Two smaller age fractions peak at 450 Ma and at 600–650 Ma. The abundance of Meso- and Palaeoproterozoic and Archean ages is very low (33%) in comparison to the Palaeozoic and Neoproterozoic ones (50%) (Fig. 11).

The Caspian marine sands from the Turkmen Cheleken Peninsula (~10 ka; Kurbanov et al., 2014) show a high number of Palaeozoic and Mesozoic ages (59%). Major peaks are present at 300 Ma and 450 Ma, and a smaller but well-defined fraction also exists for the Cretaceous at 100 Ma. Neoproterozoic ages peak at around 600 Ma, while older Proterozoic ages are almost absent, except for at around 1880 Ma. Archean ages are spread out but with no grains older than 2700 Ma (Fig. 9). By contrast, the KDE of the modern Karakum Desert sands at Choganly shows a high abundance of young ages <300 Ma (29%). The large age peaks are defined by the Mesozoic fractions at c. 100 Ma and most abundant at around 200 Ma. Palaeozoic age peaks are well-defined at 300 and 450 Ma (18%). Less abundant is the Precambrian population at around 600 Ma (8%). Meso- and Palaeoproterozoic ages are comparably rare (38%), although a group of ages at 1880 Ma is abundant (Fig. 9).

In addition to our own data, we plot relevant published data from the literature for comparison (Table 1, Fig. 12). Samples from modern Volga alluvium (data from Allen et al., 2006; Wang et al., 2011) show one single large Palaeozoic peak at 360 Ma (31%) and abundant but relatively smaller Meso- and Palaeoproterozoic age fractions between 1000 and 2000 Ma (60%). Archean ages are present with 10% (Fig. 12). By contrast, the modern Don sand sample from Wang et al. (2011) contains only few grains of Palaeozoic ages (6%), whereas the Meso- and Palaeoproterozoic fractions are abundant (82%). Archean ages are concentrated at around 2750 Ma and grains older than 2800 Ma are present ($n = 2$) (Fig. 12). The modern Dnieper sample (Wang et al., 2011) contains more Palaeozoic and Late Proterozoic ages than the Don sample (13%). These peaks are, however, less significant than the abundant Meso- and Palaeoproterozoic fractions between 1000 and 2000 Ma (82%). Archean ages are almost absent ($n = 3$) (Fig. 12). The detrital zircon U—Pb age patterns of four sandstone samples from the Pliocene Caspian Productive series (Kirmaky Suite and Balakhany Suite) sampled on the Apsheron Peninsula are separately plotted and discussed in Allen et al. (2006), who point out the great similarity of these Caspian Productive series subsamples. As combined sample here, they show a large Palaeozoic age fraction, abundant Meso- and Palaeoproterozoic ages, and several

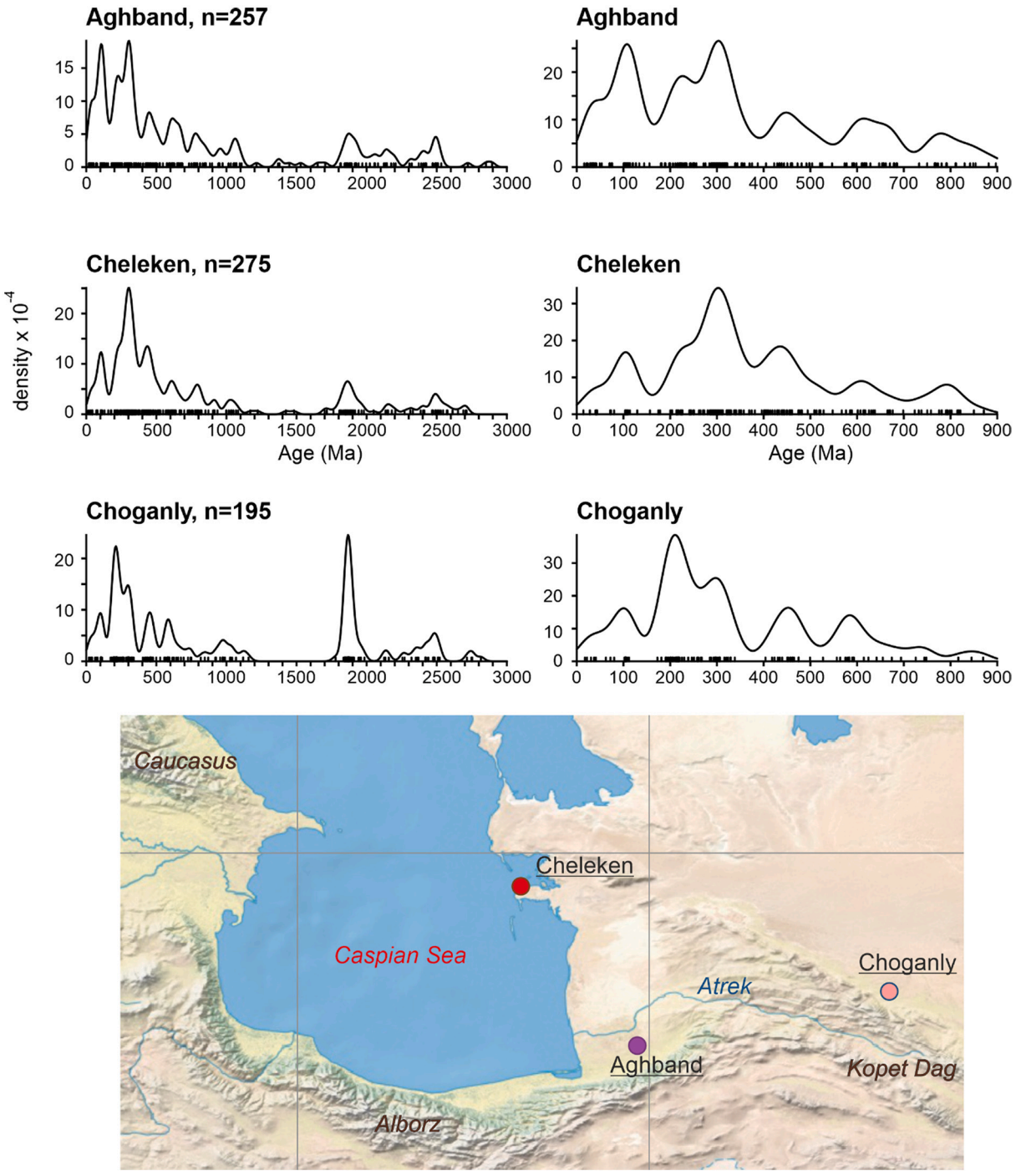

Fig. 9. KDE plots of loess from the Aghband site on the north Iranian Loess Plateau as well as of marine Caspian sand from the Cheleken Peninsula and desert sand from the Karakum Desert, Choganly site. (For interpretation of the references to colour in this figure legend, the reader is referred to the web version of this article.)

zircons of Archean age (Fig. 12; Table 2). Detrital zircons from Pliocene-Quaternary sedimentary rocks from the Taman Peninsula (sample ILN#13_700) and from the Indolo-Kuban Basin at the foothills of the Greater Caucasus (sample WC139/1, Table 1) are discussed in Vincent et al. (2013). Both samples contain several Palaeozoic ages, which are mostly concentrated around 250 Ma, and also show abundant Meso- and Palaeoproterozoic populations in their age distributions. Archean ages are scarce and most abundant at around 2600 Ma (Fig. 12). Allen et al. (2006) also analysed a Middle Jurassic sandstone sample from the eastern Greater Caucasus (Bajocian sandstone), which shows mostly Phanerozoic zircons in its low-n analysis (n = 60). The largest age fraction peaks at 240–320 Ma while ages older than 500 Ma are almost entirely missing (Fig. 12).

A distribution of zircons mostly younger than 1000 Ma can be seen for the detrital zircon data from different Neoproterozoic to Cenozoic sandstone formations from the western and eastern Alborz mountains, which are taken from Horton et al. (2008). Here, the individual low-n samples (between 9 and 59 grains each) are grouped into one Alborz sample in order to depict the detrital age distribution of the entire orogen in one plot and to allow a more meaningful comparison with other high-n data in this study. The KDE shows the largest peak at around 600 Ma and the second highest at 360 Ma (Fig. 12). A very

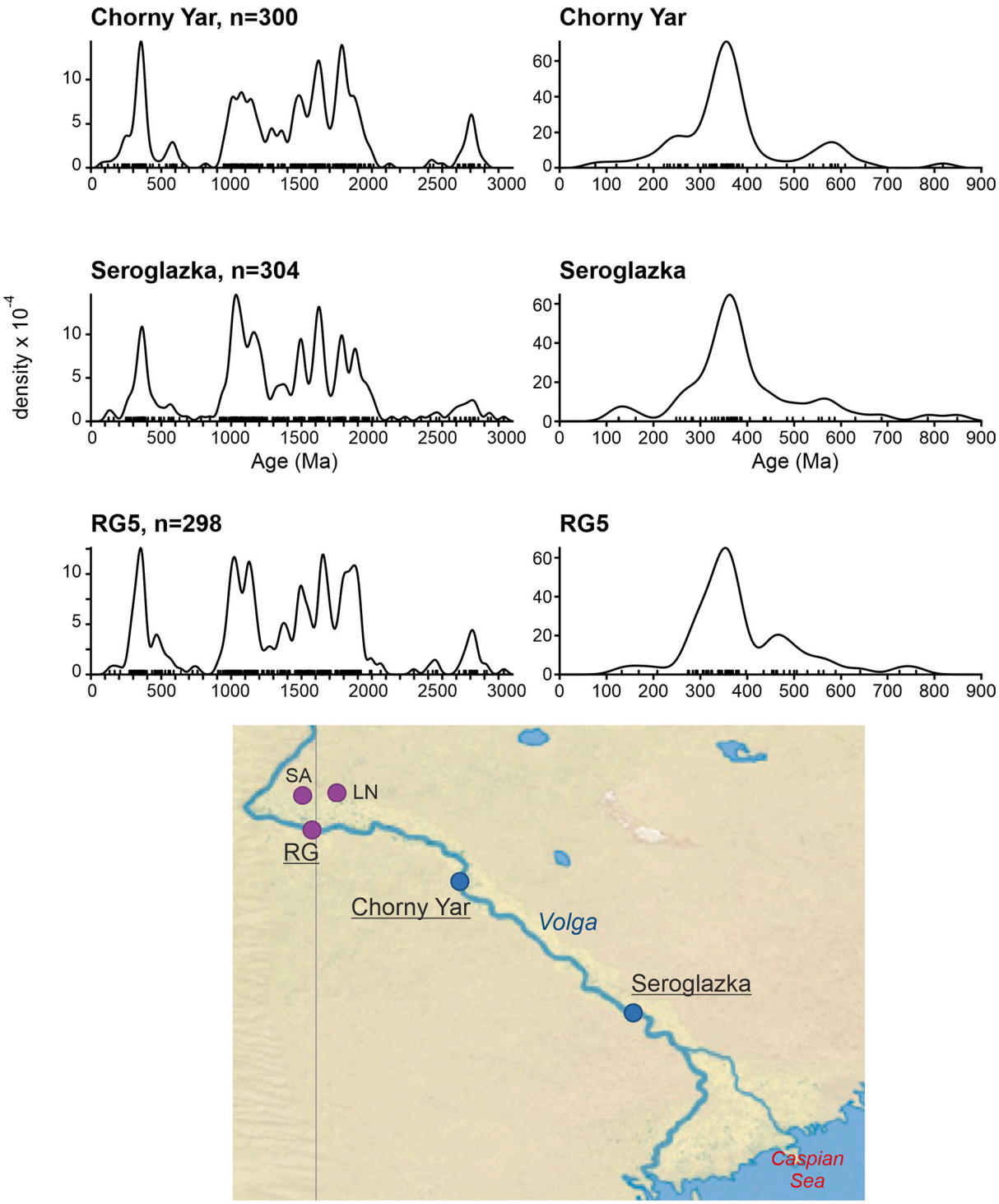

Fig. 10. KDE plots of Volga sand from Chorny Yar, Seroglazka and Raygorod, with the Chorny Yar sample being the oldest (~150–130 ka) and the Raygorod sample (RG5) the youngest (~60 ka) (Table 1, Fig. 1b).

different age distribution is observed for a sample from Siret River alluvium, taken from close to its confluence with the Danube by Ducea et al. (2018). It shows a large peak at around 320 Ma and abundant Late Neoproterozoic - Early Palaeozoic fractions forming two peaks at around 480 Ma and 620 Ma. Meso- and Palaeoproterozoic peaks are not as significant (Fig. 12). Cumulative U—Pb data from several rock samples from the surrounding area, geologically representing the North Dobrogean unit (Fig. 2), come from Balintoni and Balica (2016) and show one distinct peak at 600 Ma years, compared to which a Palaeozoic fraction at around 320 Ma, and the numerous Meso- and Palaeoproterozoic age populations are significantly smaller (Fig. 12).

5. Discussion

5.1. Lower Volga loess and its temporal and spatial source variability

Overall, all LVL samples from the 3 different sites and from different stratigraphic depths and ages show great similarity (Figs. 3 and 5). The

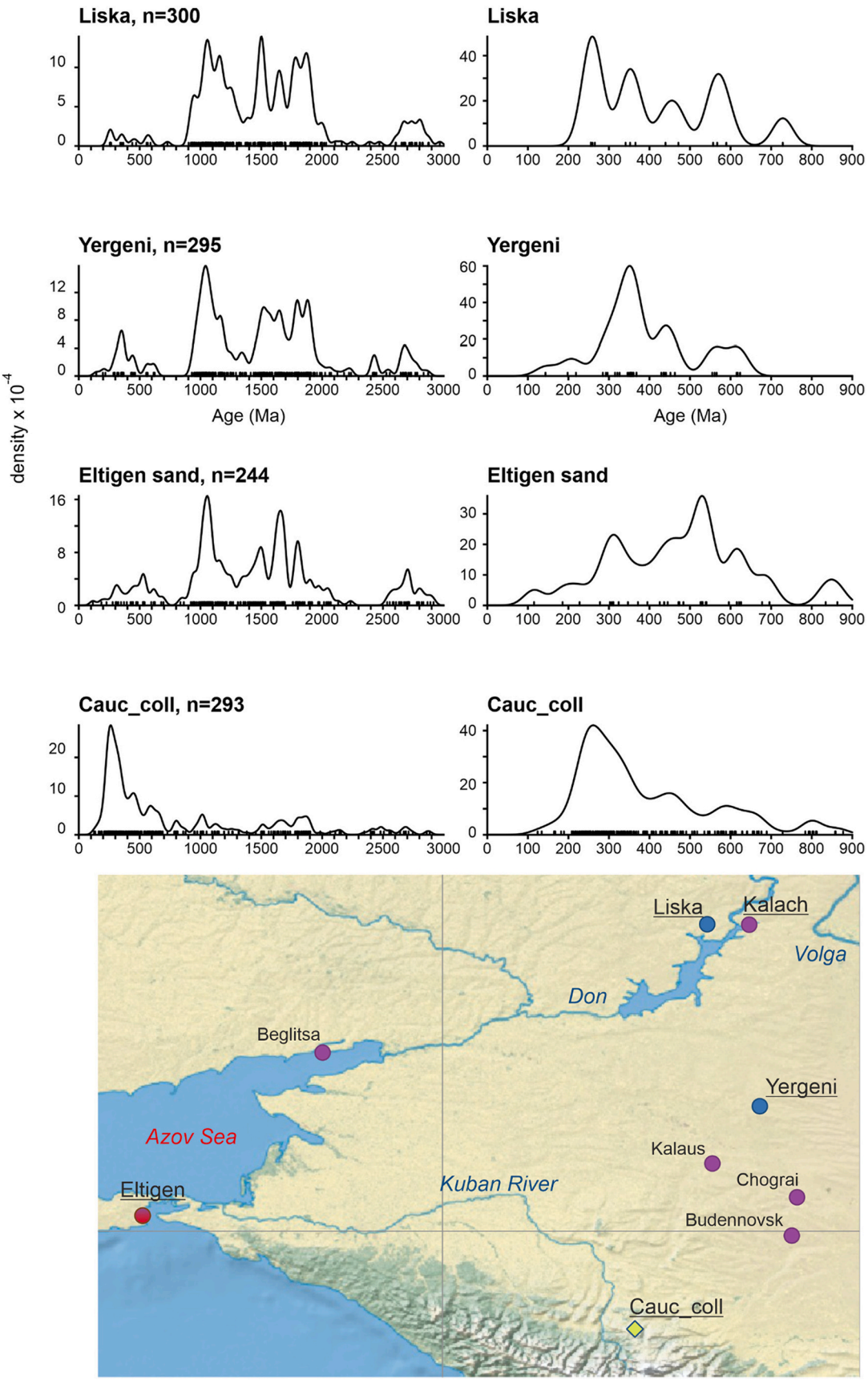

Fig. 11. KDE plots of Don sand from the Liska site, Yergeni sands from the Yergeni uplands, Black Sea sand from the Eltigen section, and of colluvium from the northern Greater Caucasus.

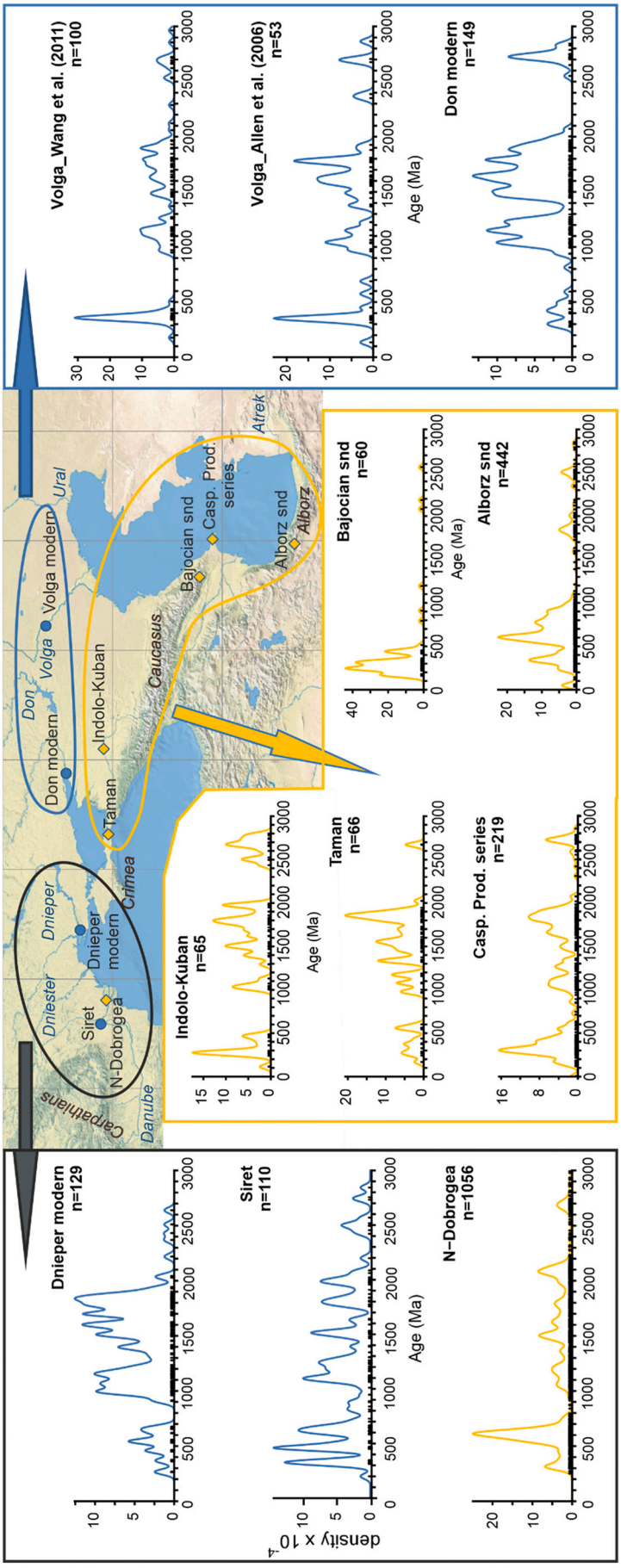

Fig. 12. KDE plots of relevant published detrital zircon data from sediments and sedimentary rocks in the study region. Published sources for these samples are given in Table 1. For colour coding see Fig. 1a, yellow diamonds denote samples from diverse sedimentary rocks. (For interpretation of the references to colour in this figure legend, the reader is referred to the web version of this article.)

Table 2
List of those samples that have been grouped together for further discussion, based on their similar zircon age distributions and verified by depositional age, geological and geographic position. See sections 5.1–5.4 for detailed explanation.

Section/ formation	Subsample	Material	Age	Reference	Combined sample
Leninsk	LN4	Loess	31.2 ± 2.2 ka	This study	LVL_20–65 ka
	LN5	Loess	56.1 ± 2.8 ka		
	LN6	Loess	63.4 ± 3.0 ka		
Raygorod	RG3	Loess	~30 ka		
	RG4	Loess	~40 ka		
Kalaus	Kalaus	Loess	MIS 3–2	This study	Manych
Chograi	Chograi	Loess	MIS 4–3		
Staiki	–	Loess	MIS 2	Pańczyk et al., 2020	EEP_Ukr
Vyazovok	–	Loess	MIS 2		
Raygorod	RG5	Fluvial sand	~60 ka	This study	Volga_150–60 ka
Seroglazka	Seroglazka	Fluvial sand	~100–85 ka		
Chorny Yar	Chorny Yar	Fluvial sand	~150–130 ka		
Chorny Yar	–	Fluvial sand	Modern	Allen et al., 2006	Volga_modern
Volgograd downstream	–	Fluvial sand	Modern	Wang et al., 2011	
Liska	Liska	Fluvial sand	Unknown Quaternary	This study	Don_Yerg
Yergeni	Yergeni	Fluvial sand	Pliocene		
Don mouth	–	Fluvial sand	Modern	Wang et al., 2011	
Indolo-Kuban	ILN#13_700	Sandstone	Pliocene-Quaternary	Vincent et al., 2013	
Taman	WC139/1	Sandstone	Pliocene-Quaternary		
Casp. Prod. series	KV LKS/3	Sandstone	Pliocene	Allen et al., 2006	Plio_Quat
	KV LKS/5				
	BQ BA/7				
	BQ BA/9				
–	Cauc_Coll	Colluvium	Modern	this study	Cauc_Jur
Bajocian	–	Sandstone	Middle Jurassic	Allen et al., 2006	

360 Ma peak, which they all have in common, comprises zircon ages corresponding to Variscan orogenesis. All samples also contain ages between 460 and 420 Ma, corresponding to Caledonian orogenesis. Ages between 540 and 630 Ma correspond to the Cadomian phase of orogenesis and are most abundant in the samples RG4 (3%), but are represented by a few grains in all other samples as well. Meso- and Palaeoproterozoic as well as Archean age distributions are very similar between all LVL samples. This indicates a similar provenance for Leninsk, Raygorod and Srednyaya Akhtuba loess during different stages of the same glacial epoch, which reflects sources with Variscan and Caledonian orogenesis age zircon assemblages in addition to the dominating Meso- and Palaeoproterozoic signal (> 70% in each sample). However, to determine whether the contributing sources changed during the time of LVL deposition, Raygorod and Leninsk samples from different stratigraphic depths are compared alongside random subsampling of grouped site data (Figs. 3-5).

At Leninsk, the three samples (Fig. 1b) all show the same peaks corresponding to Variscan and Caledonian orogenesis ages and major Proterozoic age fractions at 1050 Ma, 1180 Ma, 1320–1400 Ma, 1500 Ma, 1630 Ma, 1780 Ma, 1880 Ma as well as in the Archean, suggesting no obvious differences between them. Small changes can be observed only in the height, rather than the presence, of these peaks. Peak height differences, however, have to be interpreted with care due to the varying number of analysed grains (Fig. 5). The random subsampling of grouped Leninsk data reveals that all subsamples show a major peak at 360 Ma and a smaller age fraction at 430 Ma (Fig. 4). These peaks are also clear in the three original samples. This underpins the temporally stable, significant contribution of Variscan orogeny aged, and to a lesser extent Caledonian orogeny aged sources to Leninsk (Figs. 4 and 5). Slight differences are seen in the expression of Neoproterozoic ages between the random subsamples, while the Meso- and Palaeozoic as well as the Archean age distributions are essentially identical in terms of peak presence. This observation suggests that a slight variability in the age distribution of samples may be sampling induced, and comparison with the stratigraphically different LN samples reveals that the random subsamples in fact show greater variability in age distributions (Figs. 4 and 5). As such, the slight age spectra differences between the Leninsk samples by depth cannot be assigned to actual provenance changes. By extension, this suggests that the source for loess at Leninsk did not change significantly from 65 to 30 ka ago (Fig. 1b), at least as is observable from the applied technique.

Samples from Raygorod show more variation with stratigraphic depth. Samples RG4 and RG3, deposited at ~40 ka and ~ 30 ka, are very similar to each other, apart from the somewhat better-defined Caledonian and Cadomian orogenesis age corresponding peaks in RG4 (Fig. 3). In the Mesoproterozoic, RG4 also contains fewer grains of age c. 1300 Ma, while RG3 has a less abundant age fraction around c. 1400 Ma. However, regardless the differing number of analysed grains between the samples, this variability is comparable to that seen among the random subsamples from the grouped Raygorod data, which differ only in the peak height rather than the presence of certain age fractions (Fig. 4). This suggests that the small differences in zircon age distribution between RG3 and RG4 are within the range of sampling induced variation. However, RG2 (~20 ka) seems to show larger differences compared to the older Raygorod samples. These are notable in the absence of a 2800 Ma age fraction, the presence of a 2100 Ma age fraction, and a less distinct 1600 Ma age peak, where instead several large but diffuse age fractions occur between 1450 and 1900 Ma. Furthermore, RG2 shows a lack of ages at c. 1300 Ma and a peak at c. 1400 Ma, the opposite of RG3 (Fig. 3). Thus, while these observations may suggest an invariant dust source to Raygorod between 30 and 40 ka, there may be some temporal variability in loess provenance during MIS 2 (RG2).

Comparing the three sites together reveals that all samples from Leninsk and the two similar samples from Raygorod (RG3 and RG4) share very similar characteristics. All samples have the same Variscan and Caledonian orogenesis corresponding age fractions and the Meso- and Palaeoproterozoic age distributions are overall very similar, with differences lying within the range of sampling induced variation as discussed above. The older loess sample from Srednyaya Akhtuba with its depositional age of ~88 ka, shows an age distribution partly different to this. Presuming a close similarity between the zircon age distributions of the three LVL sites, the absence of Neoproterozoic ages between 640 and 800 Ma, as well as the absence of grains younger than 300 Ma and

older than 2800 Ma, despite their overall scarcity in LVL samples, indicate that the source input might have changed from MIS 5 to MIS 4.

Based on the analysis above, we combine the LVL data into three groups showing similar provenance signature: 1) LVL younger than 20 ka (sample RG2); 2) LVL between 60 and 20 ka (samples RG3, RG4, LN4, LN5, LN6), and; 3) LVL older than c. 80 ka (sample SA) (Table 2, Fig. 13). We note that these groupings are approximate due to low sample number, and we emphasize that we separate samples into different groups only when there are clear differences in the age spectra (i.e., presence of zircon age populations) that seem to exceed the variation seen in the subsampling experiments. In any case, overall, LVL zircon U—Pb age distributions are very similar between samples, sites and through time, indicating relatively constant sources. However, some small changes are seen, particularly for Raygorod loess deposited earlier than 20 ka and Srednyaya Akhtuba loess deposited before 80 ka, compared to all other analysed LVL samples.

5.2. Loess from the East European Plain and the Caspian Sea region

Overall, remarkable variation in loess source is seen over the region of the southern and western EEP, in the area of the Black Sea and the Caspian Sea. This variation in zircon age distribution is apparent even for closely located sites, suggesting strong variability in zircon age assemblages in different source regions, several processes of transportation and reworking prior to loess deposition, and highly site/area specific controls on aeolian sediment origins. Based on the characteristics of their zircon age KDEs, and thus their sources, the analysed loess samples are allocated to four EEP loess provinces and one Southeast Caspian loess province (discussed below). While the exact extent of these provinces can only be estimated from the results of this study, these loess provinces will be used to assign specific sources in the further discussion (5.6): The Southwest EEP province, South EEP province, North Caucasus province, Southeast EEP province and Southeast Caspian province (Fig. 14). The provenance of these loess provinces can be clearly separated from that of 'Carpathian foreland and lower Danube Basin loess' (CDB loess). A more detailed subdivision of this loess and its difference to EEP loess based on provenance and transport modes is discussed in e.g. Pańczyk et al. (2020). The comparison of our results with their data and with data from other European loess provenance studies (Ujvári et al., 2012) reinforce their findings and allow separation of the Southwest EEP province from this highly generalised 'CDB loess'. This 'CDB' loess, particularly in the Danube Basin, shows abundant Mesozoic to Neoproterozoic zircon ages, and at least south of the Carpathians and Bohemian Massif generally contains only minor or even misses Meso- and Palaeoproterozoic age fractions (Ujvári et al., 2012), which are the signature age populations that all loess provinces of the EEP, except the North Caucasus province, have in common. Below, the groupings are discussed in terms of age spectra of the constituent samples, while later on in chapter 5.6, specific sources and source variability are discussed.

5.2.1. The Southwest EEP province

This loess province comprises Russian and Ukrainian loess sites on the southwestern EEP. Its characteristic zircon age assemblage widely misses Mesozoic ages, shows small Palaeozoic age populations and abundant Meso- and Palaeoproterozoic ages (>65%). From the loess samples discussed in this study, the samples from the Pushkari, Staiki, Vyazovok and Dnieprovskie sites all show this characteristic age distribution pattern, and are relatively closely and similarly situated geographically (Fig. 8). In addition, detrital zircon U—Pb data from the

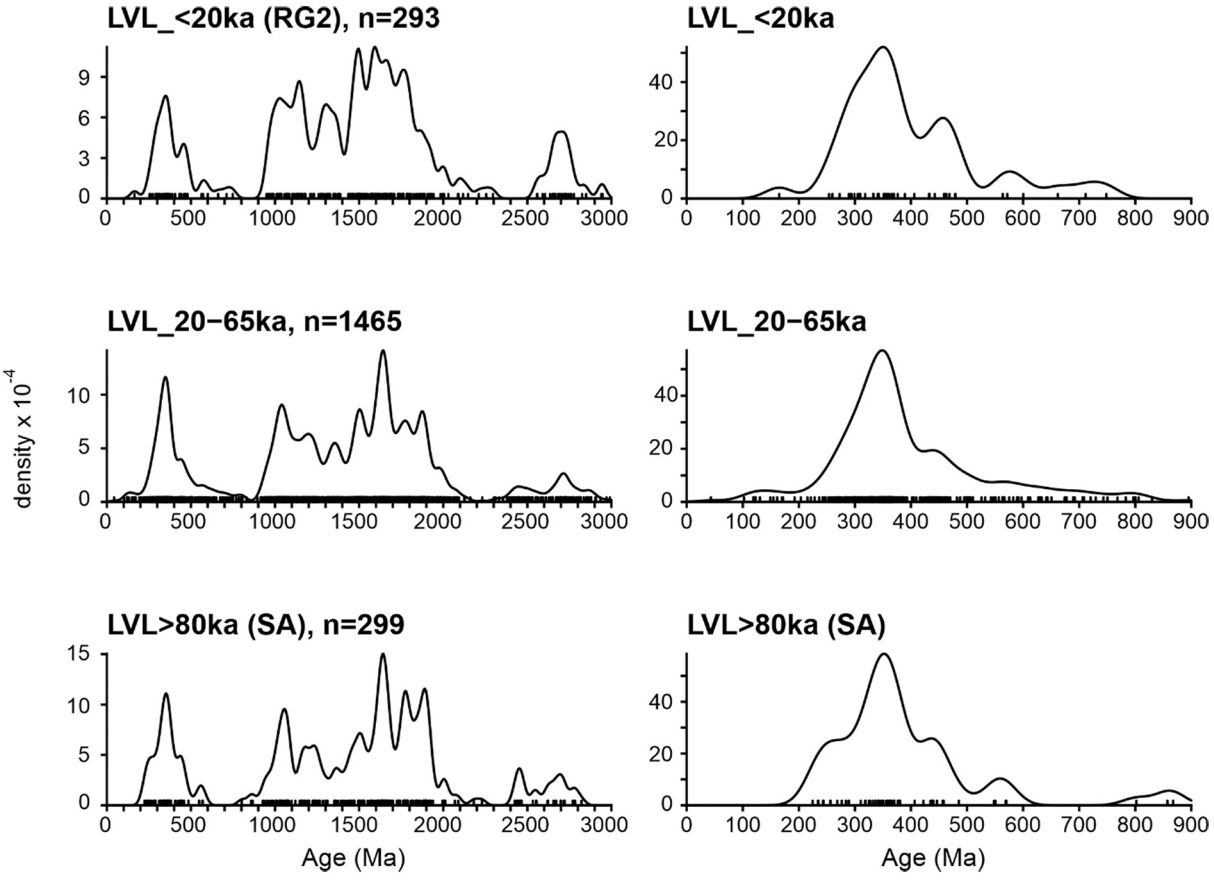

Fig. 13. KDE plots of LVL, grouped according to their similarities and differences in age distribution. Sample RG2 is treated as LVL <20 ka, samples RG3, RG4, LN4, LN5, LN6 are combined to LVL_20–65 ka and sample SA represents LVL >80 ka.

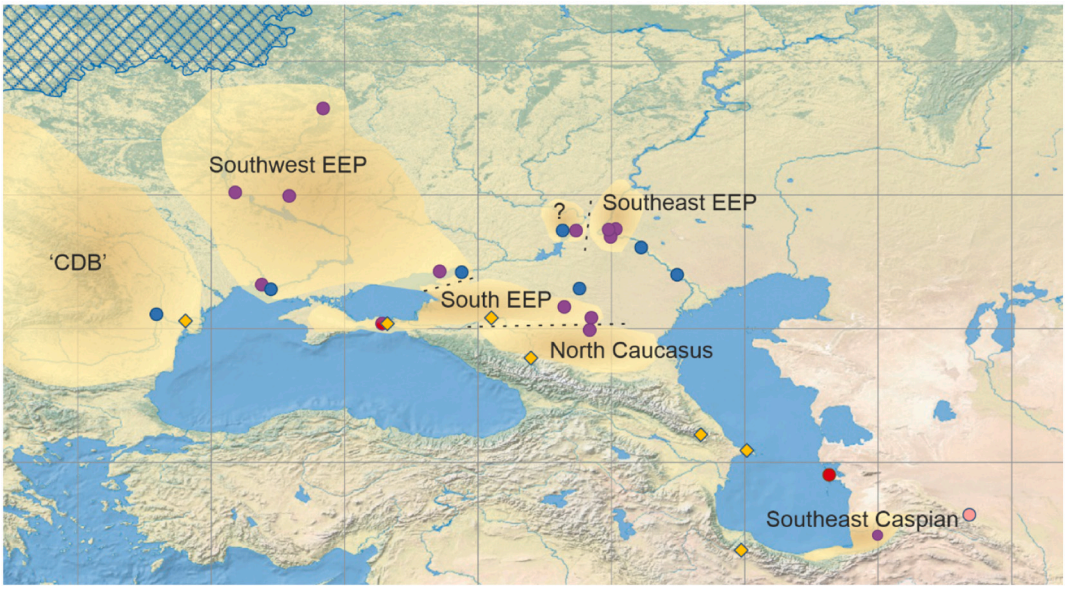

Fig. 14. Loess provinces of the EEP and in the South Caspian Sea region classified based on the detrital zircon age provenance signal of the loess samples discussed in this study. Note that the shape and extent of the loess provinces is only roughly estimated (yellow shade) and that the 'CDB' loess province is not further subdivided (please see e.g. Pańczyk et al. (2020), Ujvári et al. (2012) for provenance discussions of the subdivision of this loess province). The locations of samples considered in this study are marked, for legend see Fig. 1a. (For interpretation of the references to colour in this figure legend, the reader is referred to the web version of this article.)

Ukrainian loess site Cherepyn (Nawrocki et al., 2019) fits this provenance signal too. The Ukrainian sections along the Dnieper (Staiki, MIS 2; Dnieprovskie, MIS 6) and close to its tributaries (Vyazovok, MIS 12–2; Cherepyn, MIS 2), as well as the Russian Pushkari site (MIS 3) located close to a tributary river of the Dnieper (Desna River), lie within the drainage basin of the Dnieper, into which the Fennoscandian Ice Sheet repeatedly penetrated during the Quaternary (e.g. Chugunny and Matoshko, 1995; Gozhik, 1995). All four Southwest EEP province sites show a similar zircon age distribution, particularly in regard to Meso-, Palaeoproterozoic and Archean ages, but some differences are also seen. While the Pushkari and Dnieprovskie loess samples do not show a higher number of grains forming any broader Palaeozoic fraction and are entirely missing ages corresponding to Variscan orogenesis, the northern Ukrainian sections contain such an age fraction. Age populations corresponding to Caledonian orogenesis ages are present in all four samples, while ages corresponding to Cadomian orogenesis are nearly missing from the Pushkari sample (Fig. 8). While these differences suggest some provenance differences for the Pushkari loess compared to the three Ukrainian sites and also for the northern Ukrainian sites compared to the Black Sea site, the low number of analysed zircons for most of these samples limits their direct comparison and the pinpointing of specific sources of minor age populations. A comparison is further complicated by the somewhat different depositional age of the discussed samples. As such, they all are evaluated as representatives for the Southwest EEP loess province (Fig. 14). The two strikingly similar Ukrainian sites Staiki and Vyazovok are combined into one larger-n sample for further discussion (Table 2). A similar zircon age KDE pattern, characteristic for this loess province, is displayed in loess from Beglitsa (~30–25 ka). This site is located at the shore of the Azov Sea close to the inlet of the Don. Its loess sample shows small Palaeozoic and Late Neoproterozoic age populations, while its Meso- and Palaeoproterozoic ages are abundant (79%) and define several large peaks (Fig. 6). As such, Beglitsa loess fits most closely into the Southwest EEP loess province (Fig. 14).

5.2.2. *The South EEP province*

The main characteristics of loess from the South EEP province are a large Palaeozoic double peak at 300 Ma and 440 Ma, the presence of an age fraction at 600 Ma, abundant Meso- and Palaeoproterozoic ages, and the presence of Mesoarchean ages. This zircon age distribution pattern is shown by Eltigen loess, which is located at the tip of the Crimean Peninsula right at the Kerch Strait, which connects the Azov and Black seas. Despite the geographical proximity and the similar nature of the Beglitsa and Eltigen sections, both cropping out along the coast, the more southerly situated Eltigen loess section shows large Palaeozoic and Neoproterozoic age fractions in contrast to the Beglitsa loess, although the Meso- and Palaeoproterozoic age distributions are similar. At Eltigen, two peaks, defined by age populations at 300 and 450–530 Ma correspondent to Variscan (6%) and Caledonian (9%) orogenesis ages respectively, are well expressed. There is also a significant peak at c. 600 Ma, together with abundant Neo- and Mesoarchean ages, pointing to differences to loess from the Southwest EEP province (Figs. 6 and 14). The loess samples from the two sites Kalaus (MIS 3–2) and Chograi (MIS 4–3), located in the Manych depression, also fit into the South EEP province group, showing the characteristic abundant Palaeozoic peaks at 300 Ma and 450 Ma, a well-defined age fraction at 600–630 Ma, and abundant Archean ages, in addition to the characteristic abundance of Meso- and Palaeoproterozoic ages (Fig. 7). This allows us to outline the South EEP province as shown in Fig. 14. Due to their very similar zircon age distribution and the low-n analysis of the Chograi sample, these two Manych depression loess samples are combined to one Manych sample for further consideration (Table 2).

5.2.3. *The North Caucasus province*

This province differs from the previous ones mainly due to the low abundance of Meso-, and Palaeoproterozoic aged zircons in its loess. Its main characteristics also include a large peak at 300 Ma and a comparably smaller major age population at 440 Ma. Located on the northern foothills of the Caucasus and at a higher elevation than the close by loess sites of the South EEP province, loess from the Budennovsk section shows this characteristic zircon age distribution. While the large Variscan orogenesis aged peak at 300 Ma, as well as the age populations at 445 Ma and 600 Ma respectively, are similar to those observed for loess from the Southeast EEP province, the Meso- and Palaeoproterozoic age populations are small and Archean ages are nearly absent, which is clearly different from all the other discussed loess samples from the EEP

(Figs. 7 and 14).

5.2.4. The Southeast EEP province

The most remarkable difference between the Southeast EEP and the Southwest and South EEP loess provinces is found in the zircon age pattern of the Palaeozoic, while the Meso- and Palaeoproterozoic age distributions are similar. Representatives of the Southeast EEP province show a large Variscan orogenesis aged fraction that, in contrast to loess from the South EEP and North Caucasus provinces, peaks at 360 Ma. The LVL sites show this characteristic well (see 5.1; Fig. 14).

5.2.5. Southeast Caspian province

The age distribution of the Iranian Aghband loess section is clearly different to all analysed EEP loess samples. Mesozoic, Palaeozoic and Neoproterozoic ages are abundant, while Meso- and Palaeoproterozoic ages are nearly absent (Fig. 9). Thus, and also due to its geographical separation from the loess sites on the EEP, this section is taken to represent a separated loess province southeast of the Caspian Sea (Fig. 14).

5.2.6. Non-allocated loess sites

Loess from the Kalach site on the Don River (unknown Quaternary age) represents a particular case, which does not allow its allocation to any of the above described loess provinces. Despite its close proximity to the LVL sections, and cropping out along the Don River, it shows some remarkable differences in its zircon distribution. While the 360 Ma age peak in the sample corresponds to the timing of the Variscan orogeny just as for the LVL samples, and Meso- and Palaeoproterozoic, and Archean ages are also similarly distributed, the Mesozoic age peaks detected in the Kalach loess are absent in all other discussed samples, and indicate a different source input at this site (Figs. 6 and 14). While its Palaeozoic, Proterozoic, and Archean age distributions suggest an affiliation to the Southeast EEP province, its Mesozoic ages are not compatible. As such, it is possible that the Kalach site is a representative of yet another EEP loess province, or that some specific local input is recorded at that particular site, and that it is not representative of any larger province (Fig. 14).

5.3. River and sea sediments

In order to simplify the comparisons between regions for the later discussion (5.5, 5.6) and to enable more meaningful comparisons where samples have relatively low n, here we combine samples of similar types of material from comparable catchments in cases where their zircon age distributions are very similar. This applies to both original and published data and is undertaken independently from the grouping of loess data into loess provinces discussed above, and for which the river and sea sediments might represent sediment sources.

All three Palaeo-Volga samples (Chorny Yar, Seroglazka, RG5; Table 1) display highly comparable zircon age distributions, most notably in the large Variscan orogeny aged population at around 360 Ma (~10%) and the abundant Meso-, Palaeoproterozoic age fractions (~75%). Here, only slight differences occur in the prominence and relative abundance of some age peaks, for example the diffuse peaks of the Chorny Yar sample between 1000 and 1350 Ma in comparison to the well-defined double peak in the Seroglazka and RG5 samples (Fig. 10). The striking overall similarity suggests no significant changes in the sedimentary load of the Palaeo-Volga through time and allows grouping these three Palaeo-Volga samples into one Palaeo-Volga sample (Volga_150–60 ka; Table 2, Fig. 15). Differences between the Caledonian orogeny aged fractions of the three Paleo-Volga samples (4% in RG5; 3% in Seroglazka; 2% in Chorny Yar) are unlikely to be source diagnostic. Due to the overall small number of Caledonian aged grains ($n = 6$ in RG5, 4 in Seroglazka, 2 in Chorny Yar), the probability of overlooking this age population is high and dependent on the number of analysed zircons per sample. Modern Volga sediment samples come from Wang et al. (2011) and Allen et al. (2006), collected from the lower reaches of the Volga downstream from Volgograd and the present floodplain near Chorny Yar, the same outcrop from which our ~150–130 ka old Palaeo-Volga sand sample was taken (Table 1). The zircon age distributions of these two modern Volga samples are very similar (Fig. 12), which are therefore combined into one modern Volga sample (Table 2, Fig. 15). The modern Volga shows some differences compared to the Palaeo-Volga discussed above, most notably the low peak heights of Meso- and Palaeoproterozoic age populations (64%) in comparison to the large Variscan orogeny age fraction (20%) (Fig. 15). To compare, these age populations account for 75% and 10% in the Palaeo-Volga samples. Potentially, the observed variability from the Palaeo- to modern Volga signals changes in the catchment or the course of the Volga from the Pleistocene to today, but could also be driven by human modification of the modern Volga River.

The KDE of the Palaeo-Don alluvium from the Liska site (MIS 4–3) shows strong overall similarity to the Pliocene Yergeni sand sample. However, apart from some minor variation in the prominence and abundance of Proterozoic and Archean age populations, there is one main difference; the well-defined age fraction at c. 360 Ma among the overall low abundance Palaeozoic populations in the Yergeni sample is missing from the low abundance Palaeozoic fraction of the Palaeo-Don sample, where only 3 grains reflect this age (Fig. 11). However, the abundance of these Palaeozoic ages is still small in comparison to the Meso- and Palaeoproterozoic age fractions. This pattern is clearly different to Volga material and suggests that the provenance of the Yergeni sample is probably more closely related to the source of the Palaeo-Don than the Palaeo-Volga. It should also be considered that the analysed Yergeni sample is considerably older (Pliocene age) than the Palaeo-Don and Palaeo-Volga samples (late Quaternary). Furthermore, while the Palaeo-Volga material does not show much variation regardless of its age and sampling site (Fig. 10), the Palaeo-Don sediment may show some variability in zircon age distribution if it were of different age or sampled further downstream. The analysed modern Don sample published by Wang et al. (2011) comes from further downstream than the Palaeo-Don sample, which allows some testing of this possible geographical and temporal variation. Both Don samples show a similar zircon age distribution and considering the overall rather small differences to the Yergeni sample, these three samples are grouped together for further analysis (Don_Yerg; Table 2, Fig. 15).

The zircon age distribution of the modern Dnieper alluvium is similar to the Don and Yergeni samples, but differs by the lack of Archean ages. Furthermore, the age fraction coeval to Cadomian orogenesis is well defined (Fig. 12). Further west, and different to all other discussed river sediments, the detrital zircon U—Pb age distribution from the Siret River sample from close to its inlet to the Danube shows strong peaks in the Neoproterozoic and Palaeozoic, reflecting the Cadomian, Caledonian and Variscan phases of orogenesis in well-defined peaks (Table 1, Fig. 12). All this signals starkly different sources for the Siret River sediment compared to those supplying the rivers on the EEP. The Siret River drains into the Black Sea via the Danube, yet the ~110 ka old Black Sea sand from the Crimean Eltigen section shows little similarity to the Siret sample and rather reflects EEP input. The KDE of Eltigen sand zircon ages is comparable to the Liska Palaeo-Don alluvium, with small Phanerozoic and Neoproterozoic zircon components (12%), and abundant primarily Meso- and Palaeoproterozoic ages (75%). However, there are differences in the Palaeoproterozoic fractions older than 1800 Ma (Fig. 11). The Caspian Sea sand from the Turkmen Cheleken Peninsula, in contrast, does not show similarities with any of the discussed EEP rivers, with Mesoproterozoic ages essentially absent, and Palaeoproterozoic and Archean fractions greatly reduced, signalling a provenance history different from the Black Sea and detached from the EEP. This is in line with what is suggested from the grouping of the Southeast Caspian loess province (Fig. 15).

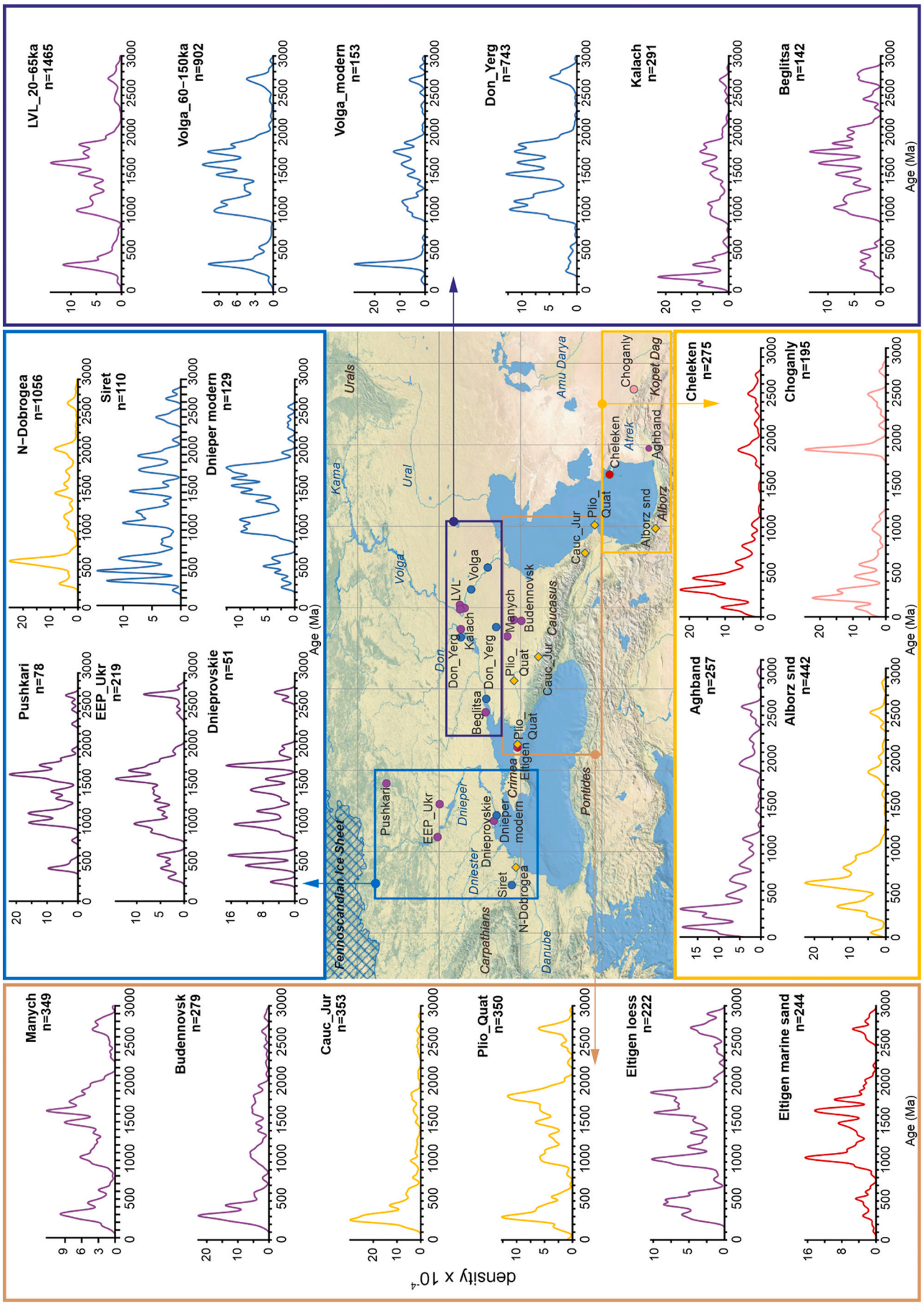

Fig. 15. Comparison of the KDE plots of all samples that are discussed in this study, divided into geographical sections independent from their potential provenance (i.e. loess provinces, section 5.2). Some plots represent combined samples from multiple samples/sites (see Table 2). For colour coding see Fig. 1a, yellow diamonds and curves denote samples from diverse sedimentary rocks. (For interpretation of the references to colour in this figure legend, the reader is referred to the web version of this article.)

5.4. Other sedimentary material

As for the river sediments, zircon U—Pb data from the other samples discussed in this study, including published data, is combined where possible to facilitate sediment provenance analyses in the Black Sea - Caspian Sea region. The modern Karakum Desert sand sample at Choganly and the Cheleken Caspian Sea sand sample (~10 ka) both show very reduced Meso-, Palaeoproterozoic and Archean zircon age abundance, which clearly contrasts to what is observed in EEP samples. However, the two samples exhibit differences in their Palaeozoic and Mesozoic age distribution (Fig. 9), further indicating differences in the provenance of these two samples (Fig. 15). Located northwest of the South Caspian Basin, a Middle Jurassic sandstone sample from the eastern Greater Caucasus (Bajocian sandstone) displays a similar age distribution to the high-n KDE of the local colluvium sample from the Greater Caucasus (Cauc_coll). Both show a large late Variscan peak at 240–320 Ma and contain very few grains of Meso- and Palaeoproterozoic ages. While the two samples also share ages of 440 Ma, differences occur as represented by a Mesozoic age fraction at 170 Ma in the Bajocian sandstone, and by an age fraction of 600 Ma in the Caucasus colluvium (Figs. 11 and 12). Given the great discrepancy in the number of analysed grains for the two samples, these small differences may be an artefact of the low zircon grain number of the Bajocian sandstone and are thus not clearly indicative of real provenance differences. These two Greater Caucasus samples are therefore combined to the sample "Cauc_Jur" for further discussion (Table 2, Fig. 15).

Further to the northwest in the northern foreland of the Greater Caucasus and geographically close to the sampling location of the Caucasus colluvium, detrital zircons from Pliocene-Quaternary sedimentary rocks from the Taman Peninsula and from the Indolo-Kuban Basin (samples ILN#13_700, WC139/1; Table 1) show similar KDEs to each other, as well as to the combined sample from the Pliocene Caspian Productive series (Kirmaky Suite and Balakhany Suite) from the Apsheron Peninsula, located on the eastern lower reaches of the Greater Caucasus, geographically close to the sampling location of the Bajocian sandstone (Fig. 12). The only notable differences are observed for Archean ages, which are present in the Indolo-Kuban and Caspian Productive series sample but nearly absent in the Taman sample. The Indolo-Kuban and Caspian Productive series samples also show a somewhat greater abundance of Palaeozoic ages compared to Meso-, Palaeoproterozoic age fractions, while Palaeozoic ages are relatively sparse in the Taman sample. However, despite the small number of analysed grains in the Indolo-Kuban and Taman samples, the zircon age distributions are comparable. Given this, and also due to the samples' similar formation age, all three samples are combined to a set of 350 zircons (sample Plio-Quat; Table 2, Fig. 15). The sample derived from the grouped Alborz sandstones, representing the detritus from the Alborz mountain range south of the Caspian Sea, as opposed to the Caucasus and its foreland, shows its largest age fraction corresponding to the timing of Cadomian orogenesis. It also contains abundant Palaeozoic ages peaking at 360 Ma. As such, it signals a different provenance to other discussed samples and is not further combined with any other data (Table 1, Fig. 15).

5.5. River sediment provenance

While the similarities and differences in the zircon age distributions of the samples discussed above already yield insights into their common or diverse provenance, we now try to trace the specific proto-sources of these river sediments. This can be done by correlating the zircon formation ages reflected in our samples with specific tectonic events in Eurasia. To do so, it is crucial to consider the geographic relationships between the discussed sediment deposits in the Pleistocene and the environmental conditions during their deposition, as well as the geology of their catchment. The Fennoscandian Ice Sheet as well as mountain glaciations of the Urals, Caucasus, and to some extent the Carpathians affected the drainage and likely also the sediment supply of the large rivers of the EEP draining into the Black Sea- Caspian Sea region (e.g. Grosswald, 1980; Fedorov, 1971; Tudryn et al., 2016). As the largest of the EEP rivers, the Volga mostly drains the Archean EEC block of Volgo-Uralia, eroding its exposed basement and sedimentary cover, but also small parts of the Archean EEC block of Sarmatia and Fennoscandia and the Ural Mountains. Potentially some drainage also comes from areas underlain by the Timan basement (Fig. 2). The course of the Volga stayed broadly the same in the Quaternary, with no remarkable changes in the drainage basin of the Upper Volga, although the lower reach of the palaeoriver, south of Volgograd, is believed to have migrated further west than today (Kroonenberg et al., 1997). Not much is known about the drainage area of the Pliocene Yergeni River, but based on the distribution of the Yergeni formation within the drainage basin of the lower reaches of the Don, it is assumed that its lower course might have been similar to the one of the Pleistocene – modern Don (Zastrozhnov, 1991; Fig. 2). The Don River mostly drains Sarmatian basement and its sedimentary cover, including the exposed Archean crust of the Voronezh Massif (e.g. Shchipansky and Bogdanova, 1996). Parts of the Scythian Platform basement and the Northern Caucasus are also within its drainage area. The drainage basin of the Dnieper comprises mostly Fennoscandian and Sarmatian basement and sedimentary cover, where it erodes into the extensive exposure of Archean crust in the Ukrainian Shield on its way to the Black Sea (Fig. 2). With this background in mind, the specific age peaks seen in the different river systems (Figs. 10, 11 and 12, Table 1) are now discussed in chronological order, starting with Archean peaks. Proto-source provenance assignments for the river sediments are made on that basis.

Old Archean crust crops out in the Voronezh Massif and Ukrainian Shield of the Sarmatian province, but exposed Archean crust older than 2800 Ma is absent from Volgo-Uralia and the part of Fennoscandia that comprises the EEP. Indeed, the scarcity of this age fraction in the Palaeo- and modern Volga samples therefore reflects well the geology of its drainage basin (Figs. 2 and 15; e.g. Bogdanova, 1986; Gorbatschev and Bogdanova, 1993; Puchtel et al., 1998; Bogdanova et al., 2008). This is also the case for the modern and Palaeo-Don (Liska) samples, which contain more grains of >2800 Ma than the Volga sediment (11 out of 300 compared to 9 out of 908) and reflect the presence of Mesoarchean crust (Voronezh Massif) within the Don River basin (Fig. 11). Even the metamorphic overprinting of this old crust at 2.8 Ga (Shchipansky and Bogdanova, 1996) might be discernible in the Palaeo-Don alluvium sample. By contrast, only 4 grains show such old ages in the Yergeni sample, spread between 2800 and 3250 Ma. This suggests that the Voronezh Massif does not lie within the Yergeni drainage basin (Fig. 11). Surprisingly, and as already noted by Wang et al. (2011), the modern Dnieper sample contains only few grains of Archean age ($n = 3$), despite draining the Ukrainian Shield (Figs. 2 and 12). While the low-n detrital zircon analysis of only one sample limits meaningful interpretation, this can potentially be explained as a result of artificial sediment trapping. The construction of dams along the river might cause larger grains from a closer source to settle preferentially in reservoirs upstream of the dams. To test whether this is the case, a comparison with Palaeo-Dnieper material from a similar location as the modern sample would be needed.

The sediments of all these EEP rivers have large ranges of Proterozoic ages in common, marking the polyphase evolution of the EEC during the assemblage of the three Archean provinces noted above (Bogdanova, 1993). The KDE of the Paleo-Don alluvium shows a weak but well-defined peak at 2000 Ma, which is absent from the Volga, the Yergeni and the Dnieper samples (Figs. 10, 11 and 12). These ages might reflect the collision of Volgo-Uralia and Sarmatia, affecting the north-eastern margin of Sarmatia, an area within the Don River basin (Fig. 2; Bogdanova et al., 2008). The large age fraction at 1800 Ma, distinguishable in all river samples, is likely to represent the collision of Volgo-Uralia - Sarmatia with Fennoscandia and formation of the EEC (Bogdanova et al., 2006, 2008; Oczlon, 2006). A smaller but still well-defined age population around 1900 Ma is present in the Volga, Don and Yergeni

material but absent from the Dnieper, and likely to derive from the orogeny that joined the two provinces Kola and Karelia in building Fennoscandia (Lapland-Kola orogen; Kuznetsov et al., 2014), the remains of which seem to be more abundant in basement of the north-eastern EEP. The abundant age populations between 1600 and 1500 Ma in all samples probably represent a phase of multiple orogenic events and related intracratonic magmatism affecting the EEC (Bogdanova et al., 2008). Ages between 1400 and 1300 Ma are abundant in the Volga and Yergeni sediments but less evident in the Don and Dnieper samples (Figs. 10, 11 and 12). These ages coincide with sill intrusions and volcanism in the South Urals (Alekseev, 1984; Bogdanova et al., 2008). Given that the Urals are within the drainage basin of the Volga, but not drained by Don and Dnieper, this suggests that this age fraction represents Uralian input. As such, the Yergeni River basin might also have included parts of the Urals. The broad age fraction between 900 and 1200 Ma, found in all river samples, matches reasonably well with the Grenville-Sveconorwegian orogeny (e.g. Bingen et al., 2003; Bogdanova et al., 2008). However, there are no geological units of this age in the catchments of the EEP rivers, so zircon grains of this age would potentially have been transported into their drainage basin by the Fennoscandian Ice Sheet during the Pleistocene glaciations. The scarcity of grains between 900 and 600 Ma for all these rivers matches with the general absence of these ages in their EEP catchment basins and shows that grains of this age were also not transported into their drainage areas from any surrounding geological terranes. In contrast, some river samples contain ages corresponding in age to Cadomian orogenesis, while others are lacking such a signal. In the Palaeo-Volga samples, an age fraction around 580 Ma might represent grains deriving from the Timanides in the area of the north-eastern margin of the EEC, an area unique on the EEP in yielding Cadomian age grains (Kuznetsov et al., 2007, 2010). That this signal is almost absent from the modern Volga samples can possibly be explained with the control of the Fennoscandian Ice Sheet on sediment reworking and transport, e.g. resulting in higher Volga river discharge than today (Fig. 15). The Timan origin of these ages appears possible also because the Don, Yergeni and Dnieper sediments, which do not drain the Timanides, contain considerably fewer corresponding ages (510–580 Ma) (Figs. 2, 11 and 12).

The Caledonian and coeval phases of orogenesis are not very well reflected in any of the EEP river sediments. Of all samples, the Palaeo-Volga and the Yergeni contain the most zircons of corresponding ages (Figs. 10 and 11). Safonova et al. (2010) argue that all Palaeozoic detrital zircon ages in their Volga sample derive from the Urals and suggest their formation in the collision of the Kazakhstan block with the Uralian arc-trench system in the Early Carboniferous, with magmatism onset as early as 500 Ma ago (Nikishin et al., 1996). Alternatively, the origin of these grains could also lie in the northwest, where the Fennoscandian Ice Sheet penetrated into the drainage basins of the EEP rivers during Pleistocene cold stages, supplying reworked sedimentary material of the EEC, potentially including the Baltic Shield (Figs. 2 and 15). However, Caledonian orogenesis aged zircons are also relatively sparse in Danish till sediments derived in part from the Scandinavian Caledonides, despite these tills lying much closer to this proto-source than the Lower Volga (Knudsen et al., 2009).

A large single peak corresponding in age to Variscan orogenesis stands out for the Volga samples. While this peak is as large as the abundant Meso- and Palaeoproterozoic ages for the Palaeo-Volga, the modern Volga material contains fewer Proterozoic zircons in comparison to this remarkably well defined Variscan peak (Fig. 15). Variscan age zircons are widespread in volcanic rocks in the southern Urals (Puchkov, 1997, 2009 and references therein). Since the Variscan signal is not significant in the age distribution of the other EEP rivers, which do not include the Ural Mountains in their drainage basins, this can be seen as strong evidence for Uralian sediment input to the Volga. The only river material for which a Variscan orogenesis age fraction is slightly enhanced compared to the other Palaeozoic age populations is the Yergeni sample. This once again indicates some subordinate drainage from the Urals by the Pliocene Yergeni River (Fig. 11). The observed difference in the abundance of Meso- to Palaeoproterozoic and Variscan ages in respect to each other between modern and Palaeo-Volga, might be explained with the construction of large dams Volga upstream, which may lead to modern sediment samples from the lower reaches of the Volga not being representative of the natural drainage contribution. It is unclear how this may have affected the palaeo and modern sediment distributions but if the Ural Mountains-derived grains pass fewer dams compared to EEC derived material, then these grains may be over-represented in Volga sediment from lower reaches. Post-Variscan zircon ages are widely missing from the samples of all EEP rivers. Given the above discussed evidence for partly Uralian provenance of the Volga sediments, this is somewhat surprising for the Volga samples, since the later stages of the Uralian orogeny occurred in the Mid-Carboniferous to Permian. This stage resulted in the formation of the Uralian Main Granite Axis, which extensively crops out especially in the central and southern Urals (Puchkov, 1997). Allen et al. (2006) explain the lack of these Late Uralian orogeny age signals in their Volga sample with a drainage pattern effect. Rivers draining the Main Granite Axis are directed eastwards rather than towards the Volga basin to the west of the Urals. Safonova et al. (2010), however, argue for the contribution of these granites to the sedimentary load of the Volga based on their detrital zircon age data. Our data suggest that this is the case at least for the Palaeo-Volga, for which several mid-Carboniferous to Permian ages are present (Fig. 10). Whether these differences represent shifts in upstream river drainage is currently unclear.

Overall, this analysis shows that the zircon age composition of the Volga samples is consistent with derivation from sediments of the Urals and especially the EEP, the latter in turn being fed by sediment sources in the Volga-Uralic, Sarmatian and Fennoscandian basement. A similar geological catchment can be inferred for the Yergeni River sample but the Uralian input appears significantly smaller. The Don does not seem to carry any Uralian material and the main source for its sedimentary load lies on the EEP as well, including more recycling of material deriving from the Samartian block than seen for the Volga and the Yergeni rivers. The Dnieper sample also shows reworking of the EEP basement and cover sequences, reflecting mostly Fennoscandian sources and surprisingly little Archean material from Sarmatia. In contrast to all these rivers, which have the largest part of their drainage basins on the EEP, the drainage basin of the Siret River mostly comprises the Carpathians (Ducea et al., 2018). This difference is also reflected in its zircon age distribution, with a diagnostic Neoproterozoic to Palaeozoic age pattern, in contrast to the zircon age spectra of the EEP rivers, where instead Neoproterozoic age fractions are widely missing (Fig. 15).

5.6. Loess provenance and Black Sea - Caspian Sea sink regions

While for the loess deposits of the three EEP loess provinces (Southwest, South and Southeast) a provenance connection to the EEP and its large rivers seems likely, the situation for the North Caucasus and Southeast Caspian loess provinces is complicated by the influence of the surrounding mountains and seas and the active tectonics in the region (Fig. 14). Particularly in respect to the topography of the Caspian Sea, the provenance of the depositional environments in the Southeast Caspian region needs to be discussed separately from those on the EEP.

5.6.1. The EEP and Caucasus

The Southwest, South, Southeast EEP loess provinces, the uncategorized province around the Kalach site, and the North Caucasus province, all indicate stark source variability across the EEP (Fig. 14). The LVL samples (MIS 5- MIS 2) represent the Southeast EEP province region defined in chapter 5.2, and these samples all show the same distinct Variscan orogeny aged Palaeozoic zircon population and wide range of Precambrian ages as the analysed Palaeo-Volga material (Fig. 15). The detrital zircon ages therefore suggest Volga River sand to be the direct near-source material for LVL. This is supported by the locality of the

loess sections along the Volga River and their stratigraphy showing Volga sands directly underlying the loess sequence in the section (Fig. 1a). Furthermore, such a relationship is also suggested by the character of the loess being relatively coarse grained with similar grain surface features as Volga River sand (Költringer et al., 2021). Thus, LVL is dominated by glacially derived material transported in a multi-step mode via the Volga River. In addition to the contribution of EEC material, a proportion of the sediment has a mountain origin in the Urals, transported to the Caspian lowland via tributaries to the Volga River and this signals the importance of both continental and mountain glaciations in the formation of LVL. However, as discussed above, there is a degree of variability between age distributions of some LVL samples potentially indicating the influence of other sources additional to the Volga, or that the Volga was more variable in its sediment load than is indicated by the samples analysed here. For example, the Khazarian transgression of the Caspian Sea (MIS 5; Tudryn et al., 2013; Shkatova, 2010) could have provided a pathway for additional detritus sourcing the LVL after its reworking by the post Khazarian Lower Volga (sample RG5). Stronger westerlies during the cold phase of loess deposition (Költringer et al., 2021could be another contributing factor for the observed slight variability (Fig. 15). Despite any differences in the age distribution of LVL of different depositional age, no major shift in provenance is detected as no exotic and specific source-diagnostic age populations are found. That some phases of the multiphase EEC evolution are more abundant in samples of different age in the LVL could simply reflect ice sheet fluctuations and changes in drainage patterns or wind strength.

In addition to the loess deposits along the Lower Volga, the North Caspian Basin represents another sedimentary sink in this region and ought to show a similar provenance to the Volga River, which directly drains into the shallow North Caspian Sea. Unfortunately, this cannot be tested here, as no marine coarse siliciclastic material from the North Caspian Sea could be analysed for this study, and no data is found in literature.

While the LVL is clearly Volga derived, the source of loess to the Kalach site on the Don River is less clear. As such, we do not include it in the Southeast EEP loess province (Fig. 14). The Proterozoic and Archean age distribution in the loess from the Kalach site indicates reworking of material from the EEC and the clearly defined and abundant Variscan orogeny aged Palaeozoic fraction is identical to the one found in Volga River sand and LVL, which suggests Uralian input via the Volga. This points to the Volga as a likely source but because Don and Volga River material display similar age distributions for their Proterozoic and Archean grains, it could also be that Don material provides the Pre-Cambrian ages, and the Palaeozoic and Mesozoic fractions reflect the input of an unknown source. Alternatively, both the Volga and the Don could contribute as sources to the Pre-Cambrian age populations, while only the Volga contribution brings the Variscan orogeny aged signal from the Urals, and the Mesozoic age populations derive from an unknown third source. As such, it is hard to tell how many and which sources contribute to the Kalach loess site, especially since the origin of its Mesozoic age fractions remains enigmatic. These striking age populations at 100 and 180 Ma cannot be found in any other of the analysed loess or secondary source material in the Northern Caspian lowland (Fig. 15), but might reflect some local yet unknown sediment input, which interestingly enough did not influence the closely located LVL (70 km east; Fig. 3). In the wider region, ages of this range are only known from the southern Transcaucasus and Lesser Caucasus (Rolland, 2017 and references therein) but transport from these far-off regions seems implausible. The location of the section with respect to the course of Palaeo-Volga and Palaeo-Don makes provenance from both rivers likely, yet the example of Kalach loess shows that it is not only large rivers that appear to have control on loess sediment sources in the region (Fig. 14). In fact, the stark spatial variation of loess on the EEP seems to be a function of the input from multiple diverse sources, as discussed further below.

Less source diversity is indicated by the Southwest EEP loess province (Fig. 14), which characteristically shows small Palaeozoic age populations and abundant Meso- and Palaeoproterozoic ages. The Beglitsa loess section, located on the shore of the Azov Sea, close to the mouth of the Don River, shows great similarity to the Don-Yergeni material, which is likely transported to the Azov Sea by the Don River (Fig. 15). Mesozoic ages are missing from both samples, and the Palaeozoic age distribution is almost identical, as are the Proterozoic age populations within the range of 900–2000 Ma. The peak at 1380 Ma, which indicates a Uralian source signal, suggests additional input from the Yergeni formation and likely not only through erosion by the Don. Smaller rivers, which drain the Yergeni uplands and contribute to the Don closer to its mouth than where the Palaeo-Don sample in this study is located (Liska section), likely supplied more Yergeni material for aeolian transport to the Beglitsa site. As such, this suggests that Palaeo-Don alluvium, transporting material from the EEC and eroding then transporting Yergeni sediment, represents the main aeolian near-source for Beglitsa loess. Furthermore, Mesoarchean ages (>2800 Ma, $n = 4$) in the Beglitsa sample are likely to come from the Voronezh Massif in the Don basin (Fig. 2). However, ages at around 2100 Ma require another explanation. These ages correlate with the timing of the Volgo-Sarmatian orogeny, which is not reflected in the Don-Yergeni sample (Fig. 15).

The loess from the Ukrainian sites Staiki and Vyazovok (combined to sample EEP_Ukr; Table 2), Dnieprovskie, and the Russian Pushkari site on the southwestern EEP are also mainly fed by the EEC and its sedimentary cover, as suggested by their great similarity to the modern Dnieper sediment, with mostly abundant Meso- and Palaeoproterozoic ages (Fig. 15). This observation reinforces the previously proposed provenance of Ukrainian loess in this province (Pańczyk et al., 2020). The low number of zircons in the Pushkari sample does not allow for detailed comparison, but its location along one of the Dnieper's tributaries suggests sediment input from a similar geological catchment. The most notable difference compared to the modern Dnieper River sediment and the Ukrainian loess (including Cherepyn; Nawrocki et al., 2019), however, is that the youngest age fraction in the Pushkari loess is of Silurian age, while the other samples also contain a limited amount (~3%) of younger zircon populations (Fig. 15). This Silurian age fraction might arguably be of Scandinavian source, however, these ages are also present in the Podolia sedimentary succession of Lower Devonian depositional age that largely crops out in the valley of the Dniester River and its tributaries (Schito et al., 2018; Kozłowska, 2019). Considering that a Carpathian origin of these Palaeozoic ages is not plausible for the Pushkari sample, the succession of the Ukrainian Podolia sedimentary basin represents a more likely contributing provenance to the loess sites within the Dnieper drainage basin. Regarding younger Palaeozoic ages, their number in the Ukrainian loess samples and the Dnieper River sample are low and in all cases these ages are rather spread and do not define larger age fractions (Figs. 8 and 12). However, the presence of young Palaeozoic ages, entirely missing in the Pushkari loess sample located further to the northeast, might indicate some reworking from the Carpathians, where Variscan metamorphism and subordinate magmatism in the range of ~350–250 Ma occurs in different tectonic units (e.g. Drăguşanu and Tanaka, 1999; Medaris et al., 2003; Ducea et al., 2018). Additionally, the Siret River sample, the Danube's largest tributary, which is sourced by the Carpathians and East European foreland (Ducea et al., 2018), shows a great abundance of Variscan age grains (~325 Ma; Fig. 15). Overall, while the abundant Meso- and Palaeoproterozoic ages indicate that reworked glaciofluvial Fennoscandian Ice Sheet deposits from Dnieper alluvium are likely to represent the biggest source to the northern Ukrainian loess sites (Buggle et al., 2008; Pańczyk et al., 2020), additional input from the Podolia sedimentary basin and the Carpathians seems to also occur, and indeed might be greater to the Dnieprovskie site on the Black Sea due to its relatively high Cadomian orogeny age peak, an age fraction, which is also abundant in the Siret sample (Fig. 15). Furthermore, Podolia and the Carpathians also represent a major sediment catchment for loess on the Ukrainian Black

Sea west coast (Roxolany; Nawrocki et al., 2018).

In summary, loess from the Southwest EEP province is sourced almost entirely from the EEC and its sedimentary cover, including some Palaeozoic input (Urals in the case of Beglitsa loess, Carpathians and Podolia for the more western sites), and no larger additional sources from other geological domains can be identified. The two large rivers, the Don and the Dnieper, provide the vast majority of material to loess sites in the Southwest EEP province.

Rivers are important also for the provenance of loess sites in the South EEP province, located in the northern foreland of the Crimea-Caucasus mountain belt between the Black Sea and Caspian Sea area (Manych and Eltigen; Figs. 1a and 14), although a greater source diversity than for the two previously discussed loess provinces is indicated. The main differences to these provinces are the large Palaeozoic peaks and a smaller but well-defined late Neoproterozoic to early Cambrian peak (Fig. 15). The Meso- and Palaeproterozoic age distributions instead show strong similarities to LVL and as such to the large EEP rivers such as the Volga, Don and Dnieper, which in turn indicates reworking of EEC material. The potential supply route for this EEC material may be the Paleo-Don, considering the geographic relationship between the discussed loess sites of the South EEP province and the courses of the rivers, as well as Archean ages >2800 Ma shown in both the Manych (combined) and Eltigen loess (Fig. 15). These ages indicate Sarmatian crust as proto-source. The Ukrainian Shield borders the Crimea to the north and is likely to supply these Archean zircons to the Eltigen site. The Manych sites, however, lie further away from where this Archean crust crops out so zircons of these ages may have been incorporated into the loess via the Palaeo-Don River through drainage of the Voronezh Massif instead (Fig. 2). However, as mentioned above, the distribution of ages <900 Ma is characteristic to loess from the South EEP province and cannot be linked to the EEC (Fig. 15). While the Palaeozoic ages have been explained with provenance from the Urals and Carpathians for the Southeast and the Southwest EEP loess provinces above, these sources are unlikely to provide such strong, well defined peaks for the South EEP province.

In order to be able to explain the origin of these age populations for the South EEP province, the geological set-up in its area needs to be discussed first. The Caucasus and the Crimean Mountains are part of the same Variscan orogen, with parts of it cropping out on the west coast of the Black Sea in the form of the North Dobrogean orogen (Fig. 2; Balintoni and Balica, 2016). The geological basement, which was uplifted during this Variscan orogenesis, is dominated by Neoproterozoic U—Pb ages (560–610 Ma; Ducea et al., 2018). This is reflected in the zircon age distribution in the cumulative sample from North Dobrogea (Fig. 15). Apart from the Variscan ages, there is also Lower Jurassic magmatism reported at least for the Crimean Mountains (Meijers et al., 2010). The northern foreland to the North Dobrogea-Crimea-Caucasus mountain range is geologically represented by the Scythian Platform, which is composed of undeformed Palaeozoic sedimentary rocks (Fig. 2; Okay and Topuz, 2017). Little is known about the basement of the Scythian Platform but e.g. Kazantsev (1982) report mainly Meso- and Neoproterozoic ages. The basement of the Scythian platform is widely covered by sedimentary rocks such as the ones sampled from the Indolo-Kuban Basin and the Taman Peninsula (Table 1, Fig. 12; part of the Plio_Quat sample, Table 2), for which the Scythian Platform and EEC represent the main sediment sources (Vincent et al., 2013). For the southwest of the Scythian Platform, the occurrence of some Early-Middle Triassic volcanic rocks are reported, and these are also sporadically found along the eastern zone of the Manych depression (Tikhomirov et al., 2004).

The Eltigen loess section is located on the southern tip of the Crimean Peninsula, and the Manych sites on the EEC block of Sarmatia, right at the border of the Scythian Platform. Ages of 550–670 Ma are likely derived from the Neoproterozoic basement of the Scythian Platform (Figs. 2 and 15). Other potential sources for these ages to the loess are absent in the proximal area. Some plutonic rocks of corresponding age are indeed reported from the Caucasus, but are mostly found in the Transcaucasus, which drains to the south of the orogen (Gamkrelidze et al., 2011). The abundant Palaeozoic ages, in contrast, are likely to be of Caucasian origin. As discussed earlier, there is no proximal source for ages corresponding to the Caledonian orogenesis on the EEP and the occurrence of such ages in its sedimentary sequence is explained by input from either the Scandinavian Caledonides or the Urals. Such an origin, however, seems unlikely for the large corresponding Palaeozoic age population in the loess in the South EEP province. Also the Scythian Platform was not affected by the Caledonian or any coeval orogeny. By contrast, corresponding Palaeozoic ages are widely reported from the Caucasus (Somin et al., 2007) and the c. 460 Ma peak observed for Eltigen and Manych loess is also present in the sedimentary rocks derived from the Caucasus (Cauc_Jur; Fig. 15).

The large Variscan orogenesis aged Palaeozoic peak in the Eltigen and Manych loess is younger than the corresponding Uralian signal observed in the Volga River and LVL samples. These Palaeozoic ages more closely correspond to the crystallization of granites in the Greater Caucasus, which are dated to ~300 Ma (Hanel et al., 1992; Somin, 2011; Fig. 15). While this reflects provenance from the Greater Caucasus, the relatively abundant ~235–250 Ma ages, poorly expressed in the Caucasus, in both samples might represent the Early-Middle Triassic volcanic rocks from the East Manych and southwestern zone of the Scythian Platform (Tikhomirov et al., 2004). However, the sporadic occurrence of these rocks in the region is inconsistent with the number of corresponding ages in the loess samples and corresponding Early-Middle Triassic ages are also largely present in the Budennovsk loess sample (Fig. 7). Even though Lower Jurassic magmatism is reported from the Crimean Mountains, Eltigen loess does not contain zircons of this age, in contrast to the Manych and Budennovsk loess, which contain a few Lower Jurassic aged grains. This suggests that these Mesozoic ages might nevertheless derive from the Caucasus, where several thermal events are recorded from the Permian to the Late Cretaceous (e.g. Rolland et al., 2016) Indeed, another sample with a significant number of these Mesozoic ages is the Pliocene age Caspian Productive Series (Fig. 12). Allen et al. (2006) inferred that this sedimentary succession is sourced from a combination of EEC material, supplied by the Palaeo-Volga, and material from the Greater Caucasus. Since no Mesozoic ages are supplied by the Palaeo-Volga, this signal therefore seems to derive from the Caucasus (Fig. 15).

Based on the discussion above, it can be concluded that Manych and Eltigen loess from the South EEP loess province (Fig. 14) are mainly derived from material eroded from the EEC via the Don River, as is reflected by the Archean and Meso-, Palaeoproterozoic age fractions. In addition, they are also partially sourced from the Greater Caucasus, which contributes the Palaeozoic and Mesozoic ages. Also, the Scythian Platform represents an additional source of material to the loess sites; mainly Neoproterozoic ages. As such, the South EEP province also seems to be controlled by multiple diverse sources.

The Northern Caucasus loess province might have a less diverse provenance than suggested for the EEP loess provinces. The sample from the Budennovsk section appears to have its main sediment source in the Caucasus. This is indicated by its Palaeozoic age peaks at ~445 and ~300 Ma, which correspond to the formation of magmatic rocks in the Greater Caucasus, as discussed above for loess from the South EEP province (Fig. 15). Also, the low abundance of Precambrian ages indicates a dominant Caucasus provenance since the samples from the Greater Caucasus (Cauc_Jur) do not show Meso-, Palaeproterozoic and Archean ages (Table 2, Figs. 12 and 15). This is a distinct difference to the EEP-sourced loess and indicates short-distance aeolian transport in the region, likely controlled by local winds. Even though mountain glaciation plays a role in the Greater Caucasus, tectonic influence might enhance erosion and sediment supply in the Caucasus as well. Despite its close proximity to the Manych sites, the age spectra at Budennovsk is remarkably different but matches its different topographic position up on the northern Caucasian foothills, whereas the Manych sites are

located in the Manych depression, and again highlights the importance of short distance aeolian transport and the control of near-sources to the loess deposits in the region. However, the Scythian Platform might contribute some material to the Budennovsk loess, which is possibly reflected in its Neoproterozoic age populations.

Besides the Budennovsk loess, the Caucasus colluvium also represents a Caucasus fed sedimentary deposit. Its age distribution signals a local source of either Phanerozoic magmatic rocks or Mesozoic sedimentary rocks, mostly reflecting the same age signal, as discussed above (Fig. 11). The presence of a clearly distinguishable Neoproterozoic to early Cambrian fraction makes it more likely that the colluvium derives from other sedimentary rocks in the Caucasus. This is explained with the fact that corresponding ages are not known from magmatic rocks in the Greater Caucasus but appear in the Transcaucasus, which might act as recycled sedimentary rocks that are cropping out in the Greater Caucasus at present. Its great similarity to the Caucasian Middle Jurassic sandstone (Allen et al., 2006) supports this idea (Figs. 11 and 12, Table 2).

All of these discussed loess provinces and geological domains surround the Black Sea, and the Don, Dnieper, and Danube are only the biggest of many contributing rivers in the area. Black Sea sand has been sampled at the Eltigen site (~110 ka), where it directly underlies the loess, which was discussed before as part of the South EEP loess province (Figs. 1a and 14). The Black Sea sand sample at Eltigen contains only few, scattered Palaeozoic ages and abundant Meso-, Palaeoproterozoic fractions, which makes it more similar to the Dnieper or Don than to the Siret or Danube, and thus signals its provenance from the EEP (Fig. 15). As summarized earlier, all terranes in the Black Sea region are characterized by Late Neoproterozoic ages and evidence for older Proterozoic or Archean components is missing, which means such input must come from the EEP (e.g. Okay and Topuz, 2017). However, it is striking that the Eltigen loess on top of the Black Sea sand signals a different provenance and additional source input from the Greater Caucasus and Scythian Platform, reflected in the abundant Palaeozoic and Neoproterozoic age fractions, which are minor in the Eltigen marine sand (Fig. 15). This suggests that the loess is formed from aeolian reworking of mixed sources from several surrounding areas, while the marine sand reflects mainly the sedimentary composition of the closest major river inlet to the Black Sea. In case of the sand at the Eltigen site, this is the Don. As such, it can be inferred that mixing between the different sea basins of the Black Sea is not significant and that marine sediments in the area of the Azov Sea are controlled by input from the Don, and those in the north-western Black Sea by the Danube in the west and the Dnieper in the north (Fig. 1a). This also reinforces that the Black Sea loess at Eltigen is not only sourced from Don alluvium or local marine sediments, as discussed above.

5.6.2. Southeast Caspian region

The Caspian Sea is divided into three parts: the North, Middle and South Caspian basins. Despite the approximately equal surface area of the three basins, the North Caspian comprises by far the smallest water volume due to its extremely shallow water depth (max. 20 m). All three basins are separated from each other by distinct swells, particularly the Middle and the South Caspian basins. The South Caspian Basin is the deepest with a maximum water depth of 1025 m and comprises the area south of the Aspheron Peninsula in Azerbaijan and Cape Kuuli in Turkmenistan (Kosarev, 2005). The Cheleken Peninsula, where our Caspian sand was sampled, lies within this area (Figs. 1a and 2). Not only the South Caspian Basin acts as a sedimentary sink in this tectonically active region, also the Southeast Caspian loess province and the Karakum Desert comprise large amounts of deposited material.

The Caspian Productive Series is discussed as one of the main geological units of the South Caspian Basin, representing a fluvio-deltaic facies, which was deposited after the complete isolation of the South Caspian Basin in the Late Miocene (e.g. Reynolds et al., 1998). In comparison with the Turkmenistan coast Caspian sand sample from the Cheleken Peninsula, the differences in the Precambrian ages are most striking. The Caspian sand does not show any influence from the EEC, as witnessed by the total absence of Mesoproterozoic ages and very limited abundance of Neo- and Palaeoproterozoic ones (Fig. 15). However, the Cheleken sample is ~10 ka old and thus significantly younger than the final depositional age of the Caspian Productive Series. It is possible that the EEC input to the South Caspian Basin decreased in the Late Pliocene after the deposition of the Caspian Productive Series was completed due to climate controls that lead to e.g. changes in river discharge or reoccurring flooding (Hinds et al., 2004). Today more than 60 rivers discharge into the South Caspian Basin from the Iranian side alone, and this river input together with coastal sea currents control the sediment distribution along the Iranian South Caspian Sea coast (Lahijani, 1997; Lahijani and Tavakoli, 2012). Alternatively, the analysed Caspian sand could represent a very local and not well-mixed sample. However, its Phanerozoic age distribution shows similarities to the KDE of the Plio-Quat sample, which includes the Productive Series (Table 2), and the distinct Palaeozoic double peak resembles the Phanerozoic age distribution of Budennovsk and Manych loess, for which the Caucasus was argued above to be the main provenance (Fig. 15). Caucasus input to the South Caspian Basin is likely due to its position and is also discussed by Allen et al. (2006). At present, coastal sediments from the western Caucasus-influenced shore of the South Caspian Sea are transported southwards via longshore drift and redeposited along the central Iranian shoreline (Lahijani and Tavakoli, 2012). Alternatively, in the case of our Turkmen coast Caspian sand sample at Cheleken, Palaeozoic ages could also reflect the geology of the Turan Platform, which is the underlying basement in this area and of mainly Palaeozoic age (Fig. 2). However, basement rocks of this domain seldom crop out through the extensive cover sequence, which accumulated from the Jurassic onwards (Natal and Cela, 2005), and a systematic provenance study of the sandstone sequence of the Turan block cover has not been conducted to date.

The distinct Cretaceous age population in the Cheleken Caspian sand KDE does not appear in any of the discussed samples from the northwest, suggesting a southern or eastern source (Fig. 15). Lukens et al. (2012) report corresponding Cretaceous ages from the Central and Southern Pamir, from where the Palaeo-Amu-Darya used to drain into the South Caspian Sea until the Mid Holocene (e.g. Hinds et al., 2004; Fig. 2). In fact, the Amu-Darya is described as an important silt carrier and of importance for loess formation in Central Asia (Suslov, 1961; Jefferson et al., 2003), and during the Pleistocene, its discharge into the South Caspian Basin was substantial, forming a large delta at its mouth (Kroonenberg et al., 2005; Torres, 2007). Considering that loess sites in the northern Black Sea - Caspian Sea region reflect far-river-transported material from the northern EEP in great abundance, long distance transport of sediment from the Pamir Mountains to the South Caspian Basin seems plausible. The same Cretaceous age fraction appears also in the Iranian loess at Aghband, located on the Iranian Loess Plateau, as well as in the sand sample from the Karakum Desert at Choganly (Fig. 15). In addition to material from the Pamir Mountains, a potential closer source for the loess at Aghband as well as for the marine and desert sands, is represented by the Alborz Mountains, and indeed, the Neoproterozoic to early Cambrian age fractions might derive from the Alborz sandstones, where these ages are highly abundant. However, the aforementioned Cretaceous ages are missing from the age distribution of the Alborz sandstones (Fig. 15). Furthermore, most of the Neoproterozoic and Phanerozoic age peaks of the Alborz and Aghband samples do not match. As such, despite their proximity, a main provenance other than the Alborz mountains is suggested for Aghband loess, and this source is also likely to act as a source to the South Caspian sand and the Karakum Desert sand to a significant extent. All three sediment samples show the same major age peaks, despite differences in abundance. Only the peak at 800 Ma is absent from the Choganly Karakum Desert sample (Fig. 15). This suggests a provenance relationship between Aghband loess, Cheleken Caspian sand and Choganly Karakum sand, although it is unclear if all three sink regions are fed from the same

proto-source(s) or act as sources to each other. Apart from the Pamir and Alborz mountains, the Altaids are another possible source to these three sites, from where corresponding Neoproterozoic and Palaeozoic ages are reported (Fig. 2, e.g. Vladimirov et al., 1997).

A more detailed investigation would be needed to answer the question of the origin of zircons in these samples, and whether long-range transport from the Pamir Mountains via the Palaeo-Amu-Darya is a substantial source pathway, or more proximal sources play a bigger role. Several more proximal potential source areas to the region would be worth more detailed investigation, especially considering the active tectonics in this region. Related high erosion rates might lead to the production of silt material without glacial influence: The Atrek and Gorgan rivers drain from the Iranian Loess Plateau and the Kopet-Dag into the South Caspian Basin, and both of these rivers are discussed as pathways for terrigenous material from the Kopet-Dag into the South Caspian Sea (Lahijani and Tavakoli, 2012; Fig. 1a). Their alluvial plains have been suggested as likely source material for loess of the Iranian loess Plateau (Kehl, 2010; Khormali and Kehl, 2011b). Besides the alluvial plains of these rivers, coastal deposits might also represent a source to the loess. Lahijani and Tavakoli (2012) found that coastal sea currents and hydrodynamics play a major role in the distribution and sorting of sedimentary material within the South Caspian Basin and lead to the accumulation of fine-grained sediments along its eastern shore.

In sum, due to the conjunction of different geological units, the presence of several surrounding orogenic ranges and their ongoing tectonic activity, and the great number of contributing rivers, among them the Pleistocene Amu-Darya, the south of the Caspian Sea represents a complex range of possible sediment sources, with great variability within a relatively small spatial area.

6. Summary and Conclusions: implications for sediment routing networks in the EEP-Black Sea-Caspian Sea region

The wide distribution of Pleistocene loess deposits on the EEP suggests a windy and dusty environment associated with periods of enhanced glaciation in the area (e.g. Költringer et al., 2021; Liang et al., 2016). Loess deposits are mostly found along the courses of large rivers on the EEP (Fig. 1a) and at least four loess provinces can be defined based on their provenance: The Southwest EEP province, the South EEP province, the Southeast EEP province, the North Caucasus province (Fig. 14). A further province (the Southeast Caspian province) borders the region to the south of the Caspian Sea. The remarkable spatial variability in zircon ages reveals that sedimentary sinks in the Black Sea - Caspian Sea region are fed from a range of sources via different transport pathways. The provenance analyses above show that all the discussed sedimentary sinks are to a greater or lesser extent controlled by the sediment supply of rivers and that these pathways enable sediment transportation of several 1000 km across the entire EEP. Comparisons of modern and palaeo-river data suggest that this routing stayed broadly the same during the Late Quaternary, notwithstanding some potential anthropogenic influences on the modern systems. During this transport, rivers actively erode into geological basement where it is exposed, e.g. in mountain regions (Urals, Caucasus) or as cratonic blocks (Voronezh Massif, Ukrainian Shield), but are mostly incising and reworking sedimentary cover sequences. This sedimentary cover is a result of previous fluvial, slope, aeolian and marine processes, which were connected to sediment derived from continental and mountain glaciation and periglaciation during the Quaternary. In particular, the Fennoscandian Ice Sheet had a major control on the erosion and reworking of bedrock and sedimentary cover, and also on drainage patterns and river discharge. Its advance and retreat during the Pleistocene (e.g. Svendsen et al., 2004) may show a direct relationship to water pulses into the Black Sea and Caspian Sea, and therefore increased sediment input from the northern and western EEP (e.g. Soulet et al., 2013; Tudryn et al., 2016). However, while large rivers are clearly the major agents for sediment distribution on the EEP, other processes also play an important role for the spatial provenance differences observed. Most sediment sinks indicate input from multiple diverse sources and therefore a more complex provenance history than can be explained by simple river transport mode alone. This becomes particularly apparent for the loess provinces discussed above (Fig. 14), and based on their discussed proto-sources and pathways (5.6) this complex history can be summarized as follows:

- The Southeast EEP province (e.g. Lower Volga loess) formed through the continental glacier provenance-river transport mode with the Volga as main transport pathway, supplying material mainly from the EEC provinces of Fennoscandia and Volgo-Uralia, combined with the mountain provenance-river transport mode from the Ural Mountains.
- The South EEP province (e.g. Manych loess, Eltigen loess) reflects the continental glacier provenance-river transport mode with the Don as one major transport pathway delivering material from the EEC provinces of Sarmatia and Volgo-Uralia, combined with mountain provenance-river transport mode from the Greater Caucasus. In addition, these sediments exhibit provenance signals indicating origin from nearby geological units, although the processes of reworking of this material prior to aeolian transport are unclear.
- The North Caucasus province (e.g. Budennovsk loess) represents a classic mountain provenance-river transport mode, where the main transport pathways (minor rivers, outwash of slope deposits etc.) provide material from the Greater Caucasus subsequently deflated and deposited as loess.
- The Southwest EEP province (e.g. Beglitsa, Vyazivok, Staiki, Pushkari) formed through the continental glacier provenance-river transport mode, for which transport pathways are represented by the two large rivers in the area, the Don and the Dnieper. These deliver material mainly from the EEC, but carry also minor sediment contributions from the Urals, Podolia and the Carpathians. These findings are in line with those presented by Pańczyk et al. (2020) and Nawrocki et al., 2018).
- The Southeast Caspian province (e.g. Aghband) might be sourced from sediments of the South Caspian Basin, the Karakum Desert, nearby and distant mountain ranges, local geological units and their cover sequences, and as such, represents a complex system of primary sources and transport pathways that require further study. Likely, tectonic activity played a role in the formation of loess deposits in this province. To date our detrital zircon dataset from loess and potential source material south of the Black-Sea, Caucasus and Caspian Sea allows only limited inference on sediment routing in the area. Based on the preliminary data here, the pathways are likely a combination of the mountain provenance-river transport mode and the mountain provenance-river transport-desert transition mode, and may involve sources as distant as the Pamir Mountains.
- In addition to these loess provinces, there is also the unassigned Kalach loess on the Don River, which clearly reflects sourcing from the EEP and an additional unknown possibly local source.

The provenance and transport modes of these loess provinces show that sediment cycling and Late Quaternary loess formation on the EEP is mainly driven by ice sheet and glacier formation driving abundant sediment supply to the region, while its distribution over a wide spatial area and long timescales is mostly undertaken via rivers prior to near source aeolian transport. However, in several cases, the origin of the sedimentary material, including loess, is neither glacial nor far travelled, and without any obvious river link. In fact, it seems that the stark variability in zircon ages and spatial diversity of loess sources on the EEP is often driven by sediment input from these multiple local sources, while the larger mass of material that often has similar protosources is contributed overall by the large rivers. In the case of the loess provinces discussed above, this larger mass comes from the EEC and its cover sequences. While the Volga supplies the Northern Caspian lowland with

material from the EEP, i.e. the EEC and its sedimentary cover, as well as with sediments from the Ural Mountains, the Don provides material from the EEP and the Yergeni Uplands. The Dnieper reflects a sedimentary catchment covering the EEP plus potentially reworking of sedimentary input from northern Europe and the eastern Carpathian foreland. As such, in sum, large rivers distribute large volumes of fairly homogenized material from eroding source regions into depocentres, while local sources show strong diversity across different parts of the study area. In contrast to this observed strong spatial variability in zircon age distributions, the samples from loess in the Lower Volga region in the Southeast EEP province indicate no significant temporal source variability during their deposition in the Late Pleistocene.

Similar to the continental deposits, the marine sediments are also controlled by the large rivers that drain into the seas. The Black Sea as well as Caspian Sea sediments signal a provenance related to the geology of the catchments of the rivers closest to the marine sediment deposit. However, in contrast to the loess, input of multiple sources does not seem to play a significant role for marine sediments. This is exemplified by the Black Sea sand sample from Beglitsa when compared to the directly overlying Beglitsa loess sample (5.6.1). While the marine sand reflects provenance from the Don River, the loess clearly indicates several distinct sources at the same location of deposition. Marine hydrodynamics driven by river discharge and longshore drift, certainly play a role for sediment distribution in seas (e.g. Lahijani and Tavakoli, 2012), however, it seems that this sediment transport occurs mainly within one topographic sea basin, without sedimentary mixing between separated basins of a single sea. In addition to river discharge, sea level changes might also control the sedimentary composition of these basins. Not only will sea level change cause the reworking of sediment in different coastal areas, but changing of the base level might also allow drainage from different geological units into the sea. Overall, the Black Sea and the Caspian Sea appear to act as sedimentary sinks rather than sources to other sediment deposits in the area, such as loess, leaving this role mainly to the fluvial deposits, as discussed above. However, some local source variation in certain loess deposits may be a result of transgressive and regressive cycles, for example in the Lower Volga loess.

Declaration of Competing Interest

The authors declare that they have no known competing financial interests or personal relationships that could have appeared to influence the work reported in this paper.

Acknowledgements

This work was funded by the Swedish Research Council (VR grant 2017-03888). The geological description of the sections in the South East European Plain was supported by the Russian Science Foundation (19-77-10077), geological research in the Cis-Caucasia region was supported by the Russian Foundation for Basic Research (19-05-01004), sampling and site descriptions at the eastern Caspian coast was supported by the Russian Science Foundation (21-18-00552). FK and AG were supported by the Russian-Iranian joint research grant (20-55-56046). We want to thank Daria Semikolennykh and Vladimir Belyaev for their help in the field, Tamara Yanina for discussions on the Ponto-Caspian stratigraphy, Andrei Panin and Elena Kurenkova for providing samples from the Don river basin, Martin Kehl for suggestions regarding Iranian loess, and Jenny Andersson from SGU for her advice on zircon separation.

Appendix A. Supplementary data

Supplementary data to this article can be found online at https://doi.org/10.1016/j.gloplacha.2022.103736.

References

Adebiyi, A.A., Kok, J.F., 2020. Climate models miss most of the coarse dust in the atmosphere. Sci. Adv. 6, 1–10. https://doi.org/10.1126/sciadv.aaz9507.

Albani, S., Mahowald, N.M., Winckler, G., Anderson, R.F., Bradtmiller, L.I., Delmonte, B., François, R., Goman, M., Heavens, N.G., Hesse, P.P., Hovan, S.A., Kang, S.G., Kohfeld, K.E., Lu, H., Maggi, V., Mason, J.A., Mayewski, P.A., McGee, D., Miao, X., Otto-Bliesner, B.L., Perry, A.T., Pourmand, A., Roberts, H.M., Rosenbloom, N., Stevens, T., Sun, J., 2015. Twelve thousand years of dust: the Holocene global dust cycle constrained by natural archives. Clim. Past 11, 869–903. https://doi.org/10.5194/cp-11-869-2015.

Aleinikoff, J.N., Muhs, D.R., Bettis, E.A., Johnson, W.C., Fanning, C.M., Benton, R., 2008. Isotopic evidence for the diversity of late Quaternary loess in Nebraska: glaciogenic and nonglaciogenic sources. Geol. Soc. Am. Bull. 120, 1362–1377.

Alekseev, A.A., 1984. Riphean-VendianMagmatismoftheWesternSlope ofthe Urals. Nauka, Moscow (in Russian).

Allen, M.B., Morton, A.C., Fanning, C.M., Ismail-Zadeh, A.J., Kroonenberg, S.B., 2006. Zircon age constraints on sediment provenance in the Caspian region. J. Geol. Soc. Lond. 163, 647–655. https://doi.org/10.1144/0016-764920-068.

Astakhov, V., 2017. Late Quaternary glaciation of the northern Urals: a review and new observations. Boreas 47, 379–389. https://doi.org/10.1111/bor.12278.

Badertscher, S., Fleitmann, D., Cheng, H., Edwards, R.L., Göktürk, O.M., Zumbühl, A., Leuenberger, M., Tüysüz, O., 2011. Pleistocene water intrusions from the Mediterranean and Caspian seas into the Black Sea. Nat. Geosci. 4, 236–239. https://doi.org/10.1038/ngeo1106.

Balintoni, I., Balica, C., 2016. Peri-Amazonian provenance of the Euxinic Craton components in Dobrogea and of the North Dobrogean Orogen components (Romania): a detrital zircon study. Precambrian Res. 278, 34–51. https://doi.org/10.1016/j.precamres.2016.03.008.

Baykal, Y., Stevens, T., Engström-Johansson, A., Skurzyński, J., Zhang, H., He, J., Lu, H., Adamiec, G., Költringer, C., Jary, Z., 2021. Detrital zircon U–Pb age analysis of last glacial loess sources and proglacial sediment dynamics in the Northern European Plain. Quat. Sci. Rev. 274, 107265 https://doi.org/10.1016/j.quascirev.2021.107265.

Bingen, B., Nordgulen, O., Sigmond, E.M.O., Tucker, R., Mansfeld, J., Hogdahl, K., 2003. Relations between 1.19–1.13 Ga continental magmatism, sedimentation and metamorphism, Sveconorwegian province, S Norway. Precambrian Res. 124, 215–241.

Black, L., Kamo, S., Williams, I.S., Mundil, R., Davis, D.W., Korsch, R.J., Foudoulis, C., 2003. The application of SHRIMP to Phanerozoic geochronology; a critical appraisal of four zircon standards. Chem. Geol. 200, 171–188.

Bogdanova, S.V., 1986. Earth Crust of the Russian Platform in the Early Precambrian (the Volga-Ural region as example). Nauka, Moscow (in Russian).

Bogdanova, S., 1993. Segments of the east European craton. In: Gee, D.G., Beckhol- men, M. (Eds.), EUROPROBE in Jablonna 1991. Institute of Geophysics, Polish Academy of Sciences-European Science Foundation, Warsaw.

Bogdanova, S., Gorbatschev, R., Grad, M., Janik, T., Guterch, A., Kozlovskaya, E., Motuza, G., Skridlaite, G., Starostenko, V., Taran, L., EUROBRIDGE and POLONAISE WorkingGroups, 2006. EUROBRIDGE: new insight into the geodynamic evolution of the East European Craton. In: Gee, D., Stephenson, R. (Eds.), European Litho- sphere Dynamics, 32. Geological Society, London, Memoir, pp. 599–625.

Bogdanova, S.V., Bingen, B., Gorbatschev, R., Kheraskova, T.N., Kozlov, V.I., Puchkov, V. N., Volozh, Y.A., 2008. The East European Craton (Baltica) before and during the assem- bly of Rodinia. Precambrian Res. 160, 23–45. https://doi.org/10.1016/j.precamres.2007.04.024.

Bridge, J., Demicco, R., 2008. Earth Surface Processes, Landforms and Sediment Deposits. Cambridge University Press.

Buggle, B., Glaser, B., Zöller, L., Hambach, U., Marković, S., Glaser, I., Gerasimenko, N., 2008. Geochemical characterization and origin of Southeastern and Eastern European loesses (Serbia, Romania, Ukraine). Quat. Sci. Rev. 27, 1058–1075. https://doi.org/10.1016/j.quascirev.2008.01.018.

Buggle, B., Hambach, U., Glaser, B., Gerasimenko, N., Marković, S., Glaser, I., Zöller, L., 2009. Stratigraphy, and spatial and temporal paleoclimatic trends in Southeastern/Eastern European loess-paleosol sequences. Quat. Int. 196, 86–106. https://doi.org/10.1016/j.quaint.2008.07.013.

Butuzova, E.A., Kurbanov, R.N., Yanina, T.A., Murray, A.S., 2019. Absolute chronology of Late Quaternary evolution stages of the Lower Volga (Seroglazka section) // Geochronology of the Quaternary period conference papers. GIN RAS, IG RAS, Moscow.

Cawood, P.A., Nemchin, A.A., Freeman, M., Sircombe, K., 2003. Linking source and sedimentary basin: Detrital zircon record of sediment flux along a modern river system and implications for provenance studies. Earth Planet. Sci. Lett. 210, 259–268. https://doi.org/10.1016/S0012-821X(03)00122-5.

Chen, J., Yang, T., Matishov, G.G., Velichko, A.A., Zeng, B., He, Y., Shi, P., Fan, Z., Titov, V.V., Borisova, O.K., Timireva, S.N., Konstantinov, E.A., Kononov, Y.M., Kurbanov, R.N., Panin, P.G., Chubarov, I.G., 2018. A luminescence dating study of loess deposits from the Beglitsa section in the Sea of Azov, Russia. Quat. Int. 478, 27–37. https://doi.org/10.1016/j.quaint.2017.11.017.

Choobari, O.A., Zawar-Reza, P., Sturman, A., 2014. The global distribution of mineral dust and its impacts on the climate system: a review. Atmos. Res. 138, 152–165.

Chugunny, Y.G., Matoshko, A.V., 1995. Dnieper glaciation—till deposits of ice-marginal zones. In: Ehlers, J., Kozarski, S., Gibbard, P. (Eds.), Glacial Deposits in North-East Europe. Balkema, Rotterdam, pp. 249–256.

Deuser, W.G., 1972. Late-Pleistocene and Holocene history of Black Sea as indicated by stable-isotope studies. J. Geophys. Res. 77, 1071–1077.

Dodonov, A.E., Zhou, L.P., Markova, A.K., Tchepalyga, A.L., Trubikhin, V.M., Aleksandrovski, A.L., Simakova, A.N., 2006. Middle-Upper Pleistocene bio-climatic and magnetic records of the Northern Black Sea Coastal Area. Quat. Int. 149, 44–54. https://doi.org/10.1016/j.quaint.2005.11.017.

Drăgușanu, C., Tanaka, T., 1999. 1.57-Ga magmatism in the South Carpathians: Implications for the pre-Alpine basement and evolution of the mantle under the European continent. J. Geol. 107 (2), 237–248. https://doi.org/10.1086/314344.

Ducea, M.N., Giosan, L., Carter, A., Balica, C., Stoica, A.M., Roban, R.D., Balintoni, I., Filip, F., Petrescu, L., 2018. U-PB detrital zircon geochronology of the lower danube and its tributaries: implications for the geology of the carpathians. Geochem. Geophys. Geosyst. 19, 3208–3223. https://doi.org/10.1029/2018GC007659.

Fedo, C.M., Sircombe, K.N., Rainbird, R.H., Hanchar, J.M., Hoskin, P.O., 2004. Detrital zircon analysis of the sedimentary record. In: Zircon: Experiments, Isotopes, and Trace Element Investigation Detrital Zircon Analysis of the Sedimentary Record.

Fedorov, P.V., 1971. Postglacial transgression of the Black Sea. Int. Geol. Rev. 14 (2), 160–164.

Frostick, L.E., Jones, S.J., 2002. Impact of periodicity on sediment flux in alluvial systems: grain to basin scale. In: Jones, S.J., Frostick, L.E. (Eds.), Sediment Flux to Basins: Causes, Controls and Consequences. Geological Scociety Special Publication, p. 191.

Froude, D.O., Ireland, T.R., Kinny, P.D., Williams, I.S., Compston, W., Williams, I.R., Myers, J.S., 1983. Ion microprobe identification of 4,100–4,200 Myr-old terrestrial zircons. Nature 304, 616–618.

Gamkrelidze, I., Shengelia, D., Tsutsunava, T., Chung, S.L., Yichiu, H., Chikhelidze, K., 2011. New data on the U–Pb zircon age of the pre-alpine crystalline basement of the Black-Sea-Central Trans- caucasian terrane and their geological significance. Bull Geor- gian Natl Acad Sci 5, 64–76.

Garzanti, E., Vermeesch, P., Andò, S., Vezzoli, G., Valagussa, M., Allen, K., Kadi, K.A., Al-Juboury, A.I.A., 2013. Provenance and recycling of Arabian desert sand. Earth-Sci. Rev. 120, 1–19. https://doi.org/10.1016/j.earscirev.2013.01.005.

Gehrels, G., Pecha, M., 2014. Detrital zircon U-Pb geochronology and Hf isotope geochemistry of Paleozoic and Triassic passive margin strata of western North America. Geosphere 10, 49–65.

Gehrels, G.E., Valencia, V., Ruiz, J., 2008. Enhanced precision, accuracy, efficiency, and spatial resolution of U-Pb ages by laser ablation-multicollector-inductively coupled plasma-mass spectrometry. Geochem. Geophys. Geosyst. 9, Q03017.

Gendler, T.S., Heller, F., Tsatskin, A., Spassov, S., Du Pasquier, J., Faustov, S.S., 2006. Roxolany and Novaya Etuliya-key sections in the western Black Sea loess area: Magnetostratigraphy, rock magnetism, and paleopedology. Quat. Int. 152–153, 89–104. https://doi.org/10.1016/j.quaint.2006.01.001.

Gobejishvili, R., Lomidze, N., Tielidze, L., 2011. Late Pleistocene (Würmian) Glaciations of the Caucasus. Dev. Quat. Sci. 15, 141–147. https://doi.org/10.1016/B978-0-444-53447-7.00012-X.

Golsovo, V., Belyaev, V., n.d. The Volga River basin report. Lomonosov Moscow State Univ. Fac. Geogr. Int. Sediment Initiat. 145.

Gorbatschev, R., Bogdanova, S., 1993. Frontiers in the Baltic Shield. Precambrian Res. 64, 3–21.

Goretskiy, G.I., 1958. About periglacial formation. Bull. Quaternary Commission 22, 3–23 (in Russian).

Gozhik, P.F., 1995. Glacial history of the Ukraine. In: Ehlers, J., Kozarski, S., Gibbard, P. (Eds.), Glacial Deposits in North-East Europe. Balkema, Rotterdam.

Grosswald, M.G., 1980. Late Weichselian ice sheet of northern Eurasia. Quat. Res. 13 (1), 1–32.

Grosswald, M.G., 1998. New approach to the ice age paleohydrol- ogy of northern Eurasia. In: Benito, G., Baker, V.R., Gregory, K.J. (Eds.), Palaeohydrology and Environmental Change. John Wiley & Sons, Chichester and New York, pp. 199–214.

Hällberg, L.P., Stevens, T., Almqvist, B., Snowball, I., Wiers, S., Költringer, C., Lu, H., Zhang, H., Lin, Z., 2020. Magnetic susceptibility parameters as proxies for desert sediment provenance. Aeolian Res. 46 https://doi.org/10.1016/j.aeolia.2020.100615.

Hanel, M., Gurbanov, A.G., Lippolt, H.J., 1992. Age and genesis of gran- ites from the Main-Range and Bechasyn zones of the western Greater Caucasus. N Jahrb Mineral Monatshefte 12, 529–544.

Harrison, S.P., Kohfeld, K.E., Roelandt, C., Claquin, T., 2001. The role of dust in climate changes today, at the last glacial maximum and in the future. Earth Sci. Rev. 54, 43–80.

Hinds, D.J., Aliyeva, E., Allen, M.B., Davies, C.E., Kroonenberg, S.B., Simmons, M.D., Vincent, S.J., 2004. Sedimentation in a discharge dominated fluvial-lacustrine system: the Neogene Productive Series of the South Caspian Basin. Azerbaijan. Mar. Pet. Geol. 21, 613–638.

Hoke, G., Schmitz, M., Bowring, S., 2014. An ultrasonic method for isolating nonclay components from clay- rich material. Geochem. Geophys. Geosyst. 15, 492–498. https://doi.org/10.1002/2013GC005125.

Horton, B.K., Hassanzadeh, J., Stockli, D.F., Axen, G.J., Gillis, R.J., Guest, B., Amini, A., Fakhari, M.D., Zamanzadeh, S.M., Grove, M., 2008. Detrital zircon provenance of Neoproterozoic to Cenozoic deposits in Iran: implications for chronostratigraphy and collisional tectonics. Tectonophysics 451, 97–122. https://doi.org/10.1016/j.tecto.2007.11.063.

Hughes, A.L.C., Gyllencreutz, R., Lohne, Ø.S., Mangerud, J., Svendsen, J.I., 2016. The last Eurasian ice sheets e a chronological database and time-slice reconstruction, DATED-1. Boreas 45, 1–45.

Jefferson, I.F., Evstatiev, D., Karastanev, D., Mavlyanova, N.G., Smalley, I.J., 2003. Engineering geology of loess and loess-like deposits: a commentary on the Russian literature. Eng. Geol. 68, 333–351. https://doi.org/10.1016/S0013-7952(02)00236-3.

Karandeeva, M.V., 1957. Geomorphology of the European part of the USSR. MSU Press, Moscow.

Karpychev, Y.A., 1993. Reconstruction ofCaspian sea-level fluctuations: radiocarbon dating coastal and bottom deposits. Radiocar- bon 35, 409–420.

Kazantsev, Y.V., 1982. Tektonika Kryma (Tectonics of the Crimea). Institute of Geology of the Bashkirskaya Republic, Acadamy of Sciences of the USSR.

Kehl, M., 2010. Quaternary loesses, loess-like sediments, soils and climate change in Iran. Relief, Boden, Paläoklima 24, Gebr. Borntraeger Science Publishers, Stuttgart, p. 208.

Kehl, M., Vlaminck, S., Köhler, T., Laag, C., Rolf, C., Tsukamoto, S., Frechen, M., Sumita, M., Schmincke, H.U., Khormali, F., 2021. Pleistocene dynamics of dust accumulation and soil formation in the southern Caspian Lowlands - new insights from the loess-paleosol sequence at Neka-Abelou, northern Iran. Quat. Sci. Rev. 253 https://doi.org/10.1016/j.quascirev.2020.106774.

Khormali, F., Kehl, M., 2011a. Micromorphology and development of loess-derived surface and buried soils along a precipitation gradient in Northern Iran. Quat. Int. 234, 109–123. https://doi.org/10.1016/j.quaint.2010.10.022.

Khormali, F., Kehl, M., 2011b. Micromorphology and development of loess-derived surface and buried soils along a precipitation gradient in Northern Iran. Quat. Int. 234, 109–123. https://doi.org/10.1016/j.quaint.2010.10.022.

Khormali, F., Shahriari, A., Ghafarpour, A., Kehl, M., Lehndorff, E., Frechen, M., 2020. Pedogenic carbonates archive modern and past precipitation change–A transect study from soils and loess-paleosol sequences from northern Iran. Quat. Int. 552, 79–90.

Knudsen, C., Kokfelt, T., Aagaard, T., Bartholdy, J., Pejrup, M., 2009. Fingerprinting sediments along the west coast of Jylland: interpreting provenance data. Geol. Surv. Denmark Greenl. Bull. 25–28 https://doi.org/10.34194/geusb.v17.5006.

Költringer, C., Stevens, T., Bradák, B., Almqvist, B., Kurbanov, R., Snowball, I., Yarovaya, S., 2020. Enviromagnetic study of Late Quaternary environmental evolution in Lower Volga loess sequences, Russia. Quat. Res. 1–25 https://doi.org/10.1017/qua.2020.73.

Költringer, C., Bradák, B., Stevens, T., Almqvist, B., Banak, A., Lindner, M., Kurbanov, R., Snowball, I., 2021. Palaeoenvironmental implications from Lower Volga loess - joint magnetic fabric and multi-proxy analyses. Quat. Sci. Rev. 267 https://doi.org/10.1016/j.quascirev.2021.107057.

Kosarev, A.N., 2005. Physico-geographical conditions of the Caspian Sea. Casp. Sea Environ. 5, 5–31. https://doi.org/10.1007/698_5_002.

Kosarev, A.N., Kostianoy, A.G., Shiganova, T.A., 2007. The sea of Azov. In: The Black Sea Environment. Springer, pp. 63–89.

Kozłowska, M., 2019. Paleosols and their sedimentary setting in the Old Red succession of Podolia, Ukraine. Palaeogeogr. Palaeoclimatol. Palaeoecol. 514, 45–64. https://doi.org/10.1016/j.palaeo.2018.09.035.

Krijgsman, W., Tesakov, A., Yanina, T., Lazarev, S., Danukalova, G., Van Baak, C.G.C., Agustí, J., Alçiçek, M.C., Aliyeva, E., Bista, D., Bruch, A., Büyükmeriç, Y., Bukhsianidze, M., Flecker, R., Frolov, P., Hoyle, T.M., Jorissen, E.L., Kirscher, U., Koriche, S.A., Kroonenberg, S.B., Lordkipanidze, D., Oms, O., Rausch, L., Singarayer, J., Stoica, M., van de Velde, S., Titov, V.V., Wesselingh, F.P., 2019. Quaternary time scales for the Pontocaspian domain: interbasinal connectivity and faunal evolution. Earth Sci. Rev. 188, 1–40.

Kroonenberg, S.B., Rusakov, G.V., Svitoch, A.A., 1997. The wandering of the Volga delta: a response to rapid Caspian sea-level change. Sediment. Geol. 107, 189–209. https://doi.org/10.1016/S0037-0738(96)00028-0.

Kroonenberg, S.B., Simmons, M.D., Alekseevski, N.I., Aliyeva, E., Allen, M.B., Aybulatov, D.N., Baba-Zadeh, A., Badyukova, E.N., Davies, C.E., Hinds, D.J., Hoogendoorn, R.M., Huseynov, D., Ibrahimov, B., Mamedov, P., Overeem, I., Rusakov, G.V., Suleymanova, S., Svitoch, A.A., Vincent, S.J., 2005. Two deltas, two basins, one river, one sea: The modern Volga delta as an analogue of the Neogene Productive Series, South Caspian Basin. In: Giosan, L., Bhattacharya, J. (Eds.), River Deltas – Concepts, Models and Examples, 83, pp. 231–256.

Kurbanov, R.N., Svitoch, A.A., Yanina, T.A., 2014. New data on marine Pleistocene stratigraphy of the Western Cheleken Peninsula. Dokl. Earth Sci. 459 (2), 1623–1626.

Kurbanov, R.N., Yanina, T.A., Murray, A., Borisova, O.K., 2018. Girkanskij etap v pozdne-pleistotsenovoj istorii Manychskoj depressii [Hyrkanian stage in the Late Pleistocene history of the Manych depression] // Vestn. Mosk. unta. Ser. 5. Geogr. №. 3, pp. 77–88 (in Russian).

Kurbanov, P.N., Yanina, T.A., Murray, A., Semikolennykh, D.V., Svistunov, M.I., Shtyrkova, E.I., 2019. The age of the Karangatian (Late Pleistocene) transgression of the Black sea // Vestn. Mosk. unta. Ser. 5. Geogr., №. 6, pp. 29–40.

Kurbanov, R., Murray, A., Thompson, W., Svistunov, M., Taratunina, N., Yanina, T., 2020. First reliable chronology for the Early Khvalynian Caspian Sea transgression in the Lower Volga River valley. Boreas. https://doi.org/10.1111/bor.12478.

Kuznetsov, N.B., Soboleva, A.A., Udoratina, O.V., Hertseva, M.V., Andreichev, V.L., 2007. Pre-Ordovician tectonic evolution and volcano-plutonic associations of the Timanides and northern Pre-Uralides, northeast part of the East European Craton. Gondwana Res. 12 (3), 305–323. https://doi.org/10.1016/j.gr.2006.10.021.

Kuznetsov, N.B., Natapov, L.M., Belousova, E.A., O'Reilly, S.Y., Griffin, W.L., 2010. Geochronological, geochemical and isotopic study of detrital zircon suites from late Neoproterozoic clastic strata along the NE margin of the East European Craton: Implications for plate tectonic mod- els. Gondwana Res. 17 (2–3), 583–601. https://doi.org/10.1016/j.gr.2009.08.005.

Kuznetsov, N.B., Belousova, E.A., Alekseev, A.S., Romanyuk, T.V., 2014. New data on detrital zircons from the sandstones of the lower Cambrian Brusov Formation (White Sea region, East-European Craton): Unravelling the timing of the onset of the Arctida-Baltica collision. Int. Geol. Rev. 56, 1945–1963. https://doi.org/10.1080/00206814.2014.977968.

Kvasov, D.D., 1979. The Late-Quaternary history of large lakes and inland seas ofEastern Europe. Annales Academiæ Scientarium Fennicæ, Series A. III. Geologica-Geographica. Suomalainen Teideakatemia, Helsinki.
Lahijani, H., 1997. Riverine sediments and stability of Iranian coast of the Caspian Sea. Ph.D. Thesis, Russian Academy of Sciences.
Lahijani, H., Tavakoli, V., 2012. Identifying provenance of South Caspian coastal sediments using mineral distribution pattern. Quat. Int. 261, 128–137. https://doi.org/10.1016/j.quaint.2011.04.021.
Lauer, T., Vlaminck, S., Frechen, M., Rolf, C., Kehl, M., Sharifi, J., Lehndorff, E., Khormali, F., 2017. The Agh Band loess-palaeosol sequence – A terrestrial archive for climatic shifts during the last and penultimate glacial–interglacial cycles in a semiarid region in northern Iran. Quat. Int. 429, 13–30. https://doi.org/10.1016/j.quaint.2016.01.062.
Lebedeva, M., Makeev, A., Rusakov, A., Romanis, T., Yanina, T., Kurbanov, R., Kust, P., Varlamov, E., 2018. Landscape Dynamics in the Caspian Lowlands Since the Last Deglaciation Reconstructed From the Pedosedimentary Sequence of Srednaya Akhtuba, Southern Russia. Geosciences 8, 492. https://doi.org/10.3390/geosciences8120492.
Lehmkuhl, F., Nett, J.J., Pötter, S., Schulte, P., Sprafke, T., Jary, Z., Antoine, P., Wacha, L., Wolf, D., Zerboni, A., Hošek, J., Marković, S.B., Obreht, I., Sümegi, P., Veres, D., Zeeden, C., Boemke, B., Schaubert, V., Viehweger, J., Hambach, U., 2020. Loess landscapes of Europe – Mapping, geomorphology, and zonal differentiation. Earth-Sci. Rev. 215, 103496 https://doi.org/10.1016/j.earscirev.2020.103496.
Leonov, Y.G., Lavrushin, Y.A., Antipov, M.P., Spiridonova, E.A., Kuz'min, Y.V., Jull, E.J. T., Burr, G.S., Jelinowska, A., Chalié, F., 2002. New age data on sediments of the transgressive phase of the Early Khvalyn transgression of the Caspian Sea. Dokl. Earth Sci. 386 (2), 748–751.
Lericolais, G., Popescu, I., Guichard, F., Popescu, S.M., Manolakakis, L., 2007. Water-level fluctuations in the Black Sea since the Last Glacial Maximum. Black Sea Flood Quest. Chang. Coastline, Clim. Hum. Settl. 437–452 https://doi.org/10.1007/978-1-4020-5302-3_18.
Li, Y., Shi, W., Aydin, A., Beroya-Eitner, M.A., Gao, G., 2020. Loess genesis and worldwide distribution. Earth-Sci. Rev. 201, 102947 https://doi.org/10.1016/j.earscirev.2019.102947.
Liang, Y., Yang, T.B., Velichko, A.A., Zeng, B., Shi, P.H., Wang, L.D., He, Y., Chen, J., Chen, Y., 2016. Paleoclimatic record from Chumbur-Kosa section in Sea of Azov region since marine isotope stage 11. J. Mount. Sci. 13, 985–999.
Licht, A., Pullen, A., Kapp, P., Abell, J., Giesler, N., 2016. Eolian cannibalism: reworked loess and fluvial sediment as the main sources of the Chinese Loess Plateau. Bull. Geol. Soc. Am. 128, 944–956. https://doi.org/10.1130/B31375.1.
Lukens, C.E., Carrapa, B., Singer, B.S., Gehrels, G., 2012. Miocene exhumation of the Pamir revealed by detrital geothermochronology of Tajik rivers. Tectonics 31, 1–12. https://doi.org/10.1029/2011TC003040.
Maher, B.A., Prospero, J.M., Mackie, D., Gaiero, D., Hesse, P.P., Balkansi, Y., 2010. Global connections between aeolian dust, climate and ocean biogeochemistry at the present day and at the last glacial maximum. Earth Sci. Rev. 99, 61–97.
Makeev, A., Lebedeva, M., Kaganova, A., Rusakov, A., Kust, P., Romanis, T., Yanina, T., Kurbanov, R., 2021. Pedosedimentary environments in the Caspian Lowland during MIS5 (Srednaya Akhtuba reference section, Russia). Quat. Int. https://doi.org/10.1016/j.quaint.2021.03.015.
Mangerud, J., Astakhov, V.I., Jacobsson, M., Svendsen, J.I., 2001. Huge Ice-age lakes in Russia. J. Quat. Sci. 16, 773–777.
Marković, S.B., Stevens, T., Kukla, G.J., Hambach, U., Fitzsimmons, K.E., Gibbard, P., Buggle, B., Zech, M., Guo, Z., Hao, Q., Wu, H., O'Hara Dhand, K., Smalley, I.J., Újvári, G., Sümegi, P., Timar-Gabor, A., Veres, D., Sirocko, F., Vasiljević, D.A., Jary, Z., Svensson, A., Jović, V., Lehmkuhl, F., Kovács, J., Svirčev, Z., 2015. Danube loess stratigraphy - Towards a pan-European loess stratigraphic model. Earth-Sci. Rev. 148, 228–258. https://doi.org/10.1016/j.earscirev.2015.06.005.
Medaris, G., Ducea, M., Ghent, E., Iancu, V., 2003. Timing of high-pressure metamorphism in the Getic-Supragetic basement nappes of the South-Carpathian mountains fold-thrust belt. Lithos 70 (3–4), 141–161. https://doi.org/10.1016/S0024-4937(03)00096-3.
Meijers, M.J.M., Vrouwe, B., van Hinsbergen, D.J.J., Kuiper, K.F., Wijbrans, J., Davies, G. R., Stephenson, R.A., Kaymakcı, N., Matenco, L., Saintot, A., 2010. Jurassic arc volcanism on Crimea (Ukraine): implications for the paleo-subduction zone configuration of the Black Sea region. Lithos 119, 412–426.
Moecher, D.P., Samson, S.D., 2006. Differential zircon fertility of source terranes and natural bias in the detrital zircon record: implications for sedimentary provenance analysis. Earth Planet. Sci. Lett. 247, 252–266.
Motavalli-Anbaran, S.H., Zeyen, H., Brunet, M.F., Ardestani, V.E., 2011. Crustal and lithospheric structure of the Alborz Mountains, Iran, and surrounding areas from integrated geophysical modeling. Tectonics 30, 1–16. https://doi.org/10.1029/2011TC002934.
Muhs, D.R., Bettis, E.A., III., 2003. Quaternary loess-Paleosol se-quences as examples of climate-driven sedimentary extremes. The Geological Society of America Special Papers 370, 53–74.
Natal, B.A., Cela, A.M., 2005. Late Palaeozoic to Triassic evolution of the Turan and Scythian platforms: the pre-history of the Palaeo-Tethyan closure, 404, pp. 175–202. https://doi.org/10.1016/j.tecto.2005.04.011.
Nawrocki, J., Gozhik, P., Łanczont, M., Pańczyk, M., Komar, M., Bogucki, A., Williams, I. S., Czupyt, Z., 2018. Palaeowind directions and sources of detrital material archived in the Roxolany loess section (southern Ukraine). Palaeogeogr. Palaeoclimatol. Palaeoecol. 496, 121–135. https://doi.org/10.1016/j.palaeo.2018.01.028.
Nawrocki, J., Bogucki, A.B., Gozhik, P., Łanczont, M., Pańczyk, M., Standzikowski, K., Komar, M., Rosowiecka, O., Tomeniuk, O., 2019. Fluctuations of the Fennoscandian Ice Sheet recorded in the anisotropy of magnetic susceptibility of periglacial loess from Ukraine. Boreas 48, 940–952. https://doi.org/10.1111/bor.12400.
Nie, J., Stevens, T., Rittner, M., Stockli, D., Garzanti, E., Limonta, M., Bird, A., Andò, S., Vermeesch, P., Saylor, J., Lu, H., Breecker, D., Hu, X., Liu, S., Resentini, A., Vezzoli, G., Peng, W., Carter, A., Ji, S., Pan, B., 2015. Loess plateau storage of Northeastern Tibetan plateau-derived yellow river sediment. Nat. Commun. 6, 8511. https://doi.org/10.1038/ncomms9511.
Nikishin, A.M., Ziegler, A., Stephenson, R.A., Cloetingh, S.A.P.L., Fume, A.V., Fokin, A., Ershov, A.V., Bolotov, S.N., Korotaev, M.V., Alekseev, A.S., Gorbachev, I., Shipilov, E.V., Lankreijer, A., Bembinova, Eyu, Shalimov, I.V., 1996. Late precambrian to triassic history of the East European craton: dynamics of sedimentary basin evolu- tion. Tectonophysics 268, 23–63.
Novenko, E.Y., 2006. Late Valdai pollen flora from loess sediments in the central East-European Plain. Paleoenvironmental reconstruction. Quat. Int. 152–153, 157–163. https://doi.org/10.1016/j.quaint.2005.12.005.
Nutman, A.P., Kalsbeek, F., Marker, M., van Gool, J.A.M., Bridgwater, D., 1999. U-Pb zircon ages of Kangâmiut dykes and detrital zircons in metasediments in the Paleoproterozoic Nagssugtoqidian Orogen (West Greenland) clues to the pre-collisional history of the orogen. Precambrian Res. 93, 87–104.
Oczlon, M.S., 2006. Terrane map of Europe. Gaea Heidelbergensis 15, 1987. In: Pettijohn, F.J., Potter, P.E., Siever, R. (Eds.), Sand and Sandstone. Springer Verlag, New York.
Okay, A.I., Topuz, G., 2017. Variscan orogeny in the Black Sea region. Int. J. Earth Sci. 106, 569–592. https://doi.org/10.1007/s00531-016-1395-z.
Paces, J.B., Miller, J.D., 1993. Precise U-Pb ages of Duluth complex and related mafic intrusions, northeastern Minnesota' geochronological insights to physical, petrogenetic, paleomagnetic, and tectonomagmatic processes associated with the 1.1 Ga midcontinent rift system. J. Geophys. Res. 98 (B8), 13997–14013.
Panaiotu, C.G., Panaiotu, E.C., Grama, A., Necula, C., 2001. Paleoclimatic record from a loess-paleosol profile in Southeastern Romania. Phys. Chem. Earth, Part A Solid Earth Geod. https://doi.org/10.1016/S1464-1895(01)00138-7.
Pańczyk, M., Nawrocki, J., Bogucki, A.B., Gozhik, P., Łanczont, M., 2020. Possible sources and transport pathways of loess deposited in Poland and Ukraine from detrital zircon U-Pb age spectra. Aeolian Res. 45 https://doi.org/10.1016/j.aeolia.2020.100598.
Panin, V., Astakhov, G., Komatsu, E., Lotsari, J. Lang, Winsemann, J., 2020. Middle and late quaternary glacial lake-outburst floods, drainage diversions and reorganization of fluvial systems in northwestern eurasia. Earth Sci. Rev. 201, 103069.
Puchkov, V.N., 1997. Structure and geodynamics of the Uralian orogen. In: Burg, J.-P., Ford, M. (Eds.), Orogeny Through Time, Geol. Soc. Am. Spec. Publ., 121, pp. 201–236.
Puchkov, V.N., 2009. The evolution of the Uralian orogen. Geol. Soc. Spec. Publ. 327, 161–195. https://doi.org/10.1144/SP327.9.
Puchtel, I.S., Hofmann, A.W., Mezger, K., Jochum, K.P., Shchipansky, A.A., Samsonov, A. V., 1998. Oceanic plateau model for continental crustal growth in the Archaean, a case study from the Kostomuksha greenstone belt, NW Baltic Shield. Earth Planet. Sci. Lett. 155, 57–74.
Pullen, A., Ibañez-Mejía, M., Gehrels, G., Ibañez-Mejía, J.C., Pecha, M., 2014. What happens when n = 1000? Creating large n geochronological datasets with LA- ICP-MS for geologic investigations. J. Anal. At. Spectrom. 29, 971–980.
Pullen, A., Ibanez-Mejia, M., Gehrels, G., Giesler, D., Pecha, M., 2018. Optimization of a laser ablation-single collector-inductively coupled plasma-mass spectrometer (thermo element 2) for accurate, precise, and efficient zircon U-Th-Pb. Geochronol.: Geochem. Geophysics Geosyst. 19 https://doi.org/10.1029/2018GC007889.
Pye, K., 1995. The nature, origin and accumulation of loess. Quat. Sci. Rev. 14, 653–667.
Reynolds, A.D., Simmons, M.D., Bowman, M.B.J., Henton, J., Brayshaw, A.C., Ali-Zade, A.A., Guliyev, I.S., Suleymanova, S.F., Ateava, E.Z., Mamedova, D.N., Koshkarly, R.O., 1998. Implications of outcrop geology for reservoirs in the Neogene Productive Series: Apsheron Peninsula, Azerbaijan. AAPG Bull. 82, 25–49.
Richards, K., 2002. Drainage basin structure, sediment delivery and the response to environmental change. In: Jones, S.J., Frostick, L.E. (Eds.), Sediment Flux to Basins: Causes, Controls and Consequences. Geological Scociety Special Publication, p. 191.
Rolland, Y., 2017. Caucasus collisional history: review of data from East Anatolia to West Iran. Gondwana Res. 49, 130–146. https://doi.org/10.1016/j.gr.2017.05.005.
Rolland, Y., Hässig, M., Bosch, D., Meijers, M.J.M., et al., 2016. A review of the plate convergence history of the East Anatolia-Transcaucasus region during the Variscan: insights from the Georgian basement and its connection to the Eastern Pontides. J. Geodyn. 96, 131–145.
Rousseau, D., Chauvel, C., Sima, A., Hatté, C., Lagroix, F., Antoine, P., Balkanski, Y., Fuchs, M., Mellett, C., Kageyama, M., Ramstein, G., Lang, A., 2014. European glacial dust deposits: Geochemical constraints on atmospheric dust cycle modeling, pp. 7666–7674. https://doi.org/10.1002/2014GL061382.Received.
Rychagov, G.I., 1997. Pleistocene History of the Caspian Sea. Moscow State University, Moscow, pp. 1–267 (in Russian).
Safonova, I., Maruyama, S., Hirata, T., Kon, Y., Rino, S., 2010. LA ICP MS U-Pb ages of detrital zircons from Russia largest rivers: Implications for major granitoid events in Eurasia and global episodes of supercontinent formation. J. Geodyn. 50, 134–153. https://doi.org/10.1016/j.jog.2010.02.008.
Schito, A., Andreucci, B., Aldega, L., Corrado, S., Di Paolo, L., Zattin, M., Szaniawski, R., Jankowski, L., Mazzolli, S., 2018. Burial and exhumation of the western border of the Ukrainian Shield (Podolia): a multi-disciplinary approach. Basin Res. 30 (S1), 532–549.
Sergeev, E.M., Larionov, A.K., Komissarova, N.N. (Eds.), 1986. Loess Rocks of the USSR. Nedra, Moscow V1, 231 pp. in Russian.

Shchipansky, A.A., Bogdanova, S.V., 1996. The Sarmatian crustal segment: precam-brian correlation between the Voronezh Massif and the Ukrainian Shield across the Dniepr-Donets Aulacogen. Tectonophysics 268, 109–125.
Shkatova, V.K., 2010. Paleogeography of the late Pleistocene Cas- pian basins: geochronometry, paleomagnetism, paleotemperature, paleosalinity and oxygen isotopes. Quat. Int. 225, 221–229.
Sirotenko, O.D., Abashina, E.E., 1992. Modelling productiveness of agroecosystems. Trudy VNIISHM 26.
Smalley, I.J., Derbyshire, E., 1990. The definition of ice-sheet and mountain loess. Area 22, 300–301.
Smalley, I., O'Hara-Dhand, K., Wint, J., Machalett, B., Jary, Z., Jefferson, I., 2009. Rivers and loess: The significance of long river transportation in the complex event-sequence approach to loess deposit formation. Quat. Int. 198, 7–18. https://doi.org/10.1016/j.quaint.2008.06.009.
Somin, M., 2011. Pre-Jurassic basement of the Greater Caucasus: brief overview. Turk. J. Earth Sci. 20, 545–610.
Somin, M., Lepekhina, E., Konilov, A., 2007. Age of hightemperature gneiss core of the Central Caucasus. Dokl. Earth Sci. 415, 690–694.
Soulet, G., Ménot, G., Bayon, G., Rostek, F., Ponzevera, E., Toucanne, S., Lericolais, G., Bard, E., 2013. Abrupt drainage cycles of the Fennoscandian Ice Sheet. Proc. Natl. Acad. Sci. U. S. A. 110, 6682–6687.
Stacey, J., Kramers, J., 1975. Approximation of terrestrial lead isotope evolution by a two-stage model. Earth Planet. Sci. Lett. 26, 207–221.
Stevens, T., Palk, C., Carter, A., Lu, H., Clift, P.D., 2010. Assessing the provenance of loess and desert sediments in northern China using U-Pb dating and morphology of detrital zircons. Bull. Geol. Soc. Am. 122, 1331–1344. https://doi.org/10.1130/B30102.1.
Stevens, T., Carter, A., Watson, T.P., Vermeesch, P., Andò, S., Bird, A.F., Lu, H., Garzanti, E., Cottam, M.A., Sevastjanova, I., 2013. Genetic linkage between the Yellow River, the Mu Us desert and the Chinese Loess Plateau. Quat. Sci. Rev. 78 https://doi.org/10.1016/j.quascirev.2012.11.032.
Suslov, S.P., 1961. Physical Geography of Asiatic Russia. Freeman, San Francisco, p. 594.
Svendsen, J.I., Alexanderson, H., Astakhov, V.I., Demidov, I., Dowdeswell, J.A., Funder, S., Gataullin, V., Henriksen, M., Hjort, C., Houmark-Nielsen, M., Hubberten, H.W., Ingólfsson, Ó., Jakobsson, M., Kjær, K.H., Larsen, E., Lokrantz, H., Lunkka, J.P., Lysså, A., Mangerud, J., Matiouchkov, A., Murray, A., Möller, P., Niessen, F., Nikolskaya, O., Polyak, L., Saarnisto, M., Siegert, C., Siegert, M.J., Spielhagen, R.F., Stein, R., 2004. Late Quaternary ice sheet history of northern Eurasia, in. Quat. Sci. Rev. Pergamon 1229–1271. https://doi.org/10.1016/j.quascirev.2003.12.008.
Taratunina, N., Rogov, V., Streletskaya, I., Thomson, W., Kurchatova, A., Yanina, T., Kurbanov, R., 2020. Late Pleistocene cryogenesis features of a loess-paleosol sequence in the Srednyaya Akhtuba reference section, Lower Volga river valley, Russia. Quat. Int. https://doi.org/10.1016/j.quaint.2020.12.015.
Tikhomirov, P.L., Chalot-Prat, F., Nazarevich, B.P., 2004. Triassic volcanism in the Eastern Fore-Caucasus: Evolution and geodynamic interpretation. Tectonophysics 381, 119–142. https://doi.org/10.1016/j.tecto.2003.10.014.
Torres, M.A., 2007. The petroleum geology of Western Turkmenistan: the Gograndag-Okarem Province. In: Yilmaz, P.O., Isaksen, G.H. (Eds.), Oil and Gas of the Greater Caspian Area: AAPG Studies in Geology, pp. 109–132.
Tudryn, A., Chalié, F., Lavrushin, Y.A., Antipov, M.P., Spiridonova, E.A., Lavrushin, V., Tucholka, P., Leroy, S.A.G., 2013. Late Quaternary Caspian Sea environment: Late Khazarian and Early Khvalynian transgressions from the lower reaches of the Volga River. Quat. Int. 292, 193–204. https://doi.org/10.1016/j.quaint.2012.10.032.
Tudryn, A., Leroy, S.A.G., Toucanne, S., Gibert-Brunet, E., Tucholka, P., Lavrushin, Y.A., Dufaure, O., Miska, S., Bayon, G., 2016. The Ponto-Caspian basin as a final trap for southeastern Scandinavian Ice-Sheet meltwater. Quat. Sci. Rev. 148, 29–43. https://doi.org/10.1016/j.quascirev.2016.06.019.
Ujvári, G., Varga, A., Ramos, F.C., Kovács, J., Németh, T., Stevens, T., 2012. Evaluating the use of clay mineralogy, Sr-Nd isotopes and zircon U-Pb ages in tracking dust provenance: An example from loess of the Carpathian Basin. Chem. Geol. 304–305, 83–96. https://doi.org/10.1016/j.chemgeo.2012.02.007.
Vandenberghe, J., 1995. Timescales, climate and river development. Quat. Sci. Rev. 14, 631–638.
Vandenberghe, J., Woo, M.-K., 2002. Modern and ancient periglacial river types. Prog. Phys. Geogr. 26, 479–506.
Velichko, A.A., Morozova, T.D., Nechaev, V.P., Rutter, N.W., Dlusskii, K.G., Little, E.C., Catto, N.R., Semenov, V.V., Evans, M.E., 2006. Loess/paleosol/cryogenic formation and structure near the northern limit of loess deposition, East European Plain, Russia. Quat. Int. 152–153, 25–41. https://doi.org/10.1016/j.quaint.2005.12.003.
Velichko, A.A., Catto, N.R., Yu Kononov, M., Morozova, T.D., Yu Novenko, E., Panin, P. G., Ya Ryskov, G., Semenov, V.V., Timireva, S.N., Titov, V.V., Tesakov, A.S., 2009. Progressively cooler, drier interglacials in southern Russia through the Quaternary: Evidence from the Sea of Azov region. Quat. Int. 198, 204–219. https://doi.org/10.1016/j.quaint.2008.06.005.
Velichko, A.A., Faustova, M.A., Pisareva, V.V., Gribchenko, Y.U.N., Sudakova, N.G., Lavrentiev, N.V., 2011. Glaciations of the east european plain. Distribution and chronology. Dev. Quat. Sci. 15, 337–359. https://doi.org/10.1016/B978-0-444-53447-7.00026-X.
Vermeesch, P., 2004. How many grains are needed for a provenance study? Earth Planet. Sci. Lett. 224, 441–451.
Vermeesch, P., 2012. On the visualisation of detrital age distributions. Chem. Geol. 312–313, 190–194. https://doi.org/10.1016/j.chemgeo.2012.04.021.
Vincent, S.J., Morton, A.C., Hyden, F., Fanning, M., 2013. Insights from petrography, mineralogy and U-Pb zircon geochronology into the provenance and reservoir potential of Cenozoic siliciclastic depositional systems supplying the northern margin of the Eastern Black Sea. Mar. Pet. Geol. 45, 331–348. https://doi.org/10.1016/j.marpetgeo.2013.04.002.
Vladimirov, A.G., Ponomareva, A.P., Shokalskii, S.P., Khalilov, V.A., Kostitsyn, Y.A., Ponomarchuk, V.A., Rudnev, S.N., Vystavnoi, S.A., Kruk, N.N., Titov, A.V., 1997. Late Paleozoic-Early Mesozoic granitoid magmatism in Altay. Russ. Geol. Geophys. 38, 755–771.
Wang, C.Y., Campbell, I.H., Stepanov, A.S., Allen, C.M., Burtsev, I.N., 2011. Growth rate of the preserved continental crust: II. Constraints from Hf and O isotopes in detrital zircons from Greater Russian Rivers. Geochim. Cosmochim. Acta. https://doi.org/10.1016/j.gca.2010.12.010.
Yanina, T.A., 2014. The Ponto-Caspian region: Environmental consequences of climate change during the Late Pleistocene. Quat. Int. 345, 88–99. https://doi.org/10.1016/j.quaint.2014.01.045.
Yanina, T.A., 2020. Environmental variability of the Ponto-Caspian and mediterranean basins during the last climatic macrocycle. Geography, Environ. Sustain. 13 (4), 6–23.
Yanina, T.A., Svitoch, A.A., Kurbanov, R., Murray, A.S., Tkach, N.T., Sychev, N.Y., 2017. Paleogeographic analysis of the results of optically stimulated luminescence dating of pleistocene deposits of the lower volgaarea. Vestn. Mosk. Univ. Seriya 5 Geogr., 20–28 (in Russian).
Yanko-Hombach, V., Kislov, A., 2018. Late Pleistocene – Holocene sea-level dynamics in the Caspian and Black Seas: Data synthesis and Paradoxical interpretations. Quat. Int. 465, 63–71. https://doi.org/10.1016/j.quaint.2017.11.030.
Zastrozhnov, A.S., 1991. [Elaboration of the regional stratigraphical scheme of the Palaeo-Don] Razrabotka regionalnoi stratigraficheskoi schemy neogenovyh otlozheniy Paleo-Dona. Volgograd Geological Survey Expedition, Volgograd (in Russian).
Zubakov, V.A., 1988. Climatostratigraphic Scheme of the Black-Sea Pleistocene and Its Correlation With the Oxygen Isotope Scale and Glacial Events, p. 24.